


APPROVAL SHEET

Title of Dissertation: HIV-1 MATRIX INTERACTIONS WITH tRNAs AND THEIR  
ROLE IN MEMBRANE TARGETING

Name of Candidate: Christy R. Gaines  
Doctor of Philosophy, 2017

Dissertation and Abstract Approved: \_\_\_\_\_

  
Dr. Michael F. Summers  
Investigator/Professor  
Howard Hughes Medical Institute  
Department of Chemistry and Biochemistry  
University of Maryland, Baltimore County

Date Approved: 10/19/17

## ABSTRACT

Title of Document: HIV-1 MATRIX INTERACTIONS WITH  
tRNAS AND THEIR ROLE IN MEMBRANE  
TARGETING

Christy Rae Gaines  
Doctor of Philosophy, 2017

Directed By: Dr. Michael F. Summers, Chemistry and  
Biochemistry

Assembly of the HIV-1 virion begins when the myristoylated matrix domain (myrMA) of the Gag polyprotein targets the Gag-genome complex to the plasma membrane through interactions between myrMA's highly basic region (HBR) and the membrane lipid phosphatidylinositol 4,5-bisphosphate [PI(4,5)P<sub>2</sub>]. In addition to interacting with PI(4,5)P<sub>2</sub>, myrMA will bind to specific tRNAs in the cytoplasm, and studies have found that treating myrMA with RNase will decrease myrMA's ability to discriminate between membranes containing and lacking PI(4,5)P<sub>2</sub>. Here we developed assays to characterize the interaction between MA and tRNA<sup>Lys3</sup>, one of the RNAs that bound to MA and the primer used during reverse transcription. NMR spectrometry mapped the RNA-binding region to the HBR, including lysine residues known to regulate membrane binding. Isothermal titration calorimetry (ITC) of basic patch mutants determined that many mutations known to affect plasma membrane binding also decreased myrMA's affinity to tRNA<sup>Lys3</sup>. ITC experiments also found that exposure of MA's N-terminal myristoyl group weakens tRNA-MA interactions, supporting the hypothesis that tRNA binding regulates membrane binding as

myristoyl exposure occurs upon binding to the plasma membrane. However,  $^1\text{H}$ -1D NMR liposome competition assays determined that the presence of tRNA alone is not enough to allow myrMA to discriminate between membranes. tRNA<sup>Lys3</sup> prevented binding to all membranes, including those containing high levels of PI(4,5)P<sub>2</sub> and those with raft-like compositions. Lowering the pH of the samples to induce myristoyl exposure did induce specific membrane binding in the presence of tRNA, suggesting some other mechanism is required in addition to tRNA interactions to regulate assembly on the plasma membrane.

HIV-1 MATRIX INTERACTIONS WITH tRNAs AND THEIR ROLE IN  
MEMBRANE TARGETING

By

Christy R. Gaines

Dissertation submitted to the Faculty of the Graduate School of the  
University of Maryland, Baltimore County, in partial fulfillment  
of the requirements for the degree of  
Doctorate of Philosophy  
2017

© Copyright by  
Christy R. Gaines  
2017



## Dedication

For my parents, Raymond and Paula Gaines, for teaching me to shoot for the stars  
and providing the unconditional love and support to do so.

And for my siblings and best friends, Alan and Julie Gaines, for knowing me better  
than I know myself and for encouraging me to push forward.

## Acknowledgements

Many people have helped me along the way. I would like to thank my advisor, Michael Summers, for providing advice and guidance as I learned to develop experiments. I would also like to thank my committee members, Paul Bieniasz, Alex Drohat, Kristen Varney, Elsa Garcin, Ryan White, and Ian Thorpe, for providing their insights and expertise to these experiments.

I could not have done this without the graduate students, post-doctoral fellows, and staff in the Summers Lab, as they played an integral role in teaching me not only how to think about science, but also how to continue when things didn't turn out well. I would particularly like to thank Sarah Keane, who served as a trusted mentor and encouraged me to follow my dreams.

Additionally, I appreciate the support of all the undergraduate and high school students of the Summers Lab, as their enthusiasm and encouragement allowed me to continue when projects started to fail. I am especially grateful to the students that worked with me, Amalia Rivera-Oven, Emre Tkacik, Phoebe Somani, Alecia Achimovich, Tawa Alabi, Ae Lim Yang, Tarik Hawkins, Noel Getachew, Matthew McDonough, Angela Zhu, Zoe Spadaro, Femi Ajayi, and Joshua Yang, as they provided not only ideas and physical contributions to the projects, but also constantly taught me new ways of approaching problems and were my major source of motivation.

While I am lucky to have made many friends in Baltimore, I would especially like to thank Stephanie Coppola, Sarah Russell, Julie Nyman, and Amanda Bowers

for always believing in me and helping me keep my sanity by teaching me that there is more to life than the next experiment.

Finally I would like to thank my family, who never let me feel forgotten even though I had moved far away. I have the most amazing siblings, Alan and Julie Gaines, who always were willing to share in my experiences. I also cannot adequately express my gratitude to my parents, who shaped me into the person I am today and were my biggest supporters through this endeavor. Thank you!

# Table of Contents

Dedication .....	ii
Acknowledgements .....	iii
List of Tables .....	vii
List of Figures .....	viii
Chapter 1: Introduction .....	1
The HIV Pandemic and the Role of Antiretroviral Therapy .....	1
The HIV-1 Replication Cycle .....	2
The HIV-1 Matrix Protein .....	5
Matrix Interactions with Nucleic Acids .....	7
tRNA <sup>Lys3</sup> .....	9
Overview of Dissertation Studies .....	12
Chapter 2: Characterization of the myrMA-tRNA Interactions .....	18
Abstract .....	18
Introduction .....	19
Materials and Methods .....	20
Protein Expression and Purification .....	20
Preparation of Labeled Protein Samples .....	23
tRNA Synthesis and Purification .....	24
Electrophoretic Mobility Shift Assays (EMSA) .....	25
Isothermal Titration Calorimetry .....	25
Analytical Size Exclusion Chromatography .....	26
Nuclear Magnetic Resonance (NMR) Experiments .....	26
Results .....	27
Initial Characterization of myrMA-tRNA Interactions and Assay Optimization .....	27
Characterization of Matrix Interactions with tRNA <sup>Lys3</sup> .....	31
Characterization of Matrix Interactions with Multiple tRNAs to Determine Specificity .....	33
Characterization of Matrix-Capsid Interactions with tRNA <sup>Lys3</sup> .....	34
Common Characteristics of tRNAs that Bind to Matrix .....	36
Discussion .....	37
Chapter 3: Role of the Highly Basic Region and Myristoyl Group on myrMA-tRNA Interactions .....	50
Abstract .....	50
Introduction .....	51
Materials and Methods .....	53
Protein Expression and Purification .....	53
tRNA Synthesis and Purification .....	54
Isothermal Titration Calorimetry .....	54
Electrophoretic Mobility Shift Assays (EMSA) .....	54
Results .....	55
Mutations that Decrease Binding to PI(4,5)P <sub>2</sub> -Containing Liposomes also Decrease Binding to tRNA <sup>Lys3</sup> .....	55
Mutations Known to Decrease Specificity of Membrane Interactions also Affect tRNA <sup>Lys3</sup> -myrMA Interactions .....	57

Myristoyl Group Exposure Inhibits myrMA-tRNA <sup>Lys3</sup> Interactions .....	58
Discussion .....	59
Chapter 4: tRNA's Role in Regulating Matrix-Membrane Interactions.....	71
Abstract .....	71
Introduction.....	72
Materials and Methods.....	73
Protein Expression and Purification.....	73
tRNA Synthesis and Purification .....	74
Liposome Preparation .....	74
1D NMR Liposome Assay.....	75
Results.....	76
Modification of the <sup>1</sup> H-1D NMR Experiment .....	76
Comparison of <sup>1</sup> H-1D NMR Binding Assay Using His-tagged and Untagged Protein .....	77
Effect of Liposome Freeze-Thaw Cycles .....	78
Effect of Buffer Choice Liposome Binding.....	79
RNA Alone is Not Sufficient to Regulate Membrane Binding .....	80
tRNA Prevents Binding to Raft-Like Liposomes .....	82
The Effect of pH on Liposome Binding .....	83
Work with Multimerized Matrix.....	84
Discussion .....	87
Chapter 5: Significance and Future Perspectives.....	104
Summary and Significance of Dissertation Studies.....	104
Future Perspectives .....	109
Appendices.....	114
Protein DNA Sequences .....	114
tRNA Sequences .....	116
Bibliography .....	117

## List of Tables

Table 3.1: Thermodynamic characterization of myrMA mutants with tRNA <sup>Lys3</sup> .....	70
Table 3.2: Characterization of myristoyl group interactions with tRNA <sup>Lys3</sup> .....	70
Table 4.1: Percent compositions of non-raft and raft liposomes .....	92
Table 4.2: Percent compositions of model MT4 plasma membrane and HIV-1 lipid envelope liposomes .....	92

## List of Figures

Figure 1.1: The HIV-1 replication cycle.....	14
Figure 1.2: Structure of the HIV-1 matrix protein.....	15
Figure 1.3: Structure of tRNA <sup>Lys3</sup> .....	16
Figure 1.4: Proposed role of tRNA in membrane binding .....	17
Figure 2.1: EMSA of T7-transcribed tRNA <sup>Lys3</sup> and myrMA .....	40
Figure 2.2: Modifications of tRNA <sup>Lys3</sup> and <i>E. coli</i> tRNA <sup>Lys</sup> .....	41
Figure 2.3: Role of magnesium on tRNA <sup>Lys</sup> -myrMA interactions .....	42
Figure 2.4: Magnesium dependence of RNA folding .....	43
Figure 2.5: Magnesium dependence of tRNA interactions with myrMA .....	44
Figure 2.6: tRNA <sup>Lys3</sup> binds near MA's basic patch .....	45
Figure 2.7: tRNA <sup>Lys3</sup> binds in a 1:1 molar ratio to myrMA .....	46
Figure 2.8: myrMA binds specifically to tRNA <sup>Lys3</sup> .....	47
Figure 2.9: tRNA <sup>Lys3</sup> interactions with myrMACA <sup>NTD</sup> .....	48
Figure 2.10: Sequence Alignment of tRNAs that bound to MA .....	49
Figure 3.1: EMSA of tRNA <sup>Lys3</sup> interactions with mutants that decrease membrane binding .....	63
Figure 3.2: Mutations that disrupt myrMA-membrane interactions also weaken myrMA's affinity for tRNA .....	64
Figure 3.3: EMSA of tRNA <sup>Lys3</sup> interactions with K32 mutants .....	65
Figure 3.4: EMSA of tRNA <sup>Lys3</sup> interactions with mutants that decrease membrane specificity .....	66
Figure 3.5: Mutations known to affect membrane specificity also decrease myrMA's affinity for tRNA .....	67

Figure 3.6: Effect of pH on myrMA-tRNA interactions .....	68
Figure 3.7: Myristoyl group exposure weakens tRNA-MA interactions .....	69
Figure 4.1: $^1\text{H}$ -1D NMR spectra of myrMA and the myrMA-tRNA <sup>Lys3</sup> complex .....	93
Figure 4.2: Comparison of the 6XHis-tagged and untagged myrMA proteins .....	94
Figure 4.3: Effect of freeze-thaw cycles on myrMA-liposome interactions .....	95
Figure 4.4: Buffer effect on liposome binding assay .....	96
Figure 4.5: Negative phospholipids, including PI(4,5)P <sub>2</sub> cannot outcompete tRNA <sup>Lys3</sup> .....	97
Figure 4.6: tRNA <sup>IleGAU</sup> prevents binding to negatively charged liposomes .....	98
Figure 4.7: Liposome binding in the presence and absence of tRNA .....	99
Figure 4.8: tRNA <sup>Lys3</sup> prevents myrMA interactions with raft-like liposomes .....	100
Figure 4.9: Reducing the pH does not allow PI(4,5)P <sub>2</sub> -containing liposomes to outcompete tRNA <sup>Lys3</sup> .....	101
Figure 4.10: Role of multimerization on tRNA binding .....	102
Figure 4.11: myrMACA does not bind to PI(4,5)P <sub>2</sub> -containing liposomes .....	103
Figure 5.1: Proposed mechanism for Gag targeting to the plasma membrane .....	113

## Chapter 1: Introduction

### *The HIV Pandemic and the Role of Antiretroviral Therapy*

Human immunodeficiency virus (HIV) is the causative agent of Acquired Immunodeficiency Syndrome (AIDS), a deadly disease that compromises the immune system through infection and death of CD4<sup>+</sup> immune cells [1]. There are two types of HIV, HIV type 1 (HIV-1) and HIV type 2 (HIV-2), with HIV-1 being the most common worldwide with a faster progression to AIDS [2]. At the end of 2015, the World Health Organization (WHO) estimated that 36.7 million people worldwide are infected with HIV [3]. While global health organizations have made large progress in containing the HIV pandemic through the distribution of antiretroviral therapy to 17.0 million people in 2015, significant challenges remain [3]. In 2015, there were 2.1 million new HIV infections, a rate that has not significantly differed from 2010, in which there were 2.2 million new infections worldwide [3]. In addition to new infections, 1.1 million people died from AIDS-related deaths worldwide in 2015 [3]. Most people living with HIV are in sub-Saharan Africa (25.6 million) [3], but 1.1 million people with HIV live in the United States [4]. In 2015, there were 39,513 new HIV infections in the U.S., with an infection rate of 12.3 people per 100,000 [5]. Over half of these new infections occurred in the Southeast region of the U.S. (20,408), with the District of Columbia having the highest rate of HIV infection (57.0 per 100,000), followed by Louisiana (24.2 per 100,000), Florida (24.0 per 100,000), Georgia (23.4 per 100,000), and Maryland (22.4 per 100,000) [5]. Additionally, 18,303 HIV-infected patients advanced to the AIDS stage of the disease in 2015,

resulting in 1,216,917 people in the U.S. advancing to this late stage of the disease since the beginning of the epidemic [5].

After HIV infection, Antiretroviral Therapy (ART) is used to control the infection and delay progression to AIDS [6]. However, as ART can only treat the infection, but not cure it, patients must take ART for the duration of their lives [1, 6]. Also, due to the lack of proofreading activity by reverse transcriptase, HIV has a high mutation rate [7], necessitating a combination of drugs with different mechanisms of action be taken in order to prevent antiretroviral resistance [6]. As of June 2016, there were over 25 antiretroviral drugs approved by the U.S. Food and Drug Administration (FDA), with 6 different mechanisms of action, targeting viral entry, reverse transcription of the viral genome, integration of viral DNA into host chromosomes, and maturation of virion after budding [6]. However, side effects and antiretroviral resistance necessitates continuing study of the mechanisms of HIV replication and assembly in order to find new viral targets [1].

### *The HIV-1 Replication Cycle*

The HIV-1 replication cycle has two phases: the early phase and the late phase (Figure 1.1). The early phase begins with HIV-1 infection, when the envelope glycoprotein (Env) on the virion surface recognizes and attaches to CD4 receptors on the target host cell. Fusion of the virion to the host cell plasma membrane occurs when chemokine receptors, including CXCR4 and CCR5, are recruited to the bound CD4 receptors [8, 9]. Uncoating of the viral genome occurs, allowing reverse transcription of the RNA viral genome into DNA [10]. This process is facilitated through the last 18 nucleotides on the 3' end of the cellular tRNA primer, tRNA<sup>Lys3</sup>,

annealing to the primer binding site on the 5' Untranslated Region (5' UTR) of the genome [11]. While tRNA<sup>Lys3</sup> is a cellular RNA, it has a channeled life cycle that limits availability in the cell, and must be packaged into virions during the late phase for annealing to the HIV genome before fusion into the newly infected cell [12].

After synthesis of the viral DNA genome, the DNA is transported to the host cell nucleus as part of the preintegration complex, composed of viral proteins integrase (IN), matrix (MA), reverse transcriptase (RT), and Vpr, in addition to host protein HMG-I(Y) [8, 13]. Vpr is essential for nuclear localization due to its ability to bind the preintegration complex to nuclear import machinery [14]. Once in the nucleus, IN can insert randomly into the host cell genome, promoting latency if the viral DNA is inserted into areas with repressive transcription environments [15]. However, IN primarily integrates the viral DNA into the host chromosomes through interactions with the LEDGF protein to direct insertion into actively transcribing genes, initiating the late phase of the replication cycle [15].

In the late phase, the cell transcribes viral RNA from the integrated DNA and transports the RNA from the nucleus to the cytoplasm for translation [8]. Initially, low levels of HIV-1 RNA are transcribed as the virus relies on cellular machinery to initiate the process [16]. Fully spliced mRNAs encoding viral proteins Tat, Nef, and Rev are able to leave the nucleus at this point, allowing the translation of the Tat protein, which upregulates transcription of the HIV-1 genome [17]. Translation and translocation of the Rev protein to the nucleus allows the unspliced and singly spliced RNAs that code for the proteins Vif, Vpr, and Vpu to exit the nucleus, as the Rev

protein binds to the Rev-response element (RRE) in the viral genome and recruits proteins necessary for nuclear export [18].

The unspliced viral genome has two fates in the cytoplasm. The unspliced RNA can form a dimer through interactions between the dimer initiation sequence (DIS) within the 5' UTR of two RNAs, and serve as the genome for new virions [19]. As a monomer, it serves as the mRNA required for translation of the viral Gag polyprotein, the structural protein of the virus [19, 20]. The Gag polyprotein is composed of the matrix (MA), capsid (CA), nucleocapsid (NC), and p6 domains [1, 8]. The N-terminally myristoylated MA domain traffics the Gag polyprotein to the plasma membrane, the CA domain can form multimers that promote assembly, and the NC domain binds to the dimeric viral genome, allowing targeting of a Gag-genome complex to the plasma membrane and assembly of a new viral particle containing a single dimeric genome [8]. A translational frameshift allows the ribosomes to also translate the Gag-Pol polyprotein from the unspliced RNA, which contains the protease (PR), reverse transcriptase (RT), and integrase (IN) domains in addition to MA, CA, and NC [8]. At the plasma membrane, MA helps incorporate Env into new virions through interactions with the TM domain of the Env precursor protein [1, 8]. Accumulation of 1700 to 3100 Gag particles leads to the budding of a new immature virion [21], a process that requires the p6 domain to recruit host cell ESCRT machinery to facilitate the virion leaving the cell [1, 21]. Maturation occurs when the viral enzyme protease (PR) cleaves the Gag polyprotein into its separate domains, allowing CA to form a shell around the NC-bound genome and creating an infectious viral particle [22].

### *The HIV-1 Matrix Protein*

The matrix (MA) domain of the HIV-1 Gag polyprotein has multiple roles in the viral replication cycle. Mature MA, which has been cleaved from the rest of the Gag polyprotein, forms a protective shell around the viral components by burying itself into the inner leaflet of the membrane surrounding the HIV-1 virus [23, 24]. The mature MA also plays a role in the early stage of the replication cycle, as it is part of the preintegration complex that efficiently transports viral DNA into the host cell nucleus for insertion into the host's genome [25]. Additionally, MA has roles in the late cycle beyond membrane targeting, as interactions between the gp41 tail of the Env protein and MA help incorporate Env into the viral membrane [1, 26].

MA is a 15kDa globular protein composed of six helices and a three-stranded mixed  $\beta$ -sheet [27] (Figure 1.2). MA crystallizes as a trimer [28], and can form hexamers of trimers on synthetic lipid bilayers [29], suggesting that it may multimerize in the cell. Sedimentation studies have indicated that multimerization increases upon exposure of a N-terminal myristoyl group [30, 31], and multimerization enhances MA's ability to bind membranes, as *in vitro* multimerization of the protein has led to increased membrane binding in liposome flotation assays [32]. Additionally, trimerization may play a role in Env incorporation, as trimerization-deficient mutants were unable to efficiently incorporate the Env protein into virions [33].

MA has two main features that facilitate its role in membrane targeting and binding. The first is a covalently bound myristoyl moiety added cotranslationally to the N-terminal glycine of the protein [1]. This 14-carbon saturated fatty acid allows

MA to anchor the Gag polyprotein to the plasma membrane, as myristoyl-deficient mutants will only associate weakly with the plasma membrane, inhibiting virus production [34, 35]. Experiments with liposomes have shown weaker membrane association *in vitro*, as myristoylated MA binds with much higher affinity than the unmyristoylated protein to the model membranes [36, 37]. The myristoyl group can take either a sequestered or exposed conformation, with regulation of the equilibrium between the two states controlled by the myristoyl switch mechanism [30]. Although studies have determined that the Gag polyprotein has a higher affinity for the membrane than the MA domain alone [38, 39], there is little overall change in the conformation of the protein between the exposed and sequestered states [30]. The equilibrium is pH-dependent, as deprotonation of His89 disrupts the salt bridge between His89 and Glu12 that stabilizes the exposed conformation [31]. The equilibrium can also be controlled by concentration, as increased concentration promotes interactions between the myristoyl groups, stabilizing the exposed conformation and increasing the multimerization of MA [30].

The second region of MA associated with membrane binding is a highly basic region spanning residues 18-32, which interact with membrane lipid phosphatidylinositol 4,5-bisphosphate [PI(4,5)P<sub>2</sub>] to target the Gag polyprotein to the inner leaflet of the plasma membrane [1, 40]. The interaction occurs between the negatively charged phosphatidylinositol headgroup and the positively charged basic patch [41-43], a common motif among membrane proteins targeting to PI(4,5)P<sub>2</sub> [44]. Depletion of PI(4,5)P<sub>2</sub> through the use of the enzyme 5ptaseIV inhibits plasma membrane targeting and viral budding, whereas constitutively expressing PI(4,5)P<sub>2</sub> in

other membranes leads to Gag retargeting to endosomes [40]. In addition to binding to PI(4,5)P<sub>2</sub>, evidence suggests that Gag assembles at raft-like microdomains enriched in cholesterol [45-49] and that the HIV-1 lipid envelope has a raft-like composition [50, 51].

Mutations to Lys30 and Lys32 in the basic patch result in the retargeting of Gag to multivesicular bodies [52, 53], as well as the inhibition of Env incorporation and viral particle production and release [36, 53-55]. A different basic patch mutant, K26T/K27T, has a higher release efficiency and the ability to retarget the Gag protein to other membranes [56]. In addition to phenotypes observed in cell culture, mutations to lysine residues found in the basic patch affect Gag's ability to bind to model membranes. Wild-type Gag binds preferentially to membranes containing PI(4,5)P<sub>2</sub>, and does not bind efficiently to liposomes containing the negative phospholipid phosphatidylserine or neutral phosphatidylcholine [36, 56-58]. Mutations of HBR residues K18, K30 and K32 decrease Gag's ability to bind to liposomes containing PI(4,5)P<sub>2</sub> [36, 53, 56]. However the K26T/K27T binds to PI(4,5)P<sub>2</sub>-containing liposomes with a similar affinity as the wild-type, but also increases the affinity for liposomes lacking PI(4,5)P<sub>2</sub> [56], indicating that not all basic residues play an equal role in membrane targeting.

#### *Matrix Interactions with Nucleic Acids*

In addition to membrane targeting, MA also has the ability to bind nucleic acids [59-64]. Initial studies focused on MA's ability to bind to RNA and DNA due to its role in the preintegration complex (PIC) [65, 66], while other studies looked at MA's RNA-binding abilities through Gag's genome-selection function [59, 67].

Immunoprecipitation assays found that MA associates with elongation factor 1- $\alpha$  (EF1- $\alpha$ ) through an RNA intermediate, and packages the protein into virions [64]. Further work to determine specificity of RNA binding used 76mer and 31mer libraries to find an optimal RNA binding sequence [60, 61].

This RNA-binding property is thought to be linked to MA's membrane selectivity, as treatment of samples with RNases decreases Gag's ability to discriminate between membranes containing PI(4,5)P<sub>2</sub> and other negatively charged phospholipids [32, 56, 68, 69]. This discrimination is due to the MA domain, as PI(4,5)P<sub>2</sub>-containing liposomes could successfully outcompete DNA for bead-bound MA [62]. NMR experiments used a 15mer RNA oligonucleotide based off the specific binding sequence to map residues affected by RNA-binding, and found that RNA binds to MA's basic patch, the membrane-binding region of the protein [63]. However, many of these assays took place *in vitro*, and could not conclude if RNA interactions with MA had a physiological relevance.

Cross-linking immunoprecipitation (CLIP) assays determined the specific RNA sequences that bound to Gag in cells, which primarily included cellular tRNAs [69]. However, low CLIP reads of tRNAs in virions suggested that tRNAs were not packaged in large numbers [69]. Bieniasz and coworkers determined that the tRNA-binding ability of Gag is mediated through the MA domain, and is specific to eight tRNAs coding for glutamic acid, glycine, lysine, and valine [69]. While tRNA<sup>GlyGCC</sup> had the highest number of reads of all tRNAs bound to MA, the primer for reverse transcription, tRNA<sup>Lys3</sup>, had the second highest read count [69]. This RNA, as well as tRNA<sup>Lys1,2</sup> which also bound to MA, is packaged into virions during assembly [70-

72]. Both tRNA<sup>GlyGCC</sup> and tRNA<sup>Lys3</sup> bound near the 5' end of the tRNAs, in a region other than the 3' end and anticodon loop that participate in reverse transcription [69].

Since the determination that MA binds to tRNAs, other studies have tried to determine the role this specific interaction plays in membrane binding. Liposome flotation assays that added T7-transcribed tRNA<sup>Lys3</sup> determined that the tRNA does not confer specificity for membrane binding while tRNA<sup>Pro</sup> does [58]; however these studies were done in the absence of magnesium, which is essential for the correct folding of unmodified tRNA<sup>Lys3</sup> [73, 74]. Membrane targeting assays using reconstituted systems observed Gag's ability to package different RNAs in the presence and absence of modified yeast tRNAs, and found that tRNA interactions with matrix allow Gag to selectively package the HIV-1 genome indicating that tRNA-MA interactions play a vital role in virion assembly [75].

#### *tRNA<sup>Lys3</sup>*

tRNA<sup>Lys3</sup> assumes the canonical L-shape associated with tRNAs [73, 76], and like other tRNAs is heavily modified [76] (Figure 1.3). tRNA<sup>Lys3</sup> is transcribed in the nucleus, where processing begins by cleavage of the 5' end by RNase P [77, 78]. The tRNA precursor is cleaved again at nucleotide 73 on the 3' end by RNase Z, allowing the addition of the CCA nucleotide sequence that will signal aminoacylation at a later step [78, 79]. Multiple enzymes then modify 15 of the nucleic bases [76], which help with translation as well as tRNA folding and structure stability [73, 74, 78]. tRNA<sup>Lys3</sup> associates with lysyl-tRNA synthase (LysRS), which aminoacylates the 3' end of the tRNA with the lysine amino acid [12, 80]. This complex brings tRNA<sup>Lys3</sup> to the ribosome, where tRNAs interact with the ribosome, elongation factors (including

EF1- $\alpha$ ), and LysRS to create a channeled life cycle that prevents the creation of free tRNA [81].

While the primary role of tRNAs are as intermediates that facilitate the translation of mRNAs to protein, some also play a role as a primer in reverse transcription for several retroviral lifecycles. Avian retroviruses tend to use tRNA<sup>Trp</sup>, whereas tRNA<sup>Pro</sup> facilitates DNA synthesis in many murine viruses [82, 83]. The primer for HIV-1, HIV-2, and simian immunodeficiency virus (SIV) is tRNA<sup>Lys3</sup>, one of three isoforms of the tRNA<sup>Lys</sup> isoacceptor [11, 12, 83]. The two other tRNAs, tRNA<sup>Lys1</sup> and tRNA<sup>Lys2</sup>, have similar structures, with one nucleic acid difference in the acceptor stem [84]. They are generally denoted together by tRNA<sup>Lys1,2</sup>, as they both use the anticodon CUU when coding for lysine [84]. The third isoform, tRNA<sup>Lys3</sup>, makes up ~40% of the total mammalian tRNA<sup>Lys</sup> pool and uses the anticodon UUU [72].

All of the three tRNA<sup>Lys</sup> isoacceptors are packaged into new virions at concentrations higher than those found in the cytoplasm, suggesting selective packaging [70, 71], which occurs independently of NC's selection of the RNA genome [71, 85]. The tRNAs are packaged according to their ratios in the cell, with 8 copies of tRNA<sup>Lys3</sup> and 12 copies of tRNA<sup>Lys1,2</sup> found in virions [72]. The presence of the Gag-Pol protein is required, as Gag alone does not incorporate tRNA<sup>Lys</sup> into virions [86]. The thumb domain of reverse transcription (RT) is thought to mediate this requirement, as deletions of Pol after the RT thumb do not affect tRNA<sup>Lys3</sup> packaging [86]. Although the tRNAs found in virions are not aminoacylated [72], mitochondrial LysRS is also packaged into the new virions [87, 88]. Interactions

between LysRS and tRNA<sup>Lys3</sup> may help facilitate selective packaging of the tRNA [87, 89, 90], however it is unknown if the tRNAs are packaged before aminoacylation or are deacylated during the packaging process [91]. Although Gag-Pol is necessary for tRNA<sup>Lys3</sup> packaging [71], LysRS only requires Gag [92]. Exogenous production of tRNA<sup>Lys3</sup> only shifts the ratio of tRNA<sup>Lys3</sup>:tRNA<sup>Lys1,2</sup> packaged, but does not affect the overall amount of tRNA<sup>Lys</sup> packaged [72]. However increased expression of LysRS results in increased tRNA<sup>Lys</sup> packaging, indicating that LysRS is the limiting factor for tRNA<sup>Lys</sup> incorporation into virions [93, 94]. Increasing the concentration of tRNA<sup>Lys3</sup> in virions promotes primer annealing to PBS and enhances infectivity of the virus [94]. Thus, the current model [82, 91] is that interactions occur between tRNA<sup>Lys3</sup>'s anticodon loop and LysRS's N-terminal anticodon binding domain [12], with interactions between Gag and LysRS resulting in packaging of tRNA<sup>Lys3</sup> [94-96] and the thumb domain of RT stabilizing the interaction of Gag, LysRS, and tRNA [97].

Annealing to the RNA genome occurs at the 3' end of tRNA<sup>Lys3</sup>, with the last 18 nucleic acid residues complementing the primer binding site (PBS) on the 5' UTR [91]. Annealing is also stabilized by interactions between the anticodon loop and an A-rich loop on the U5 stem of the genome [98, 99]. Although the exact timing of primer annealing to PBS is unknown, the process occurs before entry into the new host cell [11, 12]. The NC domain of the Gag polyprotein has the ability to chaperone annealing *in vitro* [100], as well as the immature GagΔp6 [101, 102]. Immature Gag can facilitate annealing *in vivo*, suggesting that annealing can take place before assembly [12, 103, 104]. Gag's chaperone activity may be linked to plasma

membrane binding, as annealing is enhanced upon addition of inositol phosphates [105]. However, primer annealed to PBS by Gag is less stably associated with the genome than primer annealed by NC [12, 104, 106]. Adding NC to tRNA<sup>Lys3</sup>-genome complexes annealed by Gag results in a strengthening of the interaction [106], leading to the suggestion that primer annealing occurs in a two-step process where Gag initially binds tRNA<sup>Lys3</sup> to PBS at the assembly site and NC strengthens the interaction after maturation of the virion [12]. Upon infection of a host cell, the annealed tRNA<sup>Lys3</sup>-genome complex initiates reverse transcription. RT rapidly dissociates from the genome-tRNA<sup>Lys3</sup> complex, resulting in the slow addition of the first 6 nucleotides in a process that is dependent on the modifications of tRNA<sup>Lys3</sup> [91, 98, 107, 108]. After initiation, the process transitions to an elongation phase through extended primer-template interactions [108], and the elongation phase proceeds to synthesize (-) strand DNA [91].

### *Overview of Dissertation Studies*

While many studies have researched the role MA plays in membrane binding, MA-RNA interactions remain a relatively unexplored field. At the beginning of my studies, some in the field still debated whether or not MA could bind to RNA in cells or if the interaction was only an electrostatic artifact of *in vitro* assays. The discovery that MA binds to specific tRNAs in cells, one of which is the primer for reverse transcription [69] left a need to characterize the interaction and its possible role in membrane binding. Chapter 2 describes the development of assays used to characterize the specific interaction between MA and tRNA<sup>Lys3</sup>, as well as control RNAs to determine if RNA-binding specificity could be observed *in vitro*. Chapter 3

determines the role each individual lysine in the basic patch plays in tRNA-MA interactions, and whether they contribute equally or there is some mechanism other than charge alone that regulates the interaction. Chapter 3 also investigates the role the myristoyl group plays in MA-tRNA interactions to determine if myristoyl exposure affects RNA binding.

The current proposed mechanism [56, 69] for tRNA's role in membrane binding is shown in Figure 1.4. tRNA binds to the highly basic region (HBR) of MA, suppressing binding to membranes lacking PI(4,5)P<sub>2</sub>. Upon encountering the plasma membrane, which contains PI(4,5)P<sub>2</sub>, the lipid will outcompete the tRNA for MA's HBR, favoring membrane binding. Chapter 4 describes experiments that used liposome competition assays to determine if tRNA regulates MA's ability to specifically bind to membranes, in order to test this hypothesis.

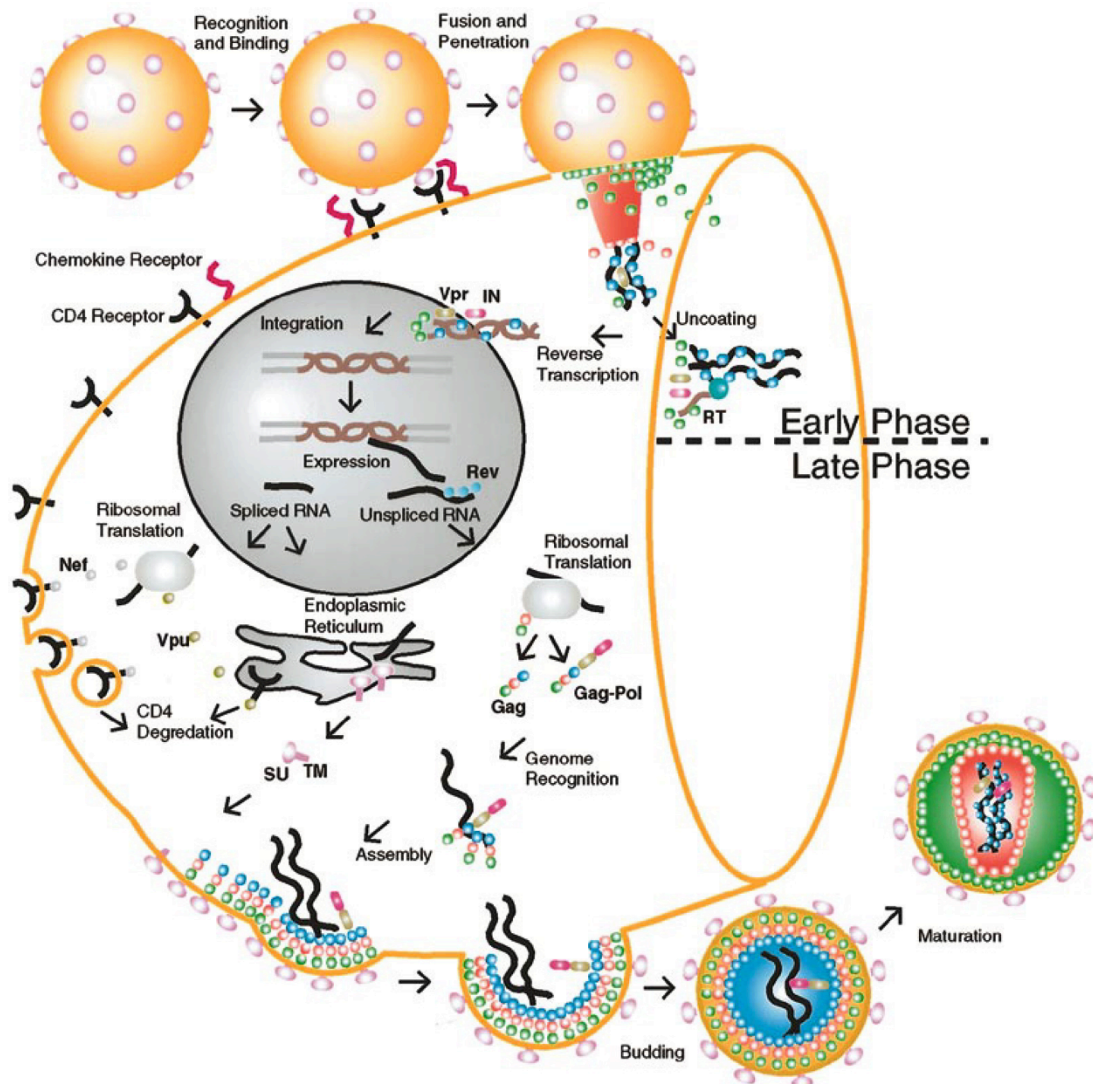


**Figure 1.1: The HIV-1 replication cycle.** The early phase of viral replication begins upon entry into the host cell, where viral uncoating allows the reverse transcription of viral RNA into DNA. This DNA is transported to the host cell nucleus and is integrated into the chromosome. The late phase begins when viral DNA is transcribed into RNA and is transported to the cytoplasm. The unspliced monomeric RNA is translated into the Gag and Gag-Pol polyproteins, which bind to the dimerized RNA genome. The matrix domain of the Gag polyprotein targets the Gag and Gag-genome complexes to the plasma membrane for virion assembly, where budding occurs to create a new virion. Maturation of the virion upon cleavage of the Gag polyprotein creates an infectious HIV-1 particle. Figure from Turner and Summers, 1999 [8].

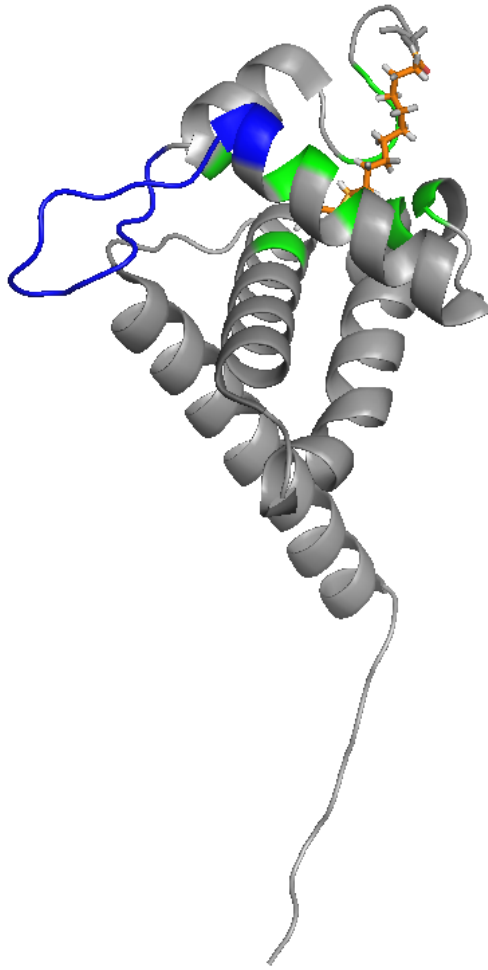


**Figure 1.2: Structure of the HIV-1 matrix protein.** The HIV-1 matrix protein is composed of 6 helices, as well as a 3 strand mixed beta sheet. The basic patch (blue) targets PI(4,5)P<sub>2</sub> on the plasma membrane. The N-terminal myristoyl group (orange) is primarily sequestered in a hydrophobic pocket (green), but can adopt an exposed conformation upon membrane binding. Figure generated in PyMOL from PDB entry 1UPH [30].

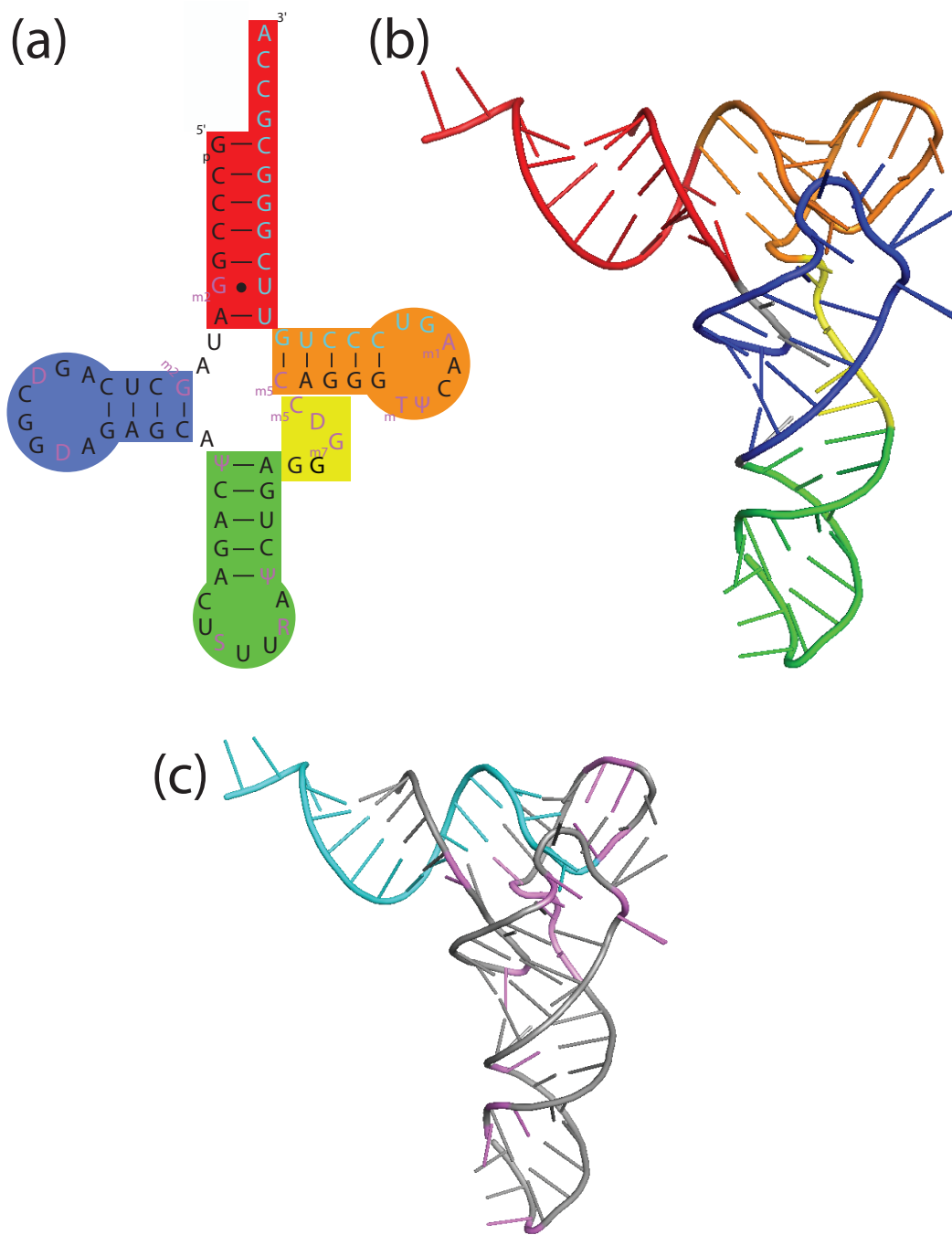


**Figure 1.3: Structure of tRNA<sup>Lys3</sup>.** (a) tRNA<sup>Lys3</sup> is composed of an acceptor stem (red) and 4 loops: the D-loop (blue), anti-codon loop (green), variable loop (yellow), and the T-loop (orange). (b) The tertiary structure of tRNA<sup>Lys3</sup>. (c) Modifications (violet) stabilize the tertiary structure of the RNA, as well as interactions between the reverse transcriptase and the primer. The 18 nucleotides that bind to the primer binding site (PBS) are in cyan. Figure generated in PyMOL from PDB entry 1FIR [76].

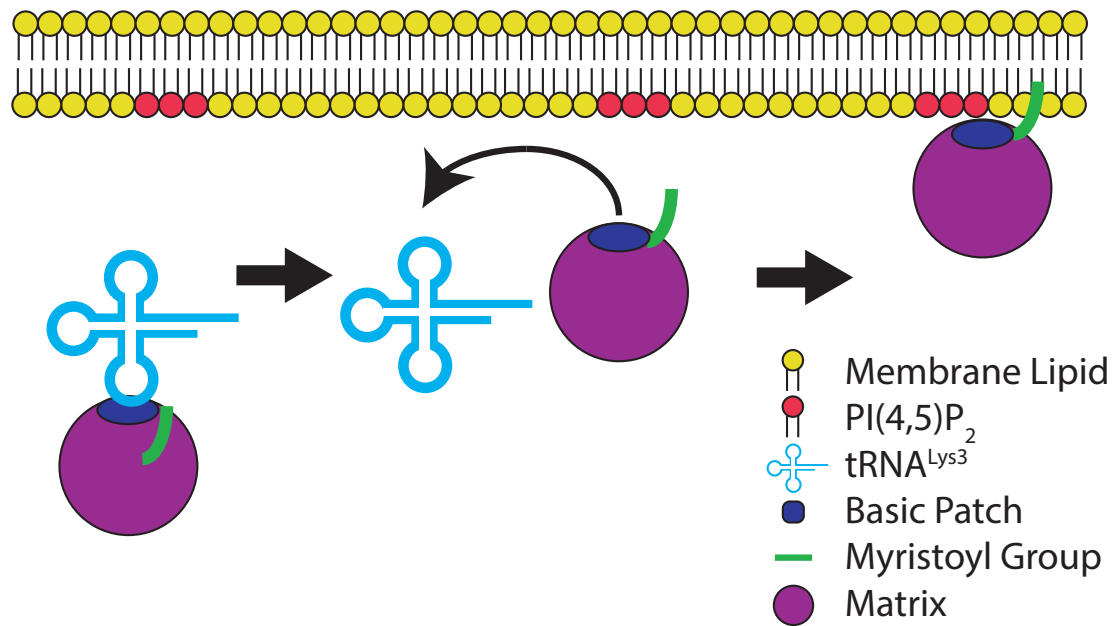


**Figure 1.4: Proposed role of tRNA in membrane binding.** tRNA binds to the highly basic region of the matrix protein, preventing nonspecific interactions with other negative phospholipids. However, upon encountering the PI(4,5)P<sub>2</sub>-containing plasma membrane, PI(4,5)P<sub>2</sub> outcompetes tRNA for the basic patch, allowing membrane binding to occur.

## Chapter 2: Characterization of the myrMA-tRNA Interactions

### *Abstract*

The matrix domain of the Gag polyprotein binds to eight specific tRNAs, one of which is tRNA<sup>Lys3</sup>, the primer used by the virus during reverse transcription and one of the tRNAs packaged into new virions. Matrix interactions with tRNAs may regulate matrix's targeting to the plasma membrane, warranting further investigation into the role tRNAs play in the assembly process. Before studying the effect of tRNA on matrix-membrane interactions, the interaction between matrix and tRNAs needed further characterization. This chapter describes development of assays to observe the matrix-tRNA<sup>Lys3</sup> interaction, determine the importance of nucleic base modifications, optimize conditions for measuring the RNA-protein interaction, and characterize interaction specificity. Upon addition of at least 5 mM MgCl<sub>2</sub> to the T7-transcribed tRNAs to induce correct folding, unmodified tRNAs can interact with matrix in an interaction similar to modified tRNAs purified from *E. coli*. Matrix binds tightly in a 1:1 molar ratio to tRNA<sup>Lys3</sup>, with a  $K_d$  of  $0.63 \pm 0.03$   $\mu$ M. Experiments with other tRNAs, including tRNA<sup>GlyGCC</sup> and tRNA<sup>IleGAU</sup>, indicate that matrix has specificity for tRNA<sup>Lys3</sup>. This interaction is similar to the one the matrix-capsid protein has for tRNA<sup>Lys3</sup>, although the addition of the capsid domain does slightly weaken matrix-tRNA interactions. Sequence analyses of the eight tRNAs that bind to matrix indicate that they all share a similar D-loop sequence, but so do other tRNAs that did not bind in the CLIP studies, necessitating further work to determine the tRNA binding site.

## Introduction

The matrix (MA) domain of the Gag polyprotein targets the protein to the plasma membrane for virion assembly [1, 8, 36, 40, 41, 53-55]. MA targets the plasma membrane through its highly basic region (HRB) and interactions with phosphatidylinositol 4,5-bisphosphate [PI(4,5)P<sub>2</sub>], as mutation of HBR residues leads to a loss of membrane specificity and retargeting of Gag to multivesicular bodies [54, 55].

In addition to binding to the plasma membrane, crosslinking immunoprecipitation (CLIP) studies have determined that MA will bind to 8 specific tRNAs in the cytoplasm [69]. While tRNA<sup>GlyGCC</sup> had the highest number of CLIP reads, the second highest reads belonged to tRNA<sup>LysUUU</sup> [69]. This tRNA, also called tRNA<sup>Lys3</sup>, plays a key role in the retroviral life cycle, as it serves as the primer for reverse transcription [11, 12, 83]. tRNA<sup>Lys3</sup> is also packaged into virions, along with its cognate tRNA synthase, LysRS [12, 82].

MA's ability to bind to RNA has been linked with its role in membrane binding. Liposome flotation assays typically use Gag protein synthesized by rabbit reticulocyte serum, which contains the machinery needed to translate protein *in vitro*, including tRNAs [56, 68]. Experiments done in the presence of RNAs remaining after the translation reaction show Gag will specifically bind to membranes containing PI(4,5)P<sub>2</sub> [56, 68]. However, upon addition of RNases that degrade RNA, Gag maintains its ability to bind to PI(4,5)P<sub>2</sub>-containing membranes, but will have increased binding to liposomes containing other negative phospholipids as it loses specificity in membrane targeting [32, 56, 68]. Other liposome flotation assays using

the lysate of HIV infected cells have shown a similar decrease in membrane specificity upon addition of RNases [69].

In order to determine the role tRNAs may play in membrane-MA interactions, I first characterized the interaction between tRNAs and MA. tRNA<sup>Lys3</sup> was selected as the RNA ligand, as there is a large body of literature on the RNA due to its role in reverse transcription, including an x-ray crystallography structure [76] and nuclear magnetic resonance (NMR) assignments for some nucleotides [73, 74, 109]. Electrophoretic mobility shift assays (EMSA) determined the conditions needed to visualize the interaction *in vitro*, providing initial data for optimization of further characterization by isothermal titration calorimetry (ITC), size exclusion chromatography (SEC), and NMR spectrometry.

### *Materials and Methods*

#### *Protein Expression and Purification*

HIV-1 NL4-3 strain myristoylated MA (myrMA) was expressed using a pETDuet vector containing genes for both HIV-1 MA and human N-myristoyltransferase. Transformed BL21-DE3-RIL *E. coli* cells (Agilent) were grown in 2-4L LB broth at 37°C until OD<sub>600</sub> ~0.6-0.7. Cells were induced using isopropyl β-thiogalactoside (1 mM) and continued to grow for 3.5-4 hours. Previous constructs used a 6XHis tag for purification, but interactions between the 6XHis tag and RNA necessitated removal of the tag and a new purification protocol. Cell pellets were resuspended in lysis buffer (50 mM NaPO<sub>4</sub>, pH 7.0, 500 mM NaCl, 2 mM EDTA, and 5 mM BME) and lysed through microfluidization. The lysed cells were centrifuged at 18000 rpm for 25 minutes at 4°C and the supernatant purified by

polyethylenimine precipitation (0.15% w/v, spinning in a beaker at 4°C for at least 20 minutes, centrifuge at 18000 rpm for 25 minutes at 4°C to separate protein from the precipitated RNA and impurities). Failure to complete the PEI precipitation resulted in RNase contamination in the protein after carrying out the rest of the purification. The protein was salted out with ammonium sulfate (at 50% saturation, spinning at 4°C in a beaker for at least 1 hour) and centrifuged at 18000 rpm for 25 minutes at 4°C to separate the precipitated matrix from impurities in the supernatant. The pellet was resuspended in cation exchange buffer (50 mM NaPO<sub>4</sub>, pH 6.0, 2 mM EDTA, 5 mM DTT) and dialyzed in 2L of the same buffer overnight at 4°C. Precipitate formed during the dialysis, most of which was impurities but some of which included the target protein. Sample loss was prevented by resuspending the ammonium sulfate pellet in at least 100 mLs buffer per 2L flask. Sample was centrifuged at 5500 rpm for 10 minutes at 10°C to pellet the precipitate and filtered through a 0.22 µm syringe filter to remove any solid particles. Ion exchange chromatography was completed using both a Q and SP column (GE Healthcare, HiPrep FF 16/10 Columns), with the Q column serving as a trap for negatively charged impurities. After removal of the Q column, myrMA was eluted with 1M NaCl added to the buffer over a 200 mL gradient, with the sample eluting near 40% elution buffer. Addition of EDTA is essential, as otherwise colored metal-binding impurities co-elute with myrMA and are difficult to remove in the further purification steps. After ion exchange, fractions containing myrMA were dialyzed overnight in hydrophobicity buffer (50 mM NaPO<sub>4</sub>, pH 7.0, 1M (NH<sub>4</sub>)<sub>2</sub>SO<sub>4</sub>, and 5 mM DTT) at 4°C. They were filtered with a 0.22 µm syringe filter and underwent hydrophobicity chromatography using a HiPrep FF

16/10 Butyl column (GE Healthcare). Samples were eluted with buffer lacking any ammonium sulfate using a 200 mL gradient, with samples eluting from the column in a broad peak near 100% elution buffer. Fractions containing myrMA were dialyzed overnight in size exclusion buffer (50 mM NaPO<sub>4</sub>, pH 7.0, 750 mM NaCl, 5 mM DTT) at 4°C, concentrated to less than 5 mL the next morning and filtered through a 0.22 µm syringe filter. Attempts to concentrate without dialyzing the protein in a high salt buffer resulted in precipitation of the protein. myrMA underwent size exclusion chromatography using a HiLoad 26/60 Superdex 75 prep grade column (GE Healthcare), where the sample eluted near 230 mL. Molecular weights and myristoylation efficiency were determined by electrospray ionization mass spectrometry (Molecular Characterization and Analysis Complex, UMBC). Myristoylated MACA<sup>NTD</sup> was expressed and purified in an identical manner. See appendices for construct sequences.

Unmyristoylated matrix [myr(-)MA] was purified using the MA gene inserted into a pET11b vector that was transformed into BL21-DE3-RIL *E. coli* cells (Agilent). Attempts to purify the untagged protein were difficult, so an N-terminal 6XHis tag with a TEV cleavage site was cloned into the protein sequence. TEV cleaves at the sequence E-N-L-W-F-Q-G between the glutamine and glycine. The sequence E-N-L-W-F-Q was inserted before the beginning of the matrix sequence so that upon TEV cleavage the protein would begin with a native glycine. Cells were grown, expressed, and lysed in an identical fashion as myrMA, with the exception that the lysis buffer did not contain EDTA. After PEI precipitation and ammonium sulfate precipitation, the sample pellets were resuspended in lysis buffer and

incubated with 10 mL HisPur Cobalt Resin (Fisher Scientific) for at least 4 hours at 4°C. Samples were eluted with 50 mM imidazole in lysis buffer and dialyzed overnight at 4°C with TEV protease (1 OD<sub>280</sub> TEV protease per 100 OD<sub>280</sub> protein) in TEV cleavage buffer (50 mM Tris, pH 8.0, 100 mM NaCl, 5 mM BME). The plasmid containing TEV protease was ordered from Addgene (pRK793, plasmid # 8827) and purified according to the protocol from the Waugh lab [110]. The following morning, 10 mL HisPur Nickel Resin (Fisher Scientific) was added to the sample and incubated for at least 4 hours. The sample underwent affinity chromatography with collection of the flow through. Resin was eluted with 200 mM imidazole and samples ran on a gel to ensure complete TEV cleavage of matrix. The flow through was dialyzed in cation exchange buffer overnight and underwent cation exchange in a similar protocol as myrMA. (The Q column is not required during purification of myr(-)MA.) Due to the lack of the myristoyl group, the cation exchange fractions were concentrated to 5 mL without dialysis and then applied to the size exclusion column, the last step in the purification.

#### *Preparation of Labeled Protein Samples*

<sup>15</sup>N-labeled samples were purified in an identical fashion as their unlabeled counterparts, but were expressed in minimal media conditions. Cells were grown to OD<sub>600</sub> = 0.6-0.7 in 4 X 1L LB flasks at 37°C, then centrifuged at 8000 rpm at 4°C for 10 minutes to pellet the cells. The cells were resuspended in ~100 mL 1X M9 Salts (47.8 mM NaHPO<sub>4</sub>, 22.0 mM KH<sub>2</sub>PO<sub>4</sub>, 8.6 mM NaCl, pH 7.3) and centrifuged again. The M9 salt wash was poured off and the samples resuspended and transferred to 1L minimal media (47.8 mM NaHPO<sub>4</sub>, 22.0 mM KH<sub>2</sub>PO<sub>4</sub>, pH 7.3, 8.6 mM NaCl, 2 mM

MgSO<sub>4</sub>, 0.1 mM CaCl<sub>2</sub>, 0.1 mM ZnCl<sub>2</sub>, 1X Trace Metals, 0.01% ampicillin, 0.1 mM chloramphenicol, and 10 mL MEM Vitamin Solution (Gibco), 4g glucose, and 1g <sup>15</sup>N-labeled NH<sub>4</sub>Cl per 1L). The cells were placed in the incubator at 30°C for one hour and then induced with 1 mM IPTG. Cells expressed overnight at 30°C and spun down the following morning for lysis and purification.

#### *tRNA Synthesis and Purification*

To form the template, DNA oligonucleotides (IDT Tech) were diluted to 1 mM with RNase-free ddH<sub>2</sub>O. 25 µL of both the forward oligonucleotide (5' strand) and reverse oligonucleotide (3' strand) were diluted with 513 µL annealing buffer (10 mM Tris, pH 7.5, 50 mM NaCl) and 437 µL RNase-free ddH<sub>2</sub>O. Sample was boiled for two minutes and slow-cooled to room temperature. After cooling, the sample was diluted to 5 mL with 4 mL RNase-free ddH<sub>2</sub>O and used in transcription reactions.

tRNAs were synthesized *in vitro* by T7 polymerase. A 30 mL reaction typically contained 12 mL H<sub>2</sub>O, 6 mL DMSO, 3 mL 10X Transcription Buffer (Made in two parts: Part A: 0.13 g spermidine hydrochloride and 0.39 g DTT in 5 mL RNase-free H<sub>2</sub>O, with 50 µL Triton X-100 added after dissolving solid reagents. Part B: Dissolve 2.43 g Tris base into 30 mM RNase-free ddH<sub>2</sub>O, pH to 8.5. Parts A and B were combined and diluted to 50 mL.), 4 mL 150 mM MgCl<sub>2</sub>, and 3 mL of stock NTPs (1 g NTP per 10 mL RNase-free ddH<sub>2</sub>O, pH 8.5) that were added in proportion to the ratios found in the target RNA, 1 mL DNA template, and 1 mL T7 polymerase.

tRNAs were purified using 10% polyacrylamide sequencing gels run overnight, followed by electroelution overnight. Washes with 2M high-purity NaCl removed residual acrylamide, and water washes removed excess ions. After addition

of  $\text{MgCl}_2$  to a concentration of 5 mM, tRNA samples were boiled for 3 minutes and snap-cooled on ice immediately before dialysis overnight in buffers used for experiments. See appendices for construct sequences.

#### *Electrophoretic Mobility Shift Assays (EMSA)*

4  $\mu\text{M}$  tRNA samples were incubated with various molar ratios of myrMA at 37°C for at least 30 minutes in buffer. Immediately after removal from the incubator, 2  $\mu\text{L}$  of 50% glycerol was added per 10  $\mu\text{L}$  sample and loaded onto a 10% 29:1 polyacrylamide Tris-Borate gel. Samples were run for ~30 minutes at 170V and gels stained with a 0.15% Stains-all solution in 60% formamide, and imaged after destaining in water. Some gels had 0.05 mM  $\text{MgCl}_2$  added to the polyacrylamide gels and TB running buffer in order to stabilize the magnesium-dependent complexes during electrophoresis. Concentrations greater than 0.2 mM  $\text{MgCl}_2$  resulted in a high resistance during the run that smeared the sample bands and melted the gels in some cases.

#### *Isothermal Titration Calorimetry*

Protein and tRNA<sup>Lys3</sup> samples were dialyzed overnight in 25 mM Tris, pH 7.0, 140 mM KCl, 10 mM NaCl, 5 mM  $\text{MgCl}_2$ , and 5 mM beta-mercaptoethanol (BME) for characterization studies. Magnesium dependence studies used 25 mM MES buffer, pH 5.5, 5 mM BME, and the noted concentration of  $\text{MgCl}_2$ . Dialysis buffer was filtered and used to dilute RNA and protein samples for ITC. A MicroCal itc200 (GE Healthcare) was used to analyze all samples. Protein samples were diluted to 25  $\mu\text{M}$  and titrated over 20 injections with 2  $\mu\text{L}$  of 400-450  $\mu\text{M}$  tRNA<sup>Lys3</sup> with a stirring

speed of 750 rpm. Averages and standard deviations of three replicate titrations were used to calculate  $K_d$ ,  $\Delta H$ ,  $\Delta S$ , and  $n$ . All samples were compared to wild-type myrMA at pH 7.0 using a Student's t-test.

#### *Analytical Size Exclusion Chromatography*

50  $\mu$ M myrMA samples were incubated with tRNA in 25 mM MES, pH 5.5, 140 mM KCl, 10 mM NaCl, 5 mM  $\text{MgCl}_2$ , and 5 mM BME for at least 45 minutes at 37°C before loading 500  $\mu$ L of sample onto a Superdex 200 10/300 GL column (GE Healthcare). Samples were run at a flow rate of 0.5 mL per minute over 1.2 column volumes.

#### *Nuclear Magnetic Resonance (NMR) Experiments*

For magnesium dependence studies, 1D  $^1\text{H}$ -NMR data were obtained on a 500 MHz Bruker Avance III spectrometer. All data were collected at 35°C using samples containing 50  $\mu$ M tRNA in 25 mM MES buffer, pH 5.5, with 10%  $\text{D}_2\text{O}$ .  $^1\text{H}$ -1D spectra were acquired with 512 transients, 1 sec relaxation delay, 32768 time domain points, and a spectral window of 16233 Hz.

Heteronuclear single quantum coherence (HSQC) experiments were collected on a 600 MHz Bruker Avance III spectrometer equipped with a cryogenic probe. Data was collected at 35°C using samples containing 50  $\mu$ M unmyristoylated matrix. Concentrated tRNA<sup>Lys3</sup> was added directly to the blank sample during titrations. Samples were processed using NvFX and analyzed using NMRViewJ (both from One Moon Scientific).

## Results

### *Initial Characterization of myrMA-tRNA Interactions and Assay Optimization*

The first goal was to create an *in vitro* system to study the interactions of the HIV-1 matrix protein and tRNAs. Of the eight tRNAs that predominately bound to matrix in CLIP studies [69], tRNA<sup>Lys3</sup> was selected due to the extensive literature characterizing the tRNA due to its role as the primer during reverse transcription [11, 12, 70, 72-74, 76, 82, 83, 90, 103, 111]. Electrophoretic mobility shift assays (EMSA) allow quick observation of protein-RNA interactions and require very little sample, making them ideal for optimizing conditions for further characterization experiments. The first experiments used *E. coli* expressed myrMA and T7-transcribed tRNA<sup>Lys3</sup>. Samples were incubated for 1 hour in 50 mM NaPO<sub>4</sub>, pH 6.5, 5 mM DTT and run on a 10% TB native gel to observe myrMA-tRNA interactions (Figure 2.1a). Multiple bands were observed in the lane containing tRNA<sup>Lys3</sup> in the absence of protein, indicating multiple conformations of the tRNA. Buffer optimization began to determine if the issue was due to the sample or the assay conditions. Tris buffer replaced NaPO<sub>4</sub>, as NaPO<sub>4</sub> had interfered with RNA samples previously in the lab. Samples were incubated for 30 minutes or an hour in 50 mM Tris, pH 6.5, 5 mM DTT buffer to try to eliminate the second band and determine a time dependence of the interaction (Figure 2.1b). Samples with higher concentrations of myrMA had smearing indicating nonspecific binding between the negatively charged tRNA and positively charged protein. In the event that the destabilization of the RNA was pH-dependent, the samples were run again incubating in Tris buffers at pH 5.5 and 7.5 (Figure 2.1c,d, respectively). Running the tRNA<sup>Lys3</sup> sample on a denaturing gel

produced one band, indicating that the results were not from degradation of the RNA, and the second band was due to RNA-RNA interactions or multiple conformers (Figure 2.1e).

In order to explain the apparent lack of specific binding, modified tRNAs were used to determine if they behaved differently from tRNAs transcribed *in vitro* using T7 polymerase. tRNAs have multiple modifications (Figure 2a) [76], which stabilize the tertiary structure of the RNA [73, 76, 112]. Unfortunately, it is difficult to obtain specific mammalian tRNAs, as they can only be purified in small quantities from bovine liver [113]. Yeast tRNAs are available commercially, but at the time they could only be obtained as a mixture instead of a single isoform. *E. coli* tRNA<sup>Lys</sup> (Figure 2.2b) was available, and was purchased from two vendors (MP Biomedicals and Sigma Aldrich). Human tRNA<sup>Lys3</sup> and *E. coli* tRNA<sup>Lys</sup> have different sequences, but both adopt the L-shape associated with most tRNAs and use the anticodon UUU during translation [76, 114]. Additionally, the main sequence differences are in four stems, which are base-paired and less likely to be involved in protein interactions. The D-loop and stem, which was implicated in matrix binding in the CLIP studies [69], only has one nucleic acid difference between tRNA<sup>Lys3</sup> and tRNA<sup>Lys</sup>. The variable loop, which interacts with the D-loop and T-loop in the tertiary structure of the tRNAs, was also very similar between the two tRNAs. EMSA assays using the modified *E. coli* tRNA<sup>Lys</sup> showed band shifts indicative of specific binding, while samples using the T7-transcribed tRNA<sup>Lys3</sup> did not (Figure 2.2c). This led to the initial conclusion that the modifications were essential for tRNA-myRNA interactions.

Continuing experiments with modified *E. coli* tRNA<sup>Lys</sup> was problematic due to the expense and difficulties obtaining the RNA, as suppliers had stopped stocking the RNA temporarily. If the tRNA modifications do not play a role, an alternate explanation is that the modifications were stabilizing the tRNA, allowing it to adopt the structure necessary to specifically interact with myrMA. Puglisi *et al.* specifically pointed to magnesium as the divalent cation required for T7-transcribed RNA to adopt the correct conformation, suggesting that 5-10 mM Mg<sup>2+</sup> was needed to initiate correct folding [73]. Another way to stabilize RNA is by the addition of salts [115], so future experiments added physiological-like (PI) concentrations of salts and 5 mM MgCl<sub>2</sub> to the samples (PI salts: 140 mM KCl, 10 mM NaCl, 5 mM MgCl<sub>2</sub>). Addition of PI salts did not allow specific bands to form in samples using the unmodified tRNA, however boiling and snap-cooling unmodified tRNA<sup>Lys3</sup> in buffer resulted in a decrease of the higher order band in the tRNA sample (Figure 2.3a).

As magnesium is positively charged, the ion migrates in a different direction as the RNA-protein complex. This could deplete the local concentration of the ion in the gel, leading to RNA destabilization and loss of complex binding. Addition of magnesium to the running buffer has helped stabilize magnesium-dependent complexes [116], and was the next condition tested. Upon the addition of 0.05 mM MgCl<sub>2</sub> to the running buffer, as well as addition of 5 mM MgCl<sub>2</sub> to the incubation buffer for the complex, specific bands similar to those seen with modified *E. coli* tRNA were seen (Figure 2.3b), indicating that the modifications are not required for myrMA-tRNA<sup>Lys3</sup> interactions, and that adequate folding of the tRNA is sufficient to observe specific binding.

In order to continue further characterize the interaction between myrMA and tRNA<sup>Lys3</sup>, the minimum amount of magnesium required for tRNA to correctly fold needed to be determined. T7-transcribed tRNA<sup>GlyGCC</sup> was used in addition to tRNA<sup>Lys3</sup> for this process, as it bound the most frequently to matrix in CLIP studies [69]. In order to monitor binding, <sup>1</sup>H-1D NMR was utilized to measure signals in the 12 to 15 ppm range for the RNAs at different magnesium concentrations. This is the imino region, which is an indicator of base pairing in the RNA. As hydrogen bonding occurs between the base pair, imino groups form between the nucleotide bases, leading to an increase in signal. With no magnesium present, both tRNA<sup>Lys3</sup> and tRNA<sup>GlyGCC</sup> show very little signal in the imino region (Figure 4). Addition of 3 mM MgCl<sub>2</sub> shows an increase in signal for both RNAs, with a further increase in signal after increasing MgCl<sub>2</sub> to a concentration of 5 mM. Boiling and snap-cooling RNA can help it adopt a uniform conformation, as the boiling process denatures the RNA, allowing it to refold during the cooling process. Boiling and snap-cooling tRNA<sup>GlyGCC</sup> resulted in a dramatic change in the imino region, implying that magnesium alone is not enough to allow the RNA to form the correct conformation. Boiling and snap cooling tRNA<sup>Lys3</sup> resulted in a slight change to the imino region, but not a large difference as seen with tRNA<sup>GlyGCC</sup>.

After titrating the tRNAs with magnesium, isothermal titration calorimetry (ITC) was used to quantify the binding between the tRNAs and matrix. These experiments were done primarily to optimize the conditions used for NMR experiments to study the complex, as described in detail in the following section, and were only run once per condition. In the absence of magnesium, both tRNA<sup>Lys3</sup> and

tRNA<sup>GlyGCC</sup> bound to myrMA in a primarily endothermic reaction (Figure 2.5a). EMSA experiments using the ITC samples showed smearing at higher myrMA:tRNA ratios instead of specific band shifts, indicating that the reaction observed through ITC was most likely a nonspecific interaction between the positive protein and the negative RNAs (Figure 2.5b,c). This is consistent with the hypothesis that the tRNAs need magnesium to assume the correct fold, which is essential for specific myrMA-tRNA interactions. The addition of 2.5 mM MgCl<sub>2</sub> resulted in a curve for an exothermic reaction, with a  $K_d$  of  $1.79 \pm 0.30$   $\mu$ M for tRNA<sup>Lys3</sup> and  $2.46 \pm 0.32$   $\mu$ M for tRNA<sup>GlyGCC</sup> (Figure 2.5d). Increasing the concentration to 5 mM MgCl<sub>2</sub> strengthened the interaction, with a  $K_d$  of  $0.227 \pm 0.023$   $\mu$ M for tRNA<sup>Lys3</sup> and  $1.07 \pm 0.13$   $\mu$ M for tRNA<sup>GlyGCC</sup> (Figure 2.5e). In both cases, tRNA<sup>Lys3</sup> bound much more strongly than tRNA<sup>GlyGCC</sup>, making it the best choice for future experiments. Additionally, EMSA analysis indicated that T7-transcribed tRNA<sup>GlyGCC</sup> formed multiple conformations even with 5 mM MgCl<sub>2</sub>, precluding it from use in future NMR experiments (Figure 2.5f,g).

#### *Characterization of Matrix Interactions with tRNA<sup>Lys3</sup>*

After optimization of interaction conditions, heteronuclear single quantum coherence (HSQC) experiments were utilized to determine the binding region on matrix (Fig. 2.6a). Experiments using myristoylated matrix and tRNA<sup>Lys3</sup> resulted in peak broadening due to an intermediate exchange regime. Isothermal titration calorimetry (ITC) experiments indicated that myrMA and an unmyristoylated mutant [myr(-)MA] had similar binding profiles at pH 7.0, indicating similar binding sites when the myristoyl group is fully sequestered (see Chapter 3). By lowering the pH

and using myr(-)MA, the RNA-protein interaction shifted into slow exchange. Removing the PI salts so that the protein was in 25 mM MES, pH 5.5, 5 mM MgCl<sub>2</sub>, and 5 mM BME yielded the best results. Residues affected by tRNA<sup>Lys3</sup> binding are near or in the basic patch of the molecule (Figure 2.6b), indicating that tRNA may compete for a similar binding site as PI(4,5)P<sub>2</sub>. In particular, residues K26, K30 and K32 shift upon binding to tRNA<sup>Lys3</sup>. These residues play a known role in targeting myrMA to the plasma membrane for viral assembly [36, 52-56]. Other residues affected by tRNA binding included another basic residue in the HBR, R22. Residues near the N-termini of helices II and V and the C-terminal of helix I also shifted upon addition of tRNA. These residues are near the basic patch of myrMA, indicating that tRNA is specifically binding in that area of the molecule. Residues near the N-terminus of helix V also bound to a 15mer RNA oligonucleotide that contained a matrix-specific binding sequence determined by SELEX [63]. That study also found evidence of binding in and near the basic patch with residues E28 and H33 [63], and while those particular residues did not shift in this experiment, nearby residues K30, L31, K32 did.

ITC was used to characterize the thermodynamics of the interaction between tRNA<sup>Lys3</sup> and HIV-1 matrix (Fig. 2.7a). The two molecules interact in a 1:1 molar ratio ( $n = 0.89 \pm 0.06$ ). myrMA and tRNA<sup>Lys3</sup> bound with a  $K_d$  of  $0.63 \pm 0.03 \mu\text{M}$  at pH 7.0 in a primarily enthalpy-driven reaction at 30°C ( $\Delta H = -5.9 \pm 0.4 \text{ kcal/mol}$ ,  $\Delta S = 8.9 \pm 1.3 \text{ cal/mol/deg}$ ), consistent with electrostatic interactions between the positively charged basic region on the myrMA protein and the negatively charged tRNA<sup>Lys3</sup> molecule.

In order to confirm the stoichiometry of the reaction, size exclusion chromatography was used to observe formation of the complex (Figure 2.7b). Both the myrMA protein and tRNA<sup>Lys3</sup> ran as single peaks. As tRNA<sup>Lys3</sup> was added to myrMA, the peak associated with myrMA decreased and a peak at a higher molecular weight appeared. The elution volume of the higher molecular weight peak corresponded with a 40 kDa complex, which is consistent with a 1:1 binding ratio. After saturation at a 1:1 tRNA:myrMA molar ratio, the complex peak did not increase in size, while the peak corresponding to the free RNA increases in area. This indicated that multiple RNAs did not bind to the protein, but remained as free tRNA after 1:1 saturation.

#### *Characterization of Matrix Interactions with Multiple tRNAs to Determine Specificity*

myrMA's ability to interact with different tRNAs was studied in order to determine specificity of the interaction. Although tRNA<sup>GlyGCC</sup> was studied during the magnesium determinations, it was not a good candidate due to the multiple conformations the T7-transcribed tRNA takes *in vitro*. tRNA<sup>IleGAU</sup> did not show any specific binding to matrix in CLIP studies [69], and was thus chosen as a control for a non-specific binder for myrMA. A single band formed in native TBM gels, suggesting that unmodified tRNA<sup>IleGAU</sup> adopts one conformation in the presence of magnesium (Figure 1.8a). A faint band formed during EMSA analysis indicative of binding between tRNA<sup>IleGAU</sup> and myrMA, but at higher concentrations of myrMA the bands became smears indicative of non-specific interactions instead of the stronger bands associated with specific interactions between tRNA<sup>Lys3</sup> and myrMA (Figure 1.8b). ITC experiments concluded that myrMA and tRNA<sup>IleGAU</sup> bound with a  $K_d$  of

$3.41 \pm 0.17 \mu\text{M}$  at pH 7.0 in a primarily enthalpy-driven reaction at  $30^\circ\text{C}$  ( $\Delta H = -9.48 \pm 0.28 \text{ kcal/mol}$ ,  $\Delta S = -6.3 \pm 0.8 \text{ cal/mol/deg}$ ) (Figure 1.8c). The reaction was approximately 5-fold weaker than the interaction with  $\text{tRNA}^{\text{Lys3}}$  ( $K_d = 0.63 \pm 0.03 \mu\text{M}$ ,  $p < 0.001$ ). Additionally, the reaction had a negative entropy value, unlike  $\text{tRNA}^{\text{Lys3}}$ 's positive value ( $p < 0.001$ ). Interestingly,  $\text{tRNA}^{\text{Lys3}}$  had a different stoichiometry of the reaction, with an  $n$  value of  $0.58 \pm 0.06$  ( $\text{tRNA}^{\text{Lys3}} = 0.89 \pm 0.06$ ,  $p = 0.003$ ). This could be due to multiple reasons. Calculation of extinction coefficients is difficult for RNAs, and it is possible that the extinction coefficient was slightly off. It is also possible that myrMA binds less specifically to  $\text{tRNA}^{\text{IleGAU}}$ , resulting in multiple binding events that are averaged together by the ITC. Based on the information from the ITC data, it appears that myrMA will bind specifically to  $\text{tRNA}^{\text{Lys3}}$ , but will also bind non-specifically to other RNAs in the absence of  $\text{tRNA}^{\text{Lys3}}$ .

#### *Characterization of Matrix-Capsid Interactions with $\text{tRNA}^{\text{Lys3}}$*

While most of the work in this dissertation uses the matrix domain alone due to the ease of purification and size limits of the NMR, the matrix domain is part of a polyprotein with multiple domains. Matrix only exists separate from the Gag polyprotein after maturation, when the capsid domain is cleaved from the matrix domain by protease [1, 8]. EMSA with the myristoylated matrix domain connected to the N-terminal domain of the capsid protein ( $\text{myrMACA}^{\text{NTD}}$ ) incubated with  $\text{tRNA}^{\text{Lys3}}$  had band shifts similar to that seen for myrMA domain alone (Figure 2.9a,b).

ITC was used to determine if the addition of the capsid domain on the myristoylated protein (myrMACA<sup>NTD</sup>) affected matrix's ability to bind to RNAs (Figure 2.9c). The interaction between myrMACA<sup>NTD</sup> had a  $K_d$  of  $0.75 \pm 0.02 \mu\text{M}$ , compared with myrMA's  $K_d$  of  $0.63 \pm 0.03 \mu\text{M}$  ( $p = 0.0034$ ), indicating that the addition of the capsid domain slightly weakens the interaction between myrMA and tRNA<sup>Lys3</sup>. The reason for this decrease in affinity was a decrease in enthalpy (myrMA:  $\Delta H = -5.9 \pm 0.4 \text{ kcal/mol}$ ; myrMACA<sup>NTD</sup>:  $\Delta H = -4.7 \pm 0.3 \text{ kcal/mol}$ ;  $p = 0.010$ ), which was slightly offset by an increase in entropy (myrMA:  $\Delta S = 8.9 \pm 1.3 \text{ kcal/mol/degree}$ ; myrMACA<sup>NTD</sup>:  $\Delta S = 12.5 \pm 0.8 \text{ kcal/mol}$ ;  $p = 0.016$ ). While there is a significant difference between the two proteins, the differences are slight compared to the effects of mutating basic patch residues (See Chapter 3). The largest effect was on the stoichiometry of the reaction, which decreased from  $0.89 \pm 0.06$  for myrMA to  $0.70 \pm 0.04$  for myrMACA<sup>NTD</sup>. While gels indicate the formation of a single complex (Figure 2.9a), the difference between the gel and the ITC data could come from multiple sources. The capsid domain is capable of self-association, which could affect the interactions between myrMA and tRNA<sup>Lys3</sup>. In solution, myrMACA<sup>NTD</sup> exists in equilibrium between a monomeric and multimeric forms. This multimerization could promote myristoyl exposure, which affects myrMA-tRNA interactions (See Chapter 3). Additionally, the act of multimerization itself could also preclude tRNA<sup>Lys3</sup> from binding due to steric hindrance, and the stoichiometry lowers as a result of the percentage of myrMACA<sup>NTD</sup> in the multimer conformation. Due to the inability of the ITC to determine which of these possible causes affected the binding of

myrMACA<sup>NTD</sup> to tRNA<sup>Lys3</sup>, future studies used the matrix domain alone to characterize the interaction between myrMA and tRNAs.

#### *Common Characteristics of tRNAs that Bind to Matrix*

The CLIP studies indicated that eight cellular tRNAs bound to matrix in cells, and indicated that binding occurred in the first 35 residues on tRNA<sup>Lys3</sup> and tRNA<sup>GlyGCC</sup>, which correspond to the 5' end of the acceptor stem and the D-loop and stem [69]. The D-loop of the tRNAs also had the highest rate of T-to-C conversions during the CLIP process, again suggesting that matrix may bind to this part of the tRNAs [69]. The D-loop of tRNA<sup>Lys3</sup> and *E. coli* tRNA<sup>Lys</sup> have nearly identical structures, as the only difference is that cytosine 17 in tRNA<sup>Lys3</sup> is replaced by deoxyuracil in *E. coli* tRNA<sup>Lys</sup> (Figure 2.2a,b). The two tRNAs have fairly similar sequences overall, with the main differences occurring in the base-paired stem loops. The CLIP studies mapped the sequence hits to the hg19 human genome to determine which RNAs bound to matrix [69]. The tRNA sequences incorporated into the hg19 genome can be accessed separately through the GtRNAdb database [117]. These sequences were deposited through various methods, including sequencing of the tRNAs themselves, but primarily through sequence analysis for sequences that appear to have a tRNA-like fold using the tool tRNAscan-SE [117]. I looked through the sequences in the GtRNAdb to determine if tRNA<sup>Lys3</sup> and the other tRNAs that bound to myrMA had a sequence similarity to each other that made them different from the other sequences. As of August 2017, the database had 610 tRNA sequences deposited, with 597 of them coding for standard amino acids. tRNA<sup>Lys3</sup> had 20 sequences associated with it in the database, as well as 24 tRNAs associated with the

CUU anticodon, as each cell has multiple copies of the tRNA genes in different chromosomes. All of the eight tRNAs observed to bind to matrix in the CLIP studies had similar D-loops (Figure 2.10). If there were differences in the loop, the differences were only by a single nucleotide, except for the case of tRNA<sup>GluUUC</sup>, which differed by two. The 5' end of the acceptor stem had more variation between the eight tRNAs, as did the anticodon stems and loops. However, other tRNAs, including ones that code for alanine, aspartate, cysteine, histidine, proline, serine, and threonine, also have similar D-loop sequences, suggesting that the tRNA-matrix interaction cannot be due to the sequence of the D-loop alone.

### *Discussion*

The aim of this work was to characterize *in vitro* the interaction seen between tRNA<sup>Lys3</sup> and the matrix domain in CLIP studies [69]. The first step required the creation of a model system in which to study the interaction. Due to issues with acquiring native mammalian, modified tRNA<sup>Lys3</sup>, early experiments determined whether alternatives could serve as substitutes. Experiments with *E. coli* tRNA<sup>Lys</sup> indicated that it could interact specifically with myrMA, but it was difficult to reliably purchase the quantities that would be necessary for future NMR and ITC experiments. Much literature exists about the structure of tRNA<sup>Lys3</sup>, as the tRNA serves as the primer during reverse transcription and is packaged into new virions [73, 74, 76]. Using NMR experiments, Puglisi *et al.* determined that modifications in the structure are necessary for correct folding of the tRNA [73]. However, they found that adding 5 to 10 mM magnesium to their unmodified samples produced spectra

similar to the modified tRNAs, suggesting that magnesium alone could allow the unmodified samples to fold correctly [74].

EMSAs comparing the myrMA-tRNA interaction using modified *E. coli* tRNA<sup>Lys</sup> versus T7-transcribed tRNA<sup>Lys3</sup> with 5 mM MgCl<sub>2</sub> indicate a similar binding profile for both RNAs, although magnesium must be added to the gel and running buffer to prevent the electric current from stripping the magnesium from the complex during electrophoresis. <sup>1</sup>H-1D NMR studies indicated that 5 mM MgCl<sub>2</sub> was sufficient to induce tRNA<sup>Lys3</sup> folding, defining one of the conditions for all subsequent experiments.

Initial characterization of the interaction indicated that tRNA<sup>Lys3</sup> binds moderately strongly to myrMA, with a  $K_d$  of  $0.63 \pm 0.03$   $\mu$ M at pH 7.0 in a 1:1 ratio. This stoichiometry was further supported by size exclusion experiments. The reaction is primarily driven by the enthalpy of the reaction, indicating that the interaction relies primarily on electrostatic interactions. This is consistent with the idea that tRNA<sup>Lys3</sup> relies on myrMA's basic patch for binding to the negative RNA [56, 69]. The hypothesis that tRNA<sup>Lys3</sup> binds to the basic patch is further supported by the HSQC titration of myrMA with tRNA<sup>Lys3</sup>, as residues that shifted upon binding are located near or in the basic patch. The interaction is not greatly affected by the addition of the N-terminal domain of capsid, as the myrMACA<sup>NTD</sup> protein had only slightly weaker affinity for tRNA than myrMA.

However, this myrMA-tRNA interaction cannot rely on charge alone, as tRNA<sup>IleGAU</sup>, a tRNA of similar size and charge [117], bound five-fold more weakly to myrMA than tRNA<sup>Lys3</sup>. There is likely some structural component of tRNA<sup>Lys3</sup> that

makes it and other tRNAs bind more tightly to matrix. While the CLIP data indicated that the structural element most likely lies in the first half of the tRNAs [69], sequence alignment of tRNAs deposited in the gtRNAdb [117] did not yield a good predictor of what that element may be. While the eight tRNAs that bound during the CLIP studies have a similar sequence in the D-loop, that sequence is fairly common among many other tRNA isoacceptors. tRNA<sup>ValUAC</sup> and tRNA<sup>GlyUCC</sup>, which do not bind well to matrix [69], have identical D-loop sequences as the other valine and glycine sequences that bind to matrix. While there are differences between these two sequences and the other isoforms of valine and glycine tRNAs, the differences occur in the stems and other regions that varied among the eight binding tRNAs.

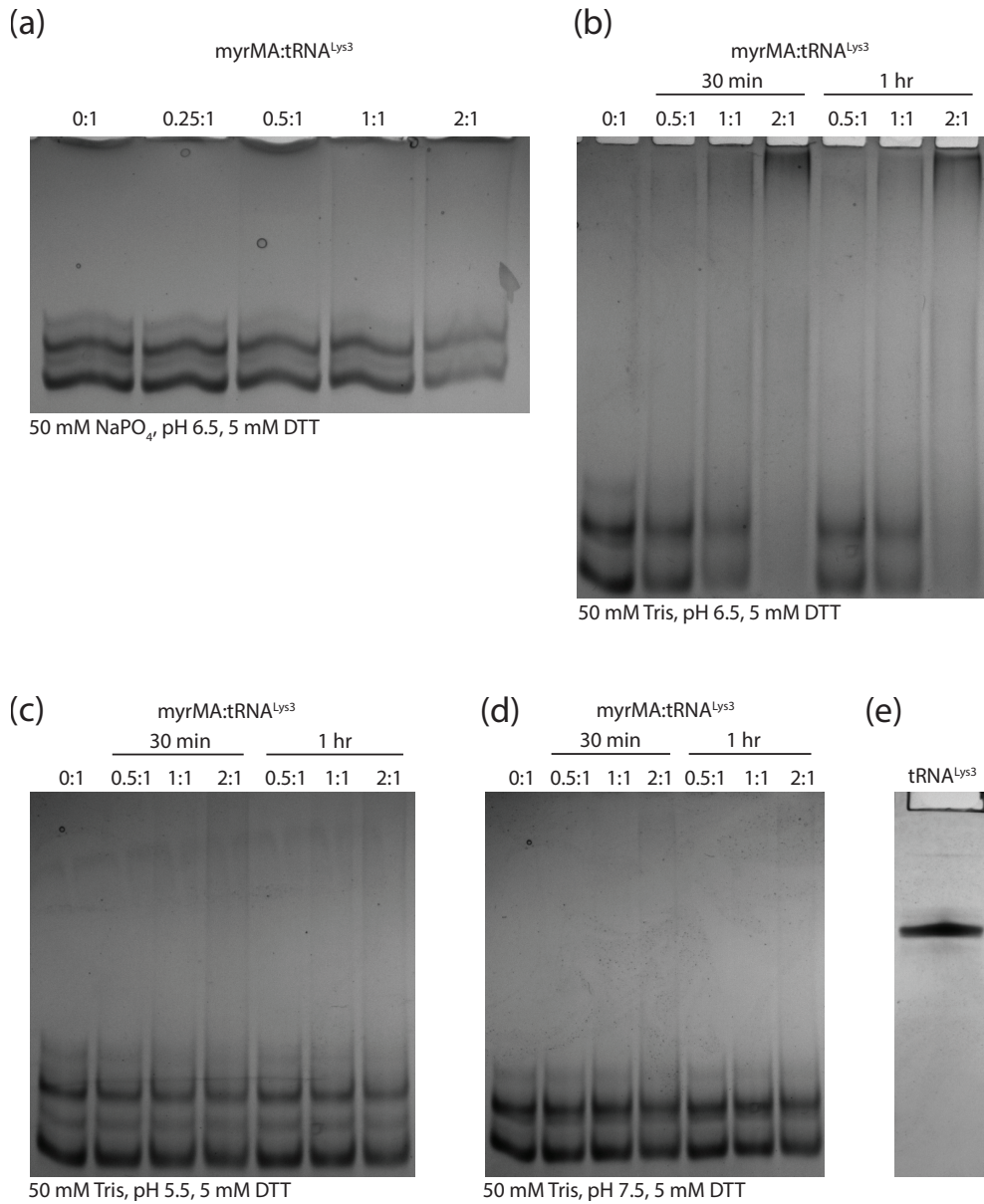


**Figure 2.1: EMSA of T7-transcribed tRNA<sup>Lys3</sup> and myrMA.** (a) Initial EMSA experiments with tRNA<sup>Lys3</sup> and myrMA did not show a band shift indicative of protein-RNA binding, but did have multiple bands due to multiple RNA conformations. (b) Multiple conformations were not due to the presence of the phosphate ion, as samples using Tris also had multiple bands, as well as aggregation at higher molar ratios of protein:RNA. The results were not pH-dependent, as similar results occurred at pH 5.5 (c) and pH 7.5 (d). Multiple bands were due to multiple RNA conformations, as tRNA<sup>Lys3</sup> ran as one band on a denaturing gel.



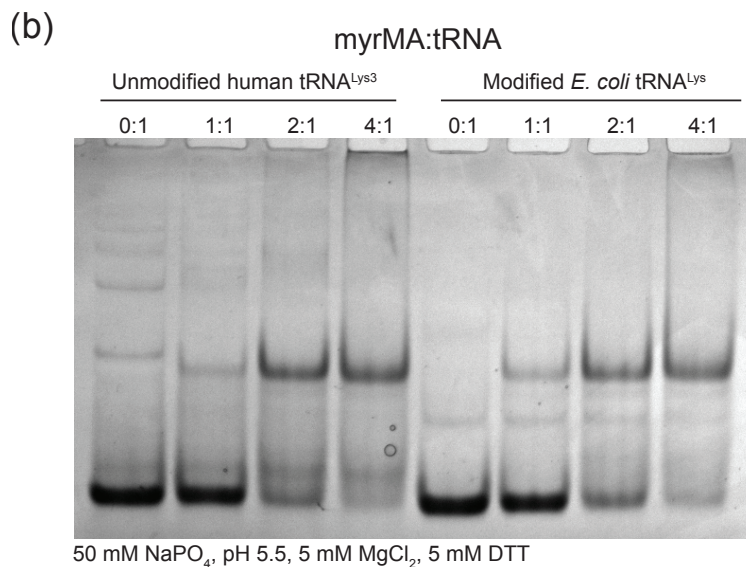
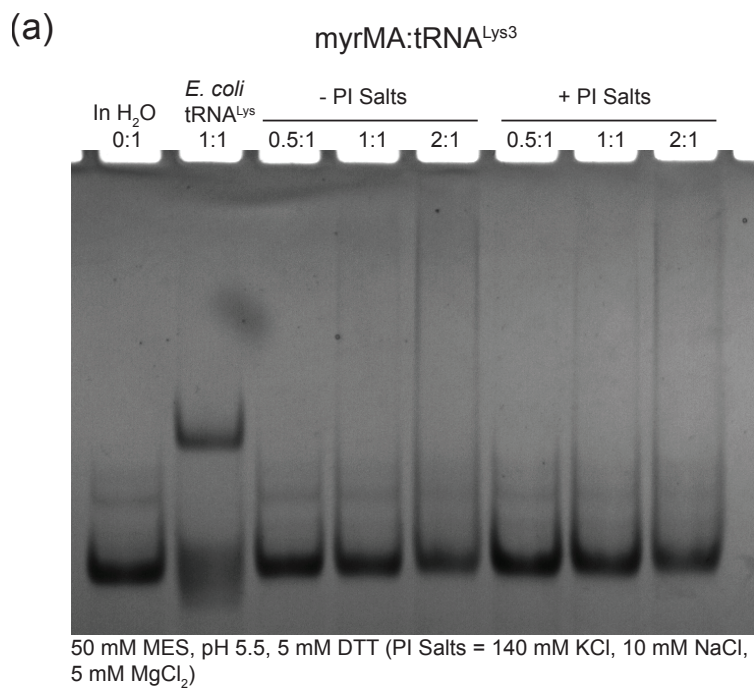


**Figure 2.3: Role of magnesium on tRNA<sup>Lys</sup>-myrMA interactions.** (a) The addition of PI salts (140 mM KCl, 10 mM NaCl, 5 mM MgCl<sub>2</sub>) was not sufficient to visualize myrMA-tRNA<sup>Lys3</sup> interactions through EMSA. (b) Addition of 0.05 mM MgCl<sub>2</sub> to the Tris-borate gel and running buffer was sufficient to induce tRNA folding, allowing T7-transcribed tRNA<sup>Lys3</sup> to specifically bind myrMA similarly to modified *E. coli* tRNA<sup>Lys</sup>.

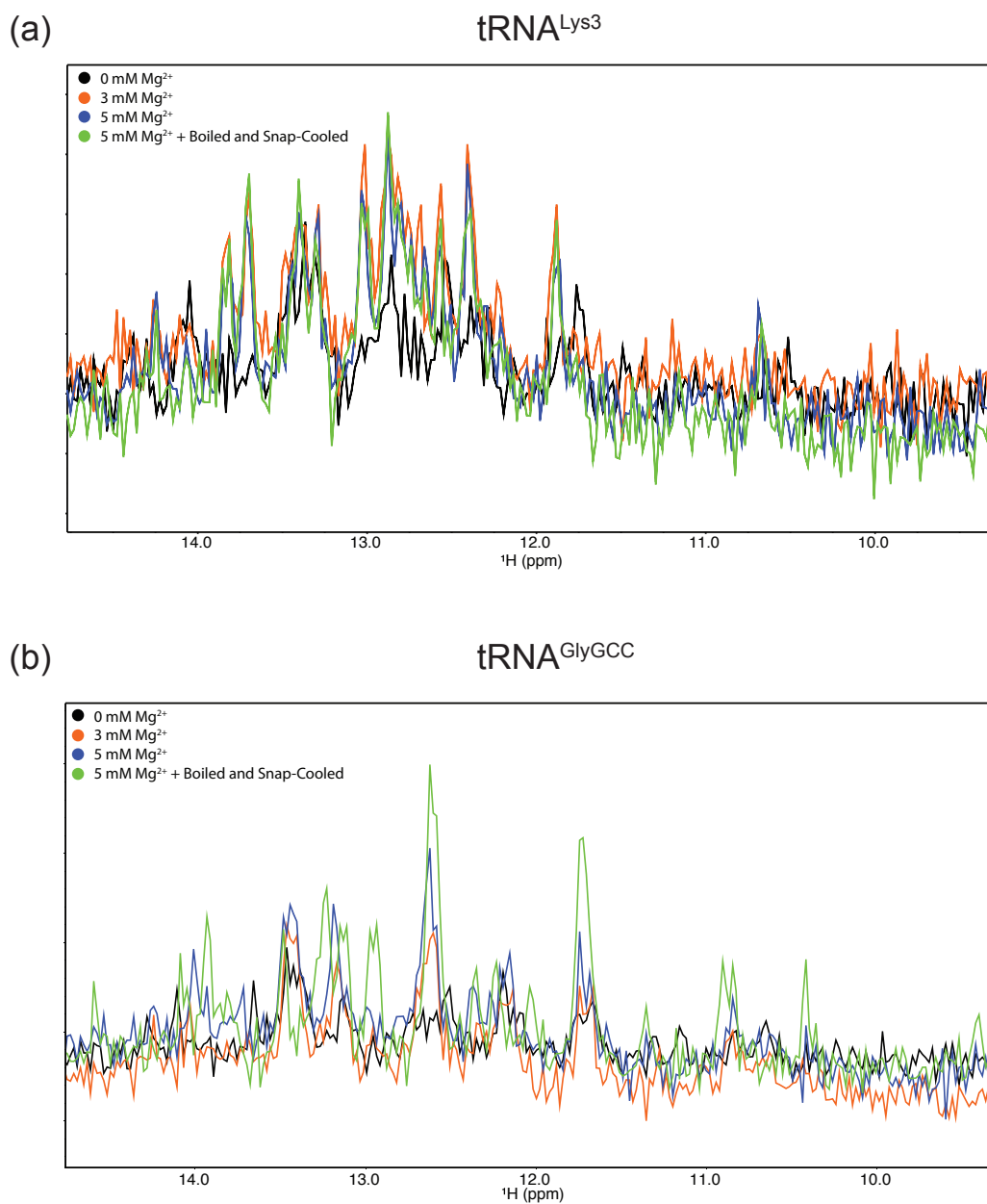


**Figure 2.4: Magnesium dependence of RNA folding.** (a) The addition of  $\text{MgCl}_2$  to  $\text{tRNA}^{\text{Lys3}}$  led to increased signal in the imino region of the 1D spectra, indicating increased base pairing. (b) Addition of  $\text{MgCl}_2$  also led to increased base pairing for  $\text{tRNA}^{\text{GlyGCC}}$ , with the process of boiling and snap-cooling dramatically affecting the fold of the tRNA.

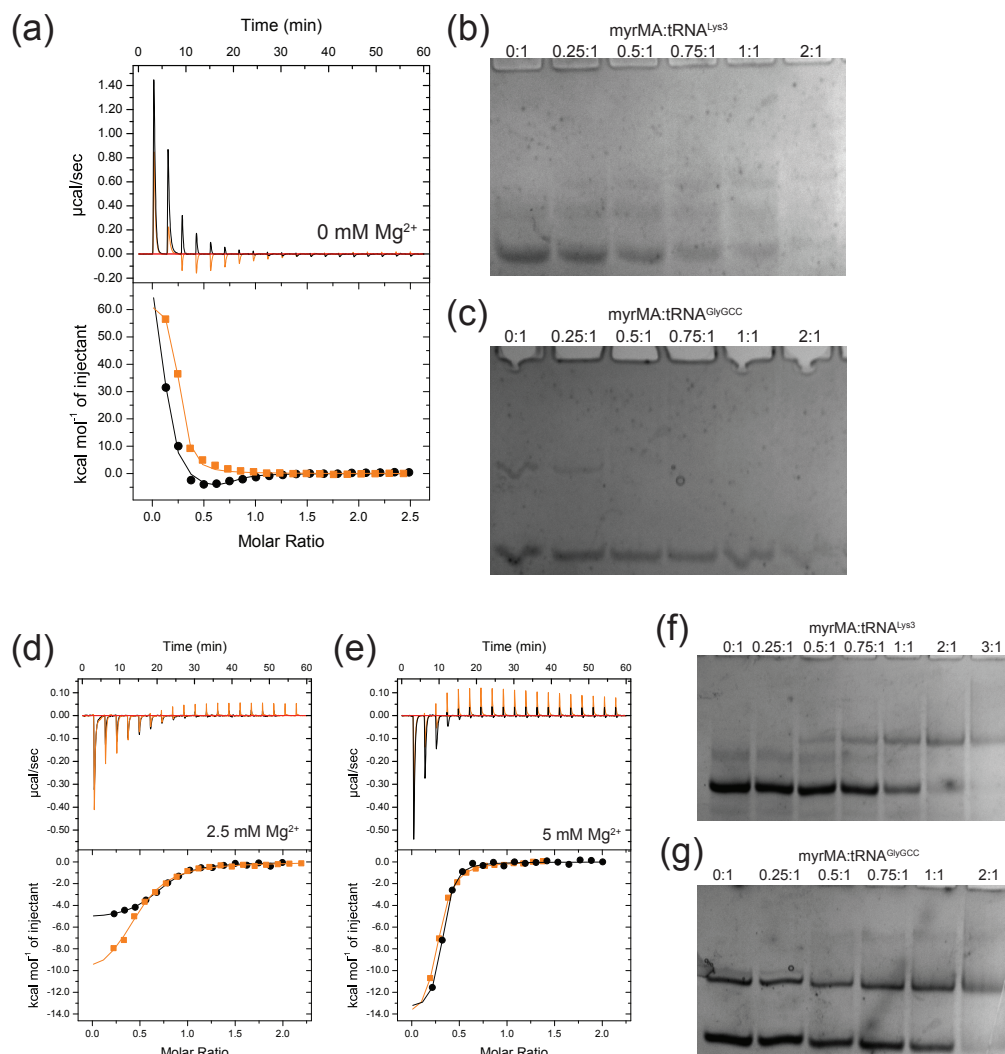


**Figure 2.5: Magnesium dependence of tRNA interactions with myrMA.** (a) Binding of myrMA to tRNA<sup>Lys3</sup> (black) and tRNA<sup>GlyGCC</sup> (orange) in the absence of magnesium results in an endothermic reaction atypical for myrMA-tRNA interactions. EMSA of the interaction with tRNA<sup>Lys3</sup> (b) and tRNA<sup>GlyGCC</sup> (c) in the absence of magnesium results in smearing indicative of nonspecific interactions. Titration of myrMA with tRNA<sup>Lys3</sup> (black) and tRNA<sup>GlyGCC</sup> (orange) in the presence of 2.5 mM MgCl<sub>2</sub> (d) and 5.0 mM MgCl<sub>2</sub> (e) results in specific binding, with tRNA<sup>Lys3</sup> binding more tightly than tRNA<sup>GlyGCC</sup> for each condition and samples with 5 mM MgCl<sub>2</sub> binding more tightly than those with 2.5 mM MgCl<sub>2</sub>. EMSA analysis of the samples with 2.5 mM MgCl<sub>2</sub> indicate that tRNA<sup>Lys3</sup> primarily takes on one conformation (f), while tRNA<sup>GlyGCC</sup> has two (g).

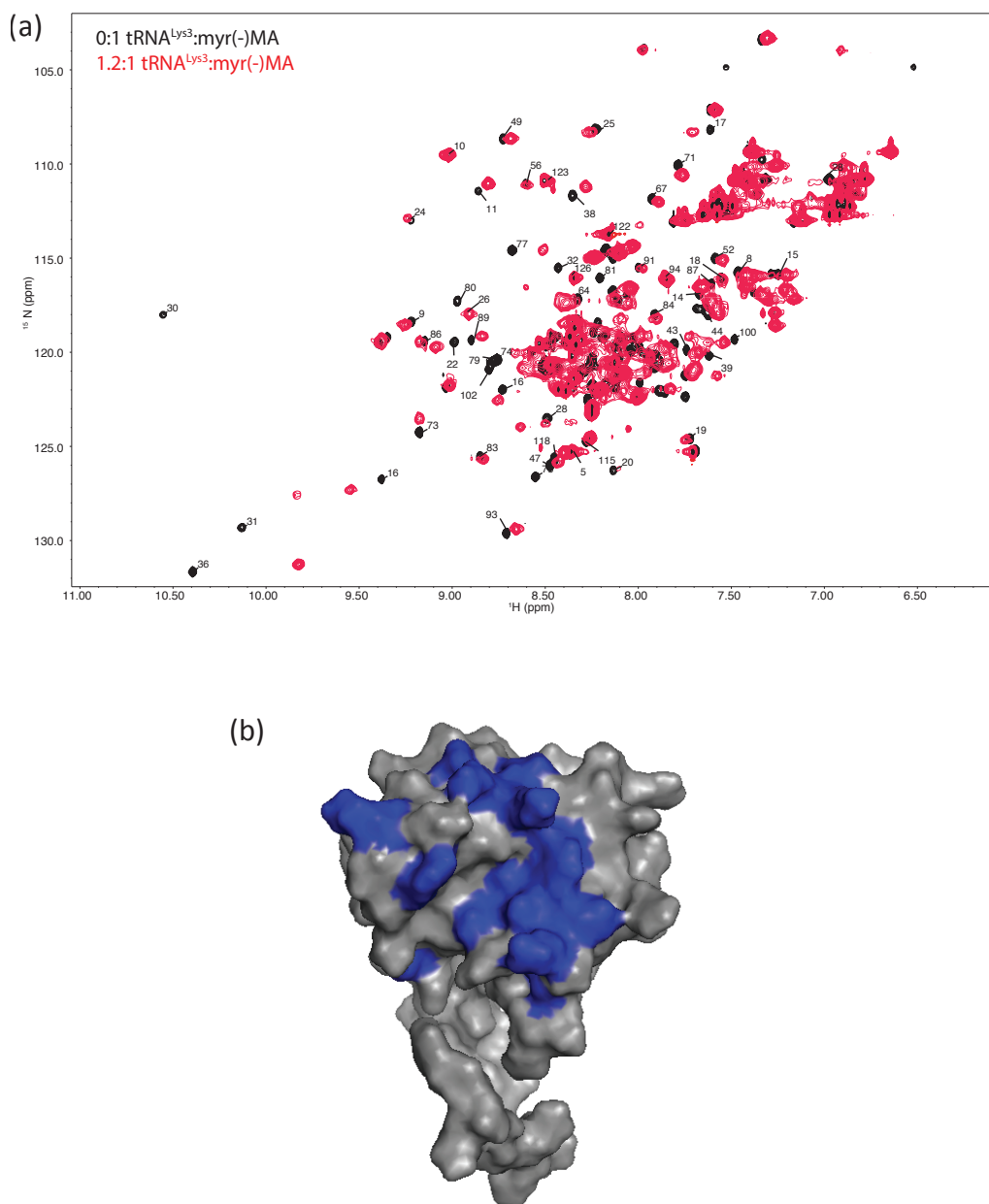


**Figure 2.6: tRNA<sup>Lys3</sup> binds near MA's basic patch.** (a) HSQC of unmyristoylated matrix (black) and the peak shifts that occur upon titration with tRNA<sup>Lys3</sup> (red). (b) Mapping the residues that shifted upon addition of tRNA indicate that binding occurs near the basic patch. Figure generated from PDB entry 2H3F with PyMOL.

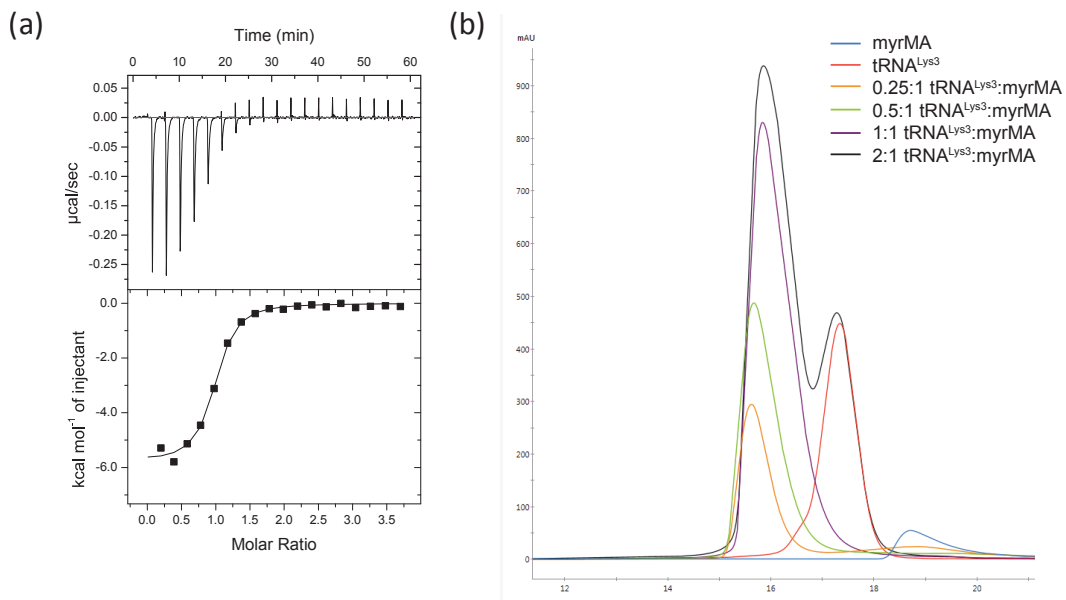


**Figure 2.7: tRNA<sup>Lys3</sup> binds in a 1:1 molar ratio to myrMA.** (a) ITC indicates that myrMA binds to tRNA<sup>Lys3</sup> in a 1:1 molar ratio with a  $K_d$  of  $0.63 \pm 0.03 \mu\text{M}$ . (b) SEC experiments show formation of a 1:1 complex of myrMA with tRNA<sup>Lys3</sup>.

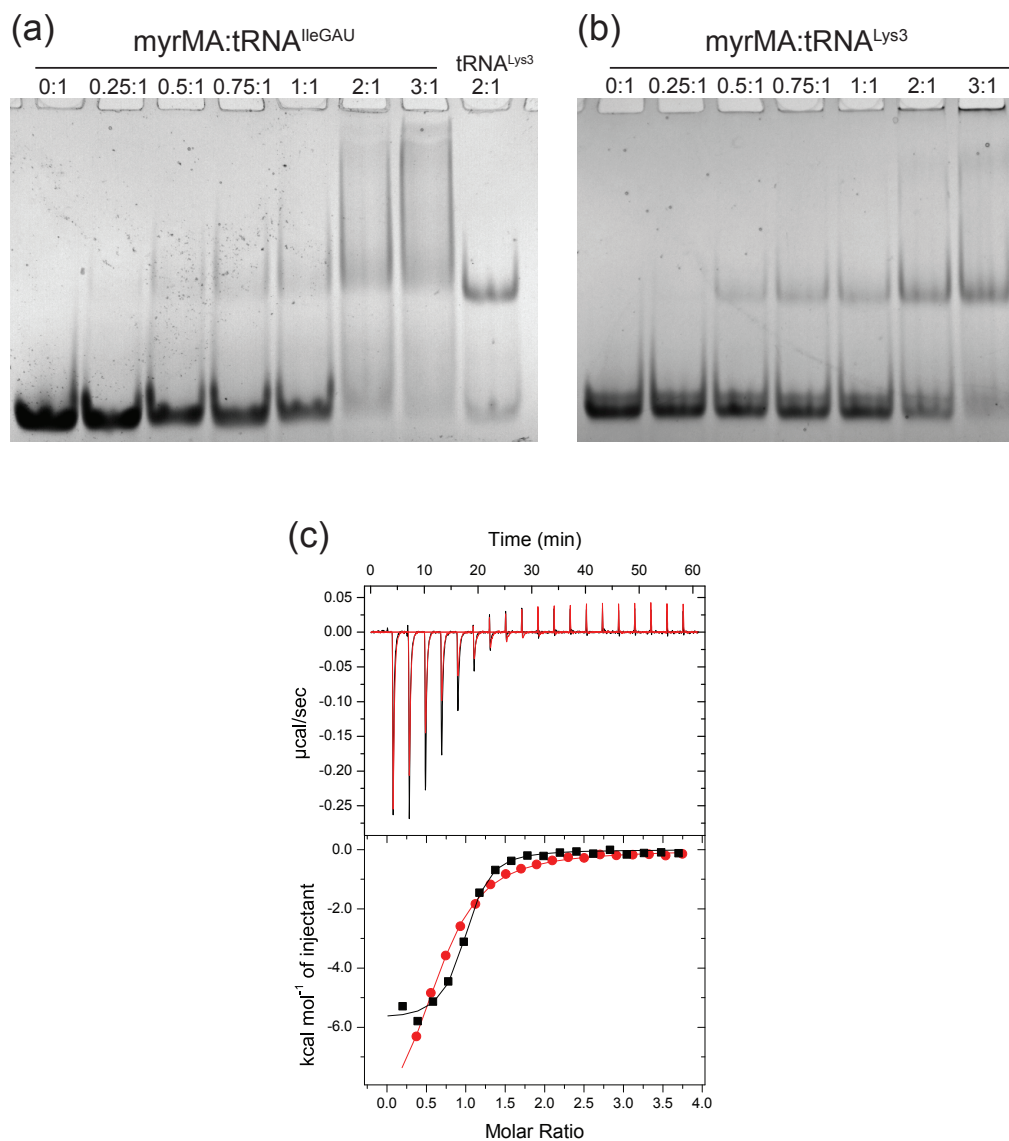


**Figure 2.8: myrMA binds specifically to tRNA<sup>Lys3</sup>.** (a) EMSA gel indicating that tRNA<sup>IleGAU</sup> forms a complex with myrMA, but not as strongly as tRNA<sup>Lys3</sup> (b), which forms a band indicative of a specific interaction instead of the smearing associated with tRNA<sup>IleGAU</sup>. (c) ITC curve of myrMA interacting with tRNA<sup>Lys3</sup> (black) and tRNA<sup>IleGAU</sup> (red).

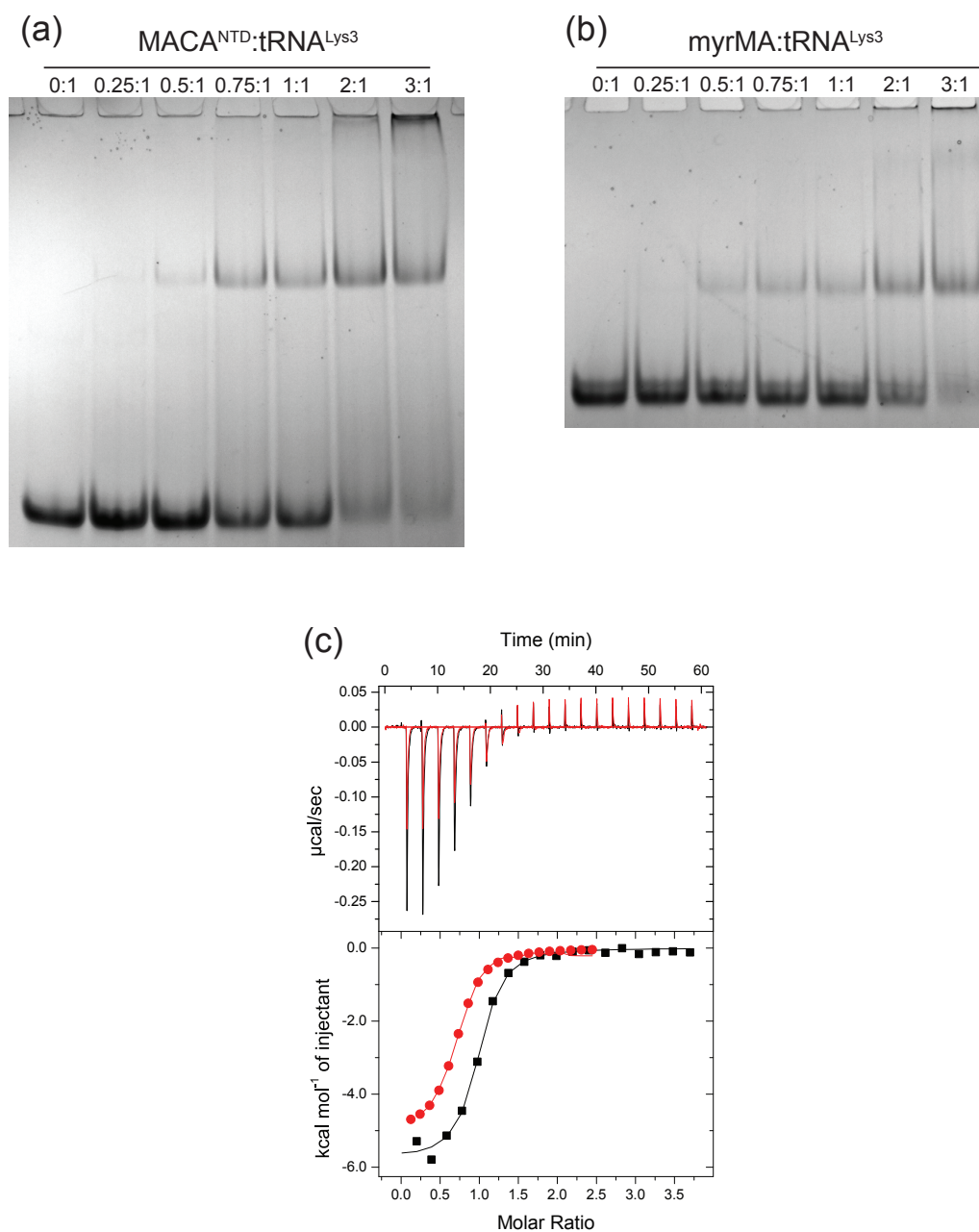


**Figure 2.9: tRNA<sup>Lys3</sup> interactions with myrMACA<sup>NTD</sup>.** (a) Myristoylated matrix-N-terminal domain capsid construct (myrMACA<sup>NTD</sup>) has a similar binding pattern to tRNA<sup>Lys3</sup> as matrix alone (b). (c) ITC curves of the myrMA domain alone (black) and myrMACA<sup>NTD</sup> (red).

Glu tRNAs  
TCCCTGGTGGTCTAGTGGTtAGGATTCTGGCGCTCTCACCGCGCGGGCCGGGTTCGATTCCCGGTCAGGGAA tRNA<sup>GluCUC</sup> (1-7 Sc: 70.0)  
TCCCACATGGTCTAGTGGTtAGGATTCTGGTTTTTCACCCAGCGGGCCGGGTTCGACTCCCGGTGTGGGAA tRNA<sup>GluUUC</sup> (2-2 Sc: 72.0)

Gly tRNAs  
GCATTGGTGGTTCAGTGGTtAGAATTCTCGCCTGCCACGCGGGAGGCCGGGTTCGATTCCCGGCCAATGCA tRNA<sup>GlyGCC</sup> (2-6 Sc: 77.9)  
GCATTGGTGGTTCAGTGGTtAGAATTCTCGCCTCCCACGCGGGAGACCCGGGTTCGAATTCGCGCCAATGCA tRNA<sup>GlyCCC</sup> (1-2 Sc: 75.5)  
GCGTTGGTGGTATAGTGGTtAGCATAGCTGCCTTCCAAGCAGTTGACCCGGGTTCGATTCCCGGCCAACGCA tRNA<sup>GlyUCC</sup> (1-1 Sc: 71.6)

Lys tRNAs  
GCCCCGGCTAGCTCAGTCCGGTAGAGCATGAGACTCTTAATCTCAGGGtCGTGGGTTCGAGCCCCACGTTGGGCG tRNA<sup>LysCUU</sup> (2-5 Sc: 78.0)  
GCCCCGGATAGCTCAGTCCGGTAGAGCATCAGACTTTTAATCTGAGGGtCCAGGGTTCAGTCCCTGTTGGGCG tRNA<sup>LysUUU</sup> (3-5 Sc: 84.0)

Val tRNAs  
GTTTCCGTAGTGTAGTGGTtATCACGTTCGCCTAACACGCGAAAGGtCCCGGTTCGAAAACCGGGCGGAAACA tRNA<sup>ValAAC</sup> ((1-5 Sc: 77.9)  
GTTTCCGTAGTGTAGTGGTtATCACGTTCGCCTCACACGCGAAAGGtCCCGGTTCGAAAACCGGGCGGAAACA tRNA<sup>ValCAC</sup> ((1-6 Sc: 78.8)  
GGTTCCA TAGTGTAGTGGTtATCACGTCTGCTTTACACGAGAGGtCCTGGGTTCGAGCCCGAGTGGAAACA tRNA<sup>ValUAC</sup> ((1-2 Sc: 78.8)

**Figure 2.10: Sequence Alignment of tRNAs that bound to MA.** Sequence alignment of the 8 tRNAs that bound to matrix in CLIP studies, along with the other isoforms of the tRNAs that did not bind for those amino acid residues (tRNA<sup>GlyUCC</sup> and tRNA<sup>ValUAC</sup>, italics). All tRNAs adopt the typical cloverleaf secondary structure, with an acceptor stem (red), D-loop and stem (blue), anticodon loop and stem (green), and T-loop and stem (orange). The D-loop was similar for all tRNAs, including those that did not bind. Differences in the D-loop are shown in pink.

## Chapter 3: Role of the Highly Basic Region and Myristoyl Group on myrMA-tRNA Interactions

### *Abstract*

Assembly of the HIV-1 virion begins when the myristoylated matrix domain (myrMA) of the Gag polyprotein targets the Gag-genome complex to the plasma membrane through interactions between myrMA's highly basic region and the membrane lipid phosphatidylinositol 4,5-bisphosphate [PI(4,5)P<sub>2</sub>]. In addition to interacting with PI(4,5)P<sub>2</sub>, myrMA will bind to specific tRNAs in the cytoplasm, and studies have found that treating myrMA with RNase will decrease myrMA's ability to discriminate between membranes containing and lacking PI(4,5)P<sub>2</sub>. In this chapter, ITC was used to determine the role specific highly basic region (HBR) residues play in tRNA interactions. Mutants of these residues either decrease myrMA's ability to bind to PI(4,5)P<sub>2</sub>-containing membranes or decrease myrMA's specificity for PI(4,5)P<sub>2</sub>. Many mutations known to affect plasma membrane binding also decreased myrMA's affinity to tRNA, with K32 mutants and the K26T/K27T mutant abolishing tRNA interactions. The role of the N-terminal myristoyl group on myrMA-tRNA interactions was also studied using ITC. Myristoyl exposure decreased myrMA's affinity for tRNA as well, suggesting that the HBR and myristoyl group play a role in both tRNA and membrane interactions.

## *Introduction*

In order for the human immunodeficiency virus (HIV) to assemble new viral particles, small numbers of viral Gag proteins target the Gag-genome complex to the plasma membrane through Gag's myristoylated matrix (myrMA) domain [118-121]. This targeting is mediated through two domains on the myrMA protein. The first is an N-terminal myristoyl group that is necessary to anchor the protein to the plasma membrane [35, 122-124]. The second is a highly basic region (HBR), including residues 16-32, which interacts with the negatively charged lipid, phosphatidylinositol 4,5-bisphosphate [PI(4,5)P<sub>2</sub>], on the plasma membrane to facilitate membrane binding [36, 40, 41, 53, 55].

Certain residues have been shown to affect Gag's ability to target to the plasma membrane, particularly basic residues in the HBR. Mutations to lysine residues 30 and 32 result in the retargeting of Gag to multivesicular bodies [52, 53], as well as inhibit Env incorporation and viral particle production and release [36, 53-55]. While also affecting the HBR, the double mutant K26T/K27T has higher release efficiency and leads to membrane retargeting [56]. In addition to phenotypes observed in cell culture, mutations to lysine residues found in the basic patch affect Gag's ability to bind to model membranes. Wild-type Gag binds preferentially to membranes containing PI(4,5)P<sub>2</sub>, and does not bind efficiently to liposomes containing the negative phospholipid phosphatidylserine or neutral phosphatidylcholine [36, 56-58]. Mutations of HBR residues K18, K30 and K32 decrease Gag's ability to bind to liposomes containing PI(4,5)P<sub>2</sub> [36, 53, 56], while in contrast, the K26/27T double mutant does not affect Gag's ability to bind to

PI(4,5)P<sub>2</sub>-containing liposomes, but instead decreases the specificity at which Gag binds to the model membranes [56].

In addition to its membrane binding properties, matrix has the ability to bind to RNA [62-64, 125]. This RNA-binding property is thought to be linked to myrMA's membrane selectivity, as treatment of samples with RNases decreases Gag's ability to discriminate between membranes containing PI(4,5)P<sub>2</sub> and other negatively charged phospholipids [32, 56, 68, 69]. This discrimination is due to the matrix domain, as PI(4,5)P<sub>2</sub>-containing liposomes could successfully outcompete DNA for bead-bound matrix [62]. CLIP studies found that MA binds to specific cellular tRNAs, including tRNA<sup>Lys3</sup> [69], an RNA that is packaged into virions and serves as the primer during reverse transcription [11, 12, 69, 76]. Membrane targeting assays using reconstituted systems indicate that tRNA interactions with matrix may also allow Gag to selectively package the HIV-1 genome [75].

I sought to determine the role each individual lysine residue contributed to the myrMA-tRNA interaction by measuring the affinity of myrMA mutants for tRNA<sup>Lys3</sup> using isothermal titration calorimetry. I also investigated the role of the N-terminal myristoyl group on myrMA-tRNA interactions. The myristoyl group can adopt either a sequestered conformation in which it is buried in myrMA's hydrophobic pocket or an exposed conformation in which the myristoyl group is exposed to the cytosol, allowing it to anchor the protein into the plasma membrane [30]. The equilibrium between the sequestered and exposed conformation can be shifted *in vitro* by changing the pH or the concentration of myrMA [30, 31], allowing observation of the

interaction between tRNA<sup>Lys3</sup> and myrMA at different points in the exposed-sequestered equilibrium.

## *Materials and Methods*

### *Protein Expression and Purification*

A detailed protein purification protocol is in Chapter 2. Briefly, myrMA was expressed using a vector containing both HIV-1 MA and human N-myristoyltransferase. Transformed BL21-DE3-RIL *E. coli* cells were grown in 2L LB broth at 37C until OD<sub>600</sub> ~0.6-0.7. Cells were induced using isopropyl D-thiogalactoside (1 mM) and continued to grow for 3.5-4 hours. Following lysing by microfluidization, the supernatant was purified by polyethylenimine precipitation (0.15% w/v) and ammonium sulfate precipitation (50% saturation). The resuspended precipitate was purified using ion exchange chromatography (Q and SP columns; GE Healthcare), hydrophobicity chromatography (Butyl column; GE Healthcare), and size exclusion chromatography (Superdex 200 G75 column; GE Healthcare). Quickchange Lightning mutagenesis kits (Agilent) were used to create mutant myrMA constructs, as well as add an N-terminal histidine tag and TEV cleavage site to a HIV-1 MA vector. myr(-)MA was expressed and lysed in a protocol identical to myrMA, but was purified after PEI precipitation by gravity cobalt affinity chromatography (ThermoFisher). TEV cleavage was followed by another cobalt affinity purification step, as well as ion exchange and size exclusion chromatography. Molecular weights and myristoylation efficiency were determined by electrospray ionization mass spectrometry.

### *tRNA Synthesis and Purification*

In-depth protocols are described in Chapter 2. Briefly, DNA oligonucleotides (IDT Tech) were annealed to form DNA templates containing a T7 promoter site and the tRNA<sup>Lys3</sup> sequence. tRNA<sup>Lys3</sup> was synthesized *in vitro* by T7 polymerase, and purified using sequencing gels, followed by electroelution, NaCl washes to remove residual polyacrylamide, and water washes to remove excess ions. After addition of MgCl<sub>2</sub> to a concentration of 5 mM, tRNA samples were boiled for 3 minutes and snap-cooled on ice immediately before dialysis for ITC.

### *Isothermal Titration Calorimetry*

Protein and tRNA<sup>Lys3</sup> samples were dialyzed overnight in 25 mM Tris, pH 7.0, (25 mM MES for samples at pH 5.5) 140 mM KCl, 10 mM NaCl, 5 mM MgCl<sub>2</sub>, and 5 mM beta-mercaptoethanol. Dialysis buffer was filtered and used to dilute RNA and protein samples for ITC. A MicroCal itc200 (GE Healthcare) was used to analyze all samples. Protein samples were diluted to 25  $\mu$ M and titrated over 20 injections with 2  $\mu$ L of 400-450  $\mu$ M tRNA<sup>Lys3</sup> with a stirring speed of 750 rpm. Averages and standard deviations of three replicate titrations were used to calculate  $K_d$ ,  $\Delta H$ ,  $\Delta S$ , and  $n$ . All samples were compared to wild-type myrMA at pH 7.0 using a Student's t-test.

### *Electrophoretic Mobility Shift Assays (EMSA)*

Protein and tRNA samples used for ITC were diluted using ITC dialysis buffer for EMSA. 4  $\mu$ M tRNA<sup>Lys3</sup> samples were incubated with various molar ratios of myrMA at 37°C for at least 30 minutes in buffer. Immediately after removal from the incubator, 2  $\mu$ L of 50% glycerol was added per 10  $\mu$ L sample and loaded onto a

10% 29:1 polyacrylamide Tris-borate gel containing 0.05 mM MgCl<sub>2</sub>. Samples ran for ~30 minutes at 170V with TB running buffer containing 0.05 mM MgCl<sub>2</sub>. Gels were stained with a 0.15% Stains-all solution in 60% formamide, and imaged after destaining in water.

## *Results*

### *Mutations that Decrease Binding to PI(4,5)P<sub>2</sub>-Containing Liposomes also Decrease Binding to tRNA<sup>Lys3</sup>*

K18T, K18/30T, and K30/32T mutations in the basic patch can decrease myrMA's ability to bind PI(4,5)P<sub>2</sub>-containing liposomes [36, 53, 56]. Additionally, the mutations affecting K30 and K32 can retarget assembly of Gag from the plasma membrane to multivesicular bodies and reduce virus release efficiency [36, 40, 52-54]. In order to determine if these residues are also involved in MA's ability to bind tRNA<sup>Lys3</sup>, we mutated K18, K30, and K32 (Figure 3.1). Initial EMSA results for mutants K30A and K18T had band shifts similar to wild-type myrMA (Figure 3.1a, b, d). Band shifts were weak for the K30T mutant (Figure 3.1c) and not detected for the K18T/K30T double mutant (Figure 3.1e), suggesting that these mutations may inhibit myrMA-tRNA interactions.

Isothermal titration calorimetry (ITC) allowed quantification of the role of each residue in myrMA-tRNA<sup>Lys3</sup> interactions. K30A decreased myrMA's affinity for tRNA<sup>Lys3</sup>, but K30T had a much greater effect (wt:  $K_d = 0.63 \pm 0.03$   $\mu$ M, K30A:  $K_d = 2.51 \pm 0.19$   $\mu$ M,  $p < 0.001$  K30T:  $K_d = 19 \pm 4$   $\mu$ M,  $p = 0.001$ ) (Figure 3.2a,d, Table 1). The enthalpy associated with tRNA binding did not significantly change for the K30A mutant compared to the wild type protein (wt:  $\Delta H = -5.9 \pm 0.4$  kcal/mol,

K30A:  $\Delta H = -6.1 \pm 0.8$  kcal/mol,  $p = 0.75$ ), but the enthalpy of reaction increased for the K30T mutant ( $\Delta H = -4.2 \pm 0.6$ ,  $p = 0.015$ ) (Figure 3.2f). Despite the change in enthalpy, the entropy of the reaction did not change for either of the mutants (wt:  $\Delta S = 8.9 \pm 1.3$  cal/mol/deg; K30A:  $\Delta S = 5.6 \pm 2.8$  cal/mol/deg,  $p = 0.14$ ; K30T:  $\Delta S = 7.8 \pm 2.4$  cal/mol/deg,  $p = 0.51$ ). The enthalpy-dependent weakening of the interaction cannot be attributed to charge loss alone, as both the K30A and K30T mutants replaced a positive charge from the basic patch with a neutral residue. The mutations did not affect the stoichiometry, as the reaction retained its 1:1 binding ratio (wt:  $n = 0.89 \pm 0.06$ , K30A:  $n = 1.09 \pm 0.16$ , K30T:  $n = 0.96 \pm 0.06$ ) (Figure 3.2e).

The K18T mutation slightly weakened the tRNA<sup>Lys3</sup>-myrMA interaction, but had the smallest effect of the mutants characterized (Figure 3.2b). The  $K_d$  of the interaction increased slightly ( $K_d = 0.84 \pm 0.9$   $\mu$ M,  $p = 0.018$ ). Unlike the threonine mutation for residue 30, the K18T mutant decreased the enthalpy of the reaction ( $\Delta H = -7.3 \pm 0.6$  kcal/mol,  $p = 0.02$ ), as well as significantly decreased the entropy of the reaction ( $\Delta S = 3.7 \pm 2.1$  cal/mol/deg,  $p = 0.02$ ) (Figure 3.2f). A decrease in affinity was seen for K18/30T ( $K_d = 17.3 \pm 0.9$   $\mu$ M), but this is not significantly different to the decrease seen for the K30T single mutant ( $p = 0.58$ ) (Figure 3.2d). K18/30T had a similar enthalpy and entropy of reaction ( $\Delta H = -4.3 \pm 0.2$  kcal/mol,  $\Delta S = 7.6 \pm 0.7$  cal/mol/deg) as the K30T mutant, suggesting that most changes result from the K30T mutation and that the K18T mutation does not have a significant additive effect on the thermodynamics of the myrMA-tRNA<sup>Lys3</sup> interaction.

K32 is essential for membrane-myrMA interactions, as mutation of this residue greatly reduces myrMA's ability to bind to PI(4,5)P<sub>2</sub>-containing liposomes

[36, 56]. Mutation of the residue also leads to decrease Env incorporation into the viral membrane [55], reduction in viral particle production [56], and decrease in viral replication overall [55]. During EMSA analysis, both the K32A and K32T mutants did not show band shifts, indicating weak tRNA<sup>Lys3</sup>-myrMA interactions (Figure 3.3). Unlike the K30A mutant, similar effects were seen for both the K32T and K32A mutants. In both the EMSA analysis and ITC, both single mutants abolished binding to tRNA<sup>Lys3</sup>, indicating that this residue is essential to myrMA's ability to bind tRNA (Figure 3.2c).

*Mutations Known to Decrease Specificity of Membrane Interactions also Affect tRNA<sup>Lys3</sup>-myrMA Interactions*

The K26/27T myrMA mutant binds to PI(4,5)P<sub>2</sub> liposomes with similar affinity as wild type myrMA, but has increased binding to liposomes containing other negatively charged lipids, such as phosphatidylserine (PS) [56]. This phenotype was also seen in membrane flotation assays upon addition of RNase to wild type myrMA, leading to the conclusion that these residues may play a role in myrMA-RNA interactions [56, 69]. EMSA gels detected band shifts for the K26T mutant, but not for the K27T or K26T/K27T mutants (Figure 3.4). ITC results indicated decreased binding for both K26T and K27T single mutants (Figure 3.5a). K27T had a greater effect than K26T, with a  $K_d$  of  $9.4 \pm 1.0 \mu\text{M}$  and  $3.2 \pm 0.6 \mu\text{M}$ , respectively (Figure 3.5b, Table 1). Binding between K26T and K27T myrMA mutants and tRNA<sup>Lys3</sup> remained at a 1:1 binding ratio, as  $n$  did not change significantly from wild type myrMA ( $n$ : wt =  $0.89 \pm 0.06$ , K26T =  $0.87 \pm 0.03$ , K27T =  $0.91 \pm 0.05$ ) (Figure 3.5c). Both mutations had similar, slight increases in enthalpy of the reaction (K26T:

$\Delta H = -5.2 \pm 0.3$  kcal/mol,  $p = 0.05$ , K27T :  $\Delta H = -5.2 \pm 0.01$ ,  $p = 0.02$ ) but only the K27T mutant had a decrease in the entropy of the reaction (K26T:  $\Delta S = 8.1 \pm 1.0$  cal/mol/deg,  $p = 0.43$ , K27T:  $\Delta S = 6.0 \pm 0.2$  cal/mol/deg,  $p = 0.02$ ) (Figure 3.5d). A cumulative effect of the mutations may be responsible for the phenotype seen in Chukkapalli *et al.* [56], as the K26/27T double mutant abolished all tRNA<sup>Lys3</sup>-myrMA interactions.

#### *Myristoyl Group Exposure Inhibits myrMA-tRNA<sup>Lys3</sup> Interactions*

myrMA's myristoyl group exists in equilibrium between the sequestered and exposed conformations [30, 31, 37, 126]. After residues in the highly basic region bind to PI(4,5)P<sub>2</sub> in the plasma membrane, the myristoyl group switches from the sequestered to the exposed conformation to anchor Gag to the membrane [36, 41]. *In vitro*, the equilibrium between the sequestered and exposed conformation will shift toward the exposed conformation upon decreasing the pH or increasing the concentration of myrMA [30, 31]. In order to test the role of the myristoyl group on tRNA<sup>Lys3</sup>-myrMA interactions, I compared the binding of myrMA to tRNA<sup>Lys3</sup> at pH 7.0 and pH 5.5 using wild-type myrMA, an unmyristoylated construct [myr(-)MA] and an exposure-deficient mutant (L8I) [127, 128]. Analysis with EMSA detected band shifts indicative of binding for all three mutants at both pH 7.0 and pH 5.5 (Figure 3.6). The L8I mutant had bands detected earlier than the wild-type protein, at ratios as low as 0.25:1 myrMA:tRNA<sup>Lys3</sup> at both pH 5.5 and pH 7.0.

ITC titrations with myr(-)MA and L8I myrMA at neutral and low pH also helped elucidate the role of the myristoyl group. At pH 7.0, when the wild-type protein is almost fully sequestered, there was no significant difference from wild type

myrMA for the mutants in stoichiometry or affinity ( $n$ : wt =  $0.89 \pm 0.06$ , L8I =  $0.85 \pm 0.05$ , myr(-)MA =  $0.91 \pm 0.04$ ;  $K_d$ : wt =  $0.63 \pm 0.03 \mu\text{M}$ , L8I =  $0.68 \pm 0.08 \mu\text{M}$ , myr(-)MA =  $0.62 \pm 0.05 \mu\text{M}$ ) (Figure 3.6a,c,d, Table 2). However, at pH 5.5 the stoichiometry decreased slightly as the protein became more exposed ( $n$ : wt =  $0.62 \pm 0.03$ , L8I =  $0.74 \pm 0.11$ , myr(-)MA =  $0.83 \pm 0.04$ ) (Figure 3.6b,d). This could be due to myrMA's ability to self-associate upon myristoyl exposure [30, 31], effectively decreasing the amount of myrMA available to bind in the sample cell. Myristoyl exposure also led to a significant decrease in affinity at pH 5.5 for the wild type protein (wt:  $K_d = 1.2 \pm 0.3 \mu\text{M}$ ,  $p = 0.001$ , L8I:  $K_d = 1.6 \pm 1.0 \mu\text{M}$ ,  $p = 0.20$ , myr(-)MA:  $K_d = 0.41 \pm 0.08 \mu\text{M}$ ,  $p = 0.01$ ) (Figure 3.6c). The enthalpy of the reaction was similar for both of the mutants at both pH 7.0 and 5.5, but the enthalpy of the reaction increased for the wild-type protein when the pH was decreased to 5.5 ( $\Delta H = -3.25 \pm 0.14 \text{ kcal/mol}$ ). The same held true for the entropy of the reaction, with only myrMA at pH 5.5 significantly deviating from the results of the wild-type protein at pH 7.0 ( $\Delta S = 16.3 \pm 0.8 \text{ cal/mol/deg}$ ,  $p = 0.001$ ) (Figure 3.6e).

### Discussion

tRNA<sup>Lys3</sup> binds near the basic patch region of myrMA, suggesting some regulatory role for membrane binding. Although recent work suggests T7-transcribed tRNA<sup>Lys3</sup> may not bind specifically to Gag *in vitro* [129], this may be due to the instability of non-modified tRNA<sup>Lys3</sup> in the absence of magnesium [74]. Using electrophoretic mobility shift assays, it was determined that 5 mM MgCl<sub>2</sub> was sufficient to fold tRNA<sup>Lys3</sup> in order to induce specific binding (Figure 2.3b).

In addition to playing a role in myrMA-PI(4,5)P<sub>2</sub> interactions, the highly basic region plays an important role in myrMA-RNA interactions. The interaction is primarily driven by the enthalpy of the reaction, although the entropy is positive. Enthalpy-driven reactions are hallmarks of electrostatic interactions, which is supported by the decrease in enthalpy associated with the K30T, K18/30T, K26T, and K27T mutants, which remove positive charge from the basic patch. Interestingly, although the mutation decreased myrMA's positive charge, the K18T mutation decreased the enthalpy of the reaction further. This enthalpy decrease was offset by an increase in the entropy of the reaction, leading to only very slight weakening of the interaction. Of all of the basic patch mutations, K18T had the smallest effect. Additionally, the K18/30T mutant behaved similarly to the K30T mutant, indicating little or no additive effects of mutating K18. K18 is on the opposite side of the basic patch from the other residues studied, near the end of helix I, and its minor role in the interaction may indicate that myrMA-tRNA interactions occur closer to the N-terminus of helix II, near the beta-turn where K30 and K32 are located.

Both K32A and K32T mutants weakened binding to the point that the thermodynamics of the interaction could not be calculated. The K32 residue plays a very important role in PI(4,5)P<sub>2</sub> binding, as single mutations such as K32E and K32A have reduced myrMA's affinity for PI(4,5)P<sub>2</sub>-containing liposomes and interrupted viral replication [36, 55]. While this residue has had the most prominent effect on membrane binding, it also appears to hold a similar crucial role in tRNA binding, as it was the only residue examined in this study that could abolish binding in a single mutation.

K30 also plays a role in membrane targeting, but does not appear to have as large of an effect as K32 [36]. There was a similar effect in the mutants' ability to disrupt tRNA-myrMA interactions. Additionally, the results indicated that not all residue substitutions had the same effect. The K30A mutant weakened the interaction 4-fold, compared to a 30-fold difference for the K30T mutant. The entropy of the reaction did not significantly change for either mutant, indicating that the differences in binding are related to the enthalpy of the reaction. Mutating K30 to the hydrophobic residue alanine did not significantly decrease the enthalpy of the reaction, indicating that the loss of the positive charge is not the main reason for the weakening of the interaction. The electronegative mutation to threonine had a much greater effect on tRNA-myrMA interactions despite the fact that the mutation was of similar size as the alanine mutation. The larger effect of the threonine mutation may be due to the electronegative nature of the hydroxyl group, which may create a repulsive force to the negatively charged tRNA.

Mutants of residues K18, K30, and K32 all reduce myrMA's ability to bind to both PI(4,5)P<sub>2</sub>-containing liposomes, as well as to tRNA<sup>Lys3</sup> [56]. The K26/27T double mutant, while also able to retarget Gag to MVBs, has a different phenotype that reduces the specificity of myrMA to PI(4,5)P<sub>2</sub>-containing liposomes [56]. The K26/27T binds to liposomes of negative charge with a similar affinity as liposomes that contain PI(4,5)P<sub>2</sub>[56]. Both K26T and K27T mutants weakened the interaction between myrMA and tRNA<sup>Lys3</sup>, with slight increases in enthalpy. The K27T mutant bound with 3-fold less affinity than K26T, indicating that it plays more of a role in the interaction. However, neither single mutation could abolish binding, unlike the

K26/27T double mutant, indicating that these residues act synergistically in the tRNA-myrMA interaction. All four lysine residues with the greatest effect (K26, K27, K30, and K32) form a cluster on the basic patch structured loop, indicating that this area is important for tRNA-myrMA interactions. ITC cannot give the exact location of the tRNA-myrMA interaction, but it is likely that structural work will indicate that the basic patch region plays a crucial role. If so, it is likely that PI(4,5)P<sub>2</sub> competes for the same binding location as tRNA.

This hypothesis is further supported by the results investigating the role of the myristoyl group. Previous models suggest that the myristoyl group only becomes exposed upon forming higher-order multimers or upon binding to the plasma membrane [30, 31, 36]. tRNA<sup>Lys3</sup> has decreased affinity for myrMA with an exposed myristoyl group, which may account for the ability of PI(4,5)P<sub>2</sub> to outcompete tRNA for the basic patch. As the Gag polyprotein moves toward the plasma membrane, the pH of the cell begins to decrease due to the pH gradient inside the cell [130]. Other studies have suggested that HIV-1 infection lowers the pH of the cell overall [131], making it more likely for the myrMA protein to become exposed and bind nonspecifically to cellular membranes. The tRNA molecules may prevent binding to membranes other than the plasma membrane by shifting the equilibrium toward the sequestered conformation of the myristoyl group, until the Gag protein comes into contact with a PI(4,5)P<sub>2</sub>-containing membrane, at which point the PI(4,5)P<sub>2</sub> can outcompete tRNA<sup>Lys3</sup>.

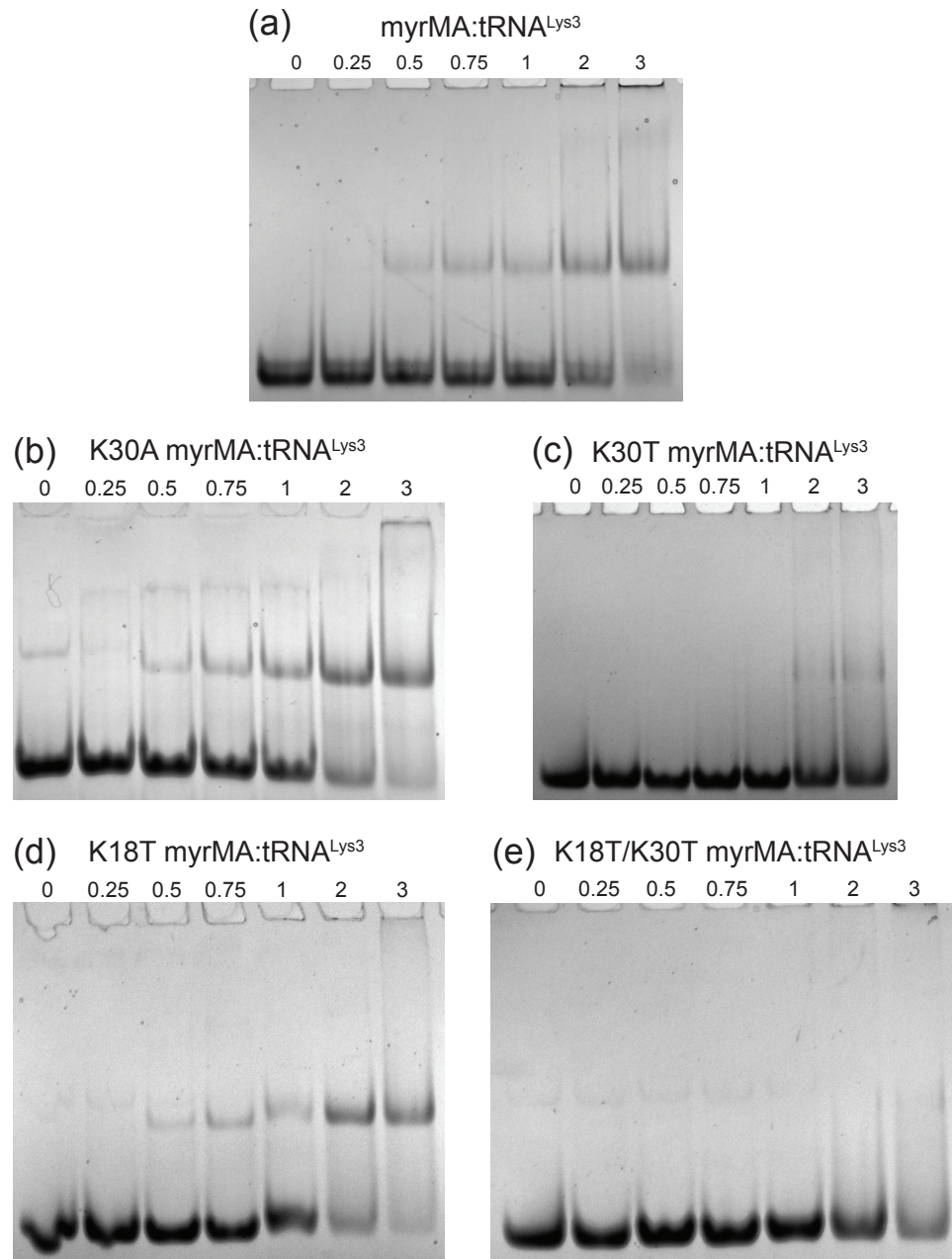


**Figure 3.1: EMSA of tRNA<sup>Lys3</sup> interactions with mutants that decrease membrane binding.** EMSA analysis of the wild-type (a), K30A (b), K30T (c), K18T(d), and K18T/K30T (e) mutants suggest that only the K30T and K18T/K30T mutants disrupt myrMA-tRNA<sup>Lys3</sup> interactions.

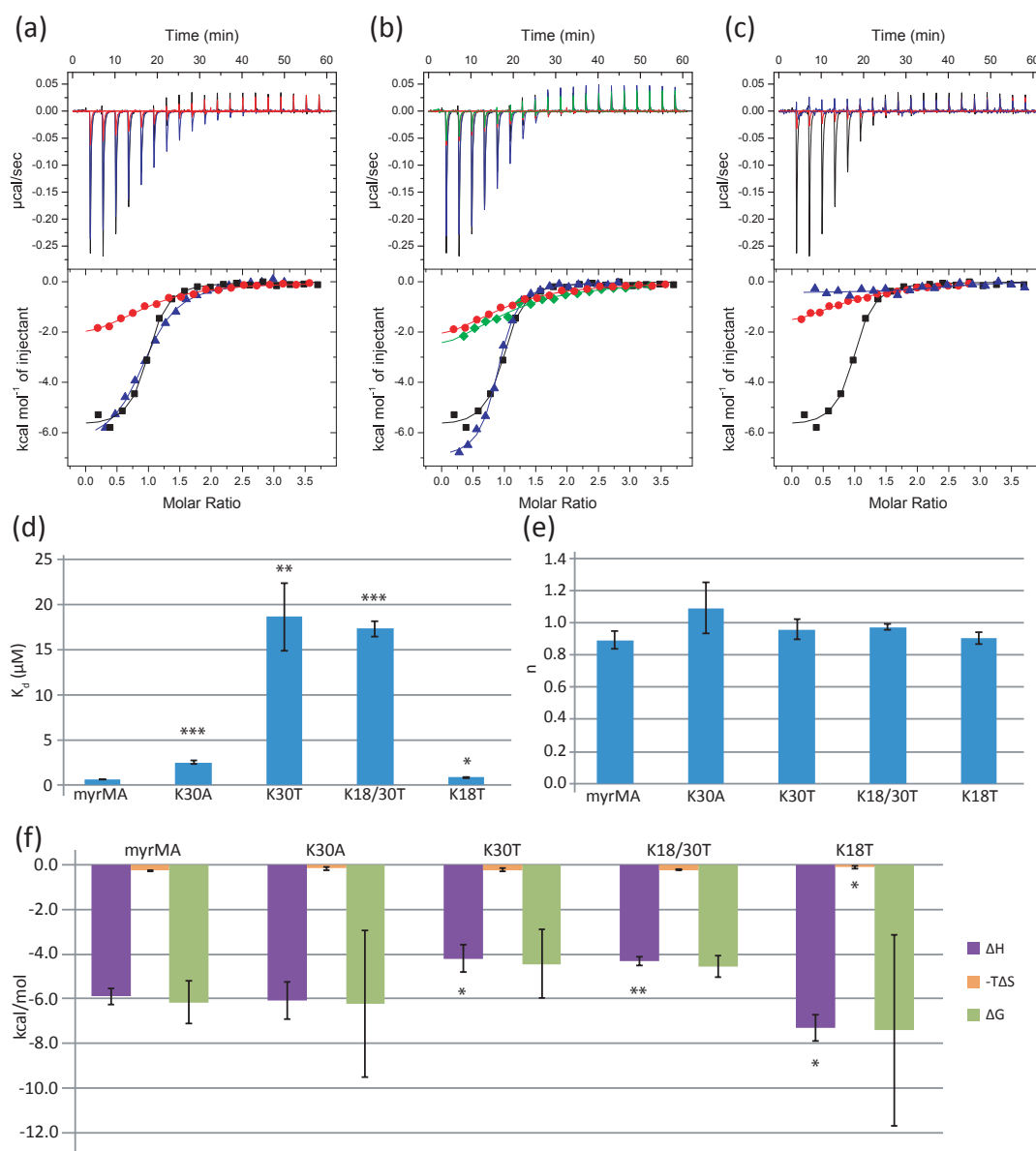


**Figure 3.2: Mutations that disrupt myrMA-membrane interactions also weaken myrMA's affinity for tRNA.** (a) ITC titration curves of K30A (blue) and K30T (red) mutants compared to wild type myrMA (black). (b) Titration curves comparing K18T (blue) mutant, K30T mutant (red), and the K18T/K30T double mutant (green). (c) ITC data for the K32A (blue) and the K32T (red) mutants. (d) Graph of  $K_d$  values for K18 and K30 mutants. K32 mutants did not bind and are not included in this graph. (e) Graph of the  $n$  values determined by ITC. (f) Thermodynamic profiles of the K18 and K30 mutants. \* $p < 0.05$ , \*\* $p < 0.01$ , \*\*\* $p < 0.001$

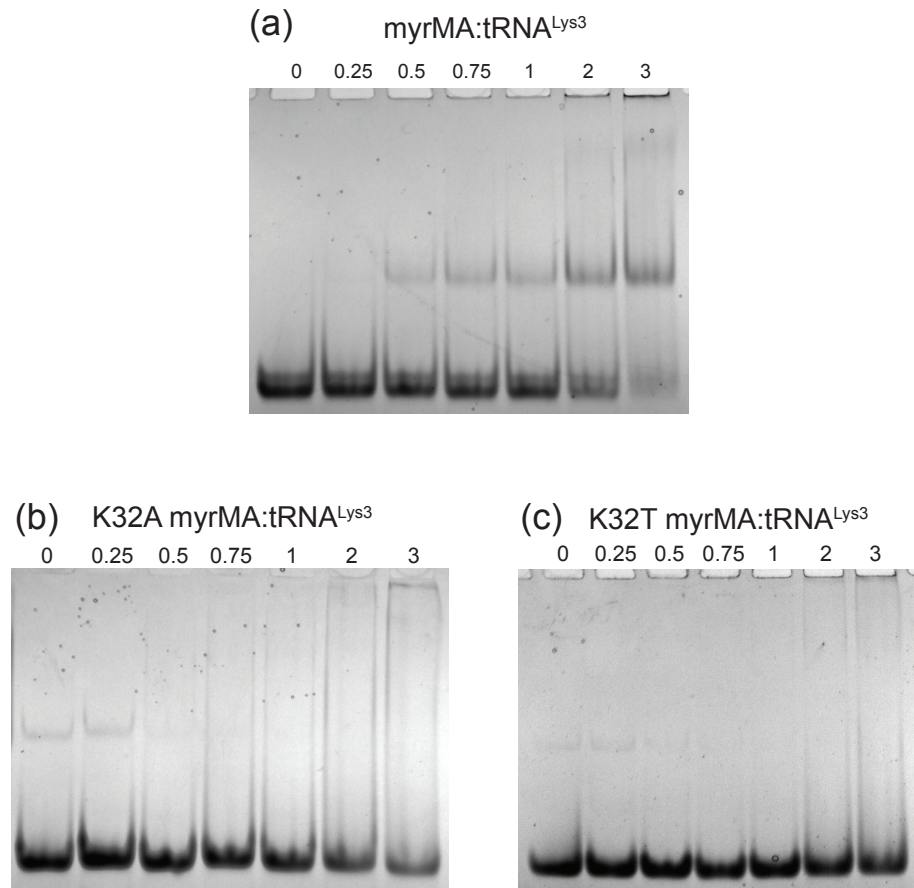


**Figure 3.3: EMSA of tRNA<sup>Lys3</sup> interactions with K32 mutants.** EMSA analysis of the wild-type (a), K32A (b), and K32T (c), mutants suggest that mutations to the K32 residue greatly disrupt myrMA-tRNA interactions.

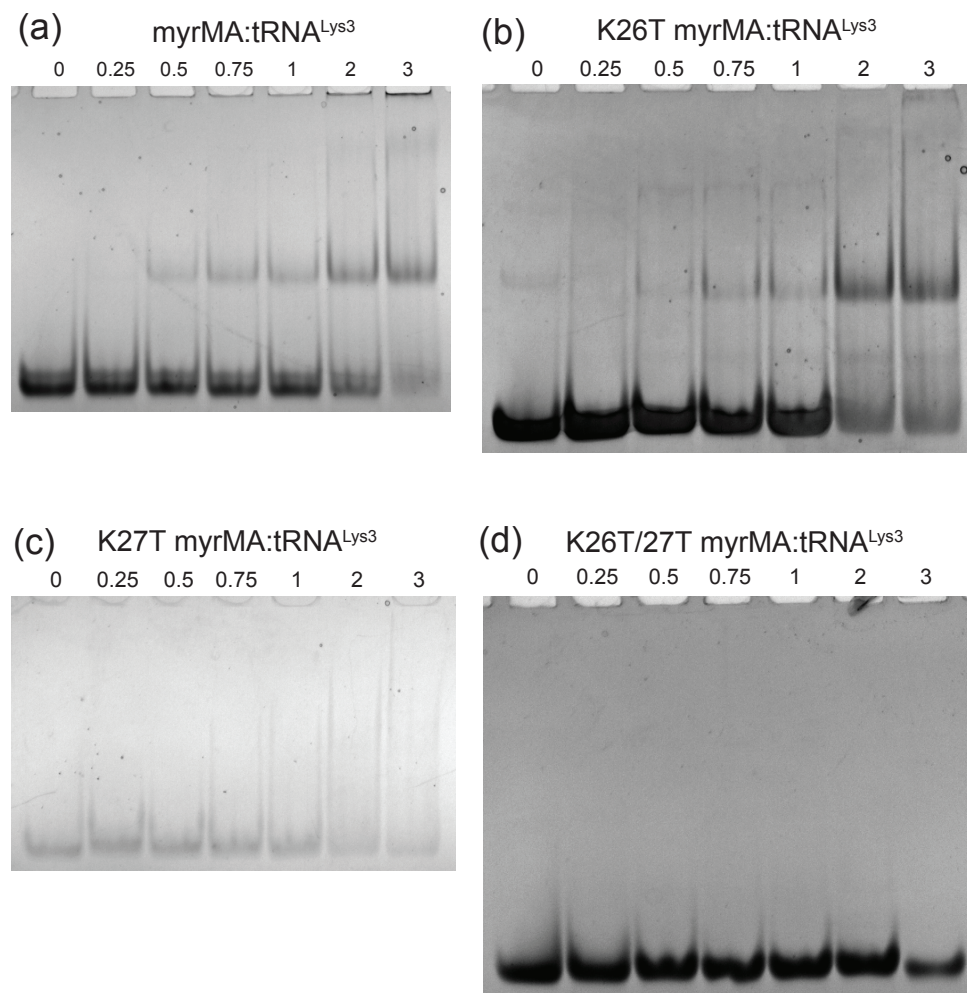


**Figure 3.4: EMSA of tRNA<sup>Lys3</sup> interactions with mutants that decrease membrane specificity.** EMSA analysis of the wild-type (a), K26T (b), K27T (c), and K26T/K27T mutants suggest that mutations to the K26T residue do not affect binding to tRNA as strongly as the K27T and K26T/K27T mutants.

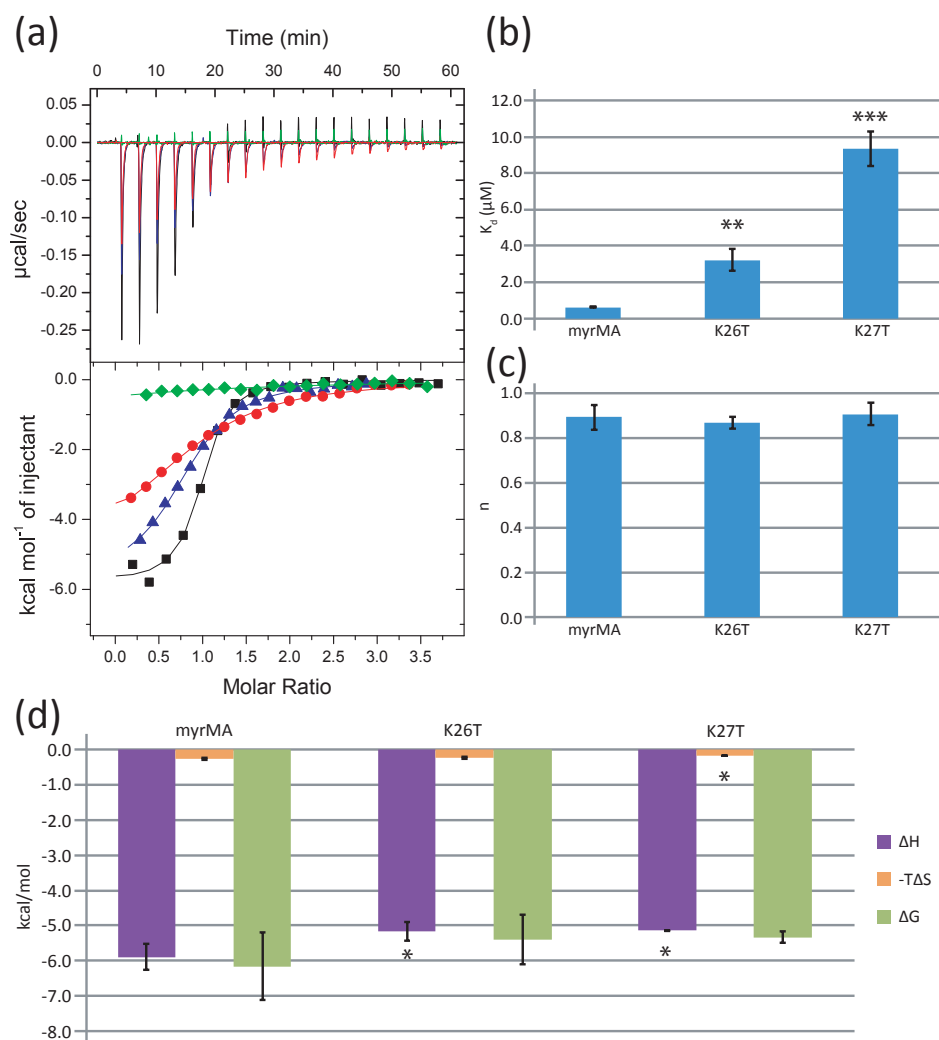


**Figure 3.5: Mutations known to affect membrane specificity also decrease myrMA's affinity for tRNA.** (a) ITC data for the K27T (blue), K26T (red) and K26T/K27T (green) myrMA mutants. (b) Graph of binding affinities for K26 and K27 mutants. (c) Stoichiometries for K26T and K27T mutants compared to wild type myrMA. (d) Thermodynamic profile for the K26T and K27T mutants. \* $p < 0.05$ , \*\* $p < 0.01$ , \*\*\* $p < 0.001$

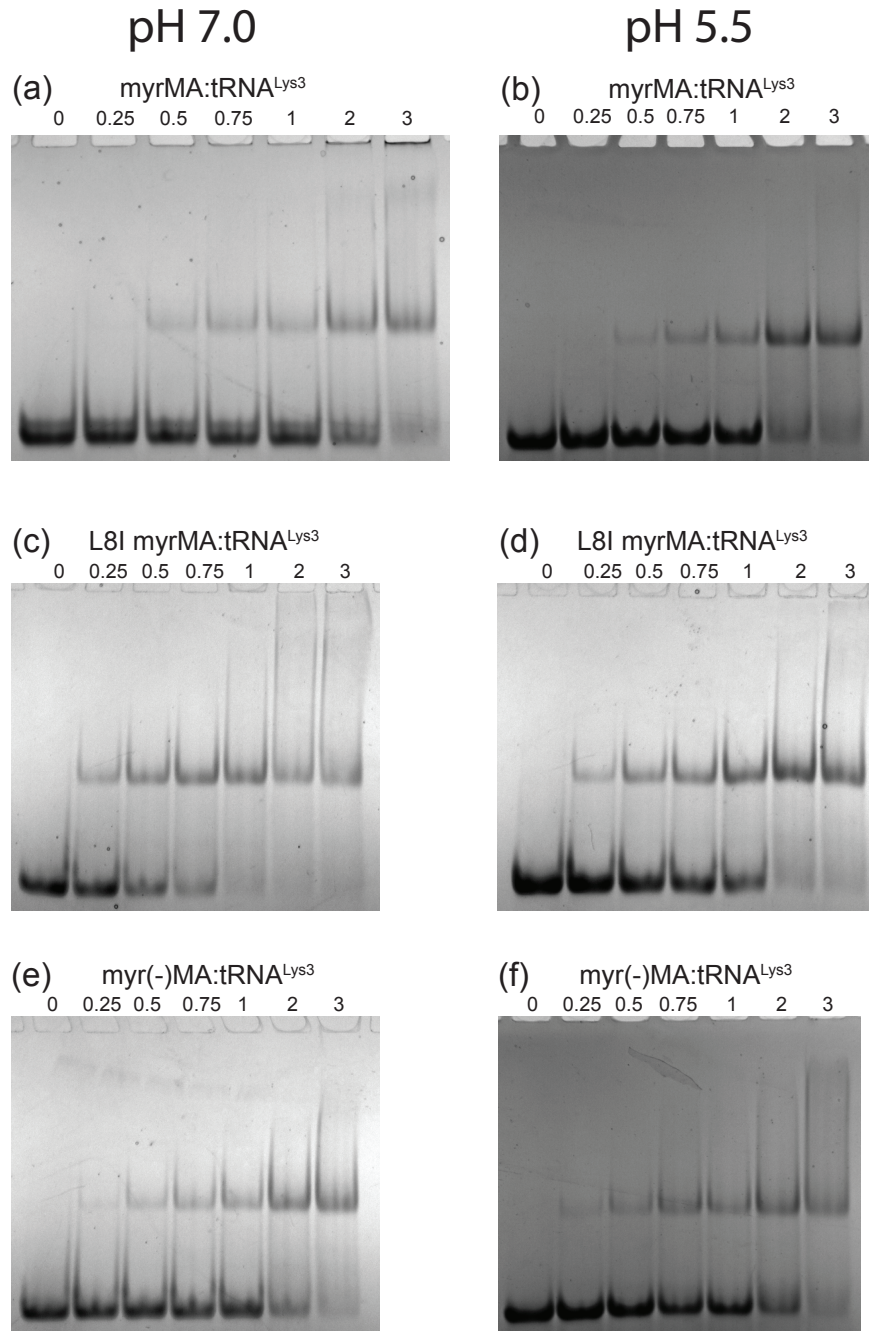


**Figure 3.6: Effect of pH on myrMA-tRNA interactions.** EMSA analysis at pH 7.0 of the wild-type (a), myristoyl-deficient mutant L8I myrMA (c), and unmyristoylated protein (e). Similar binding was seen at pH 5.5 for the three proteins (b, d, and f, respectively).

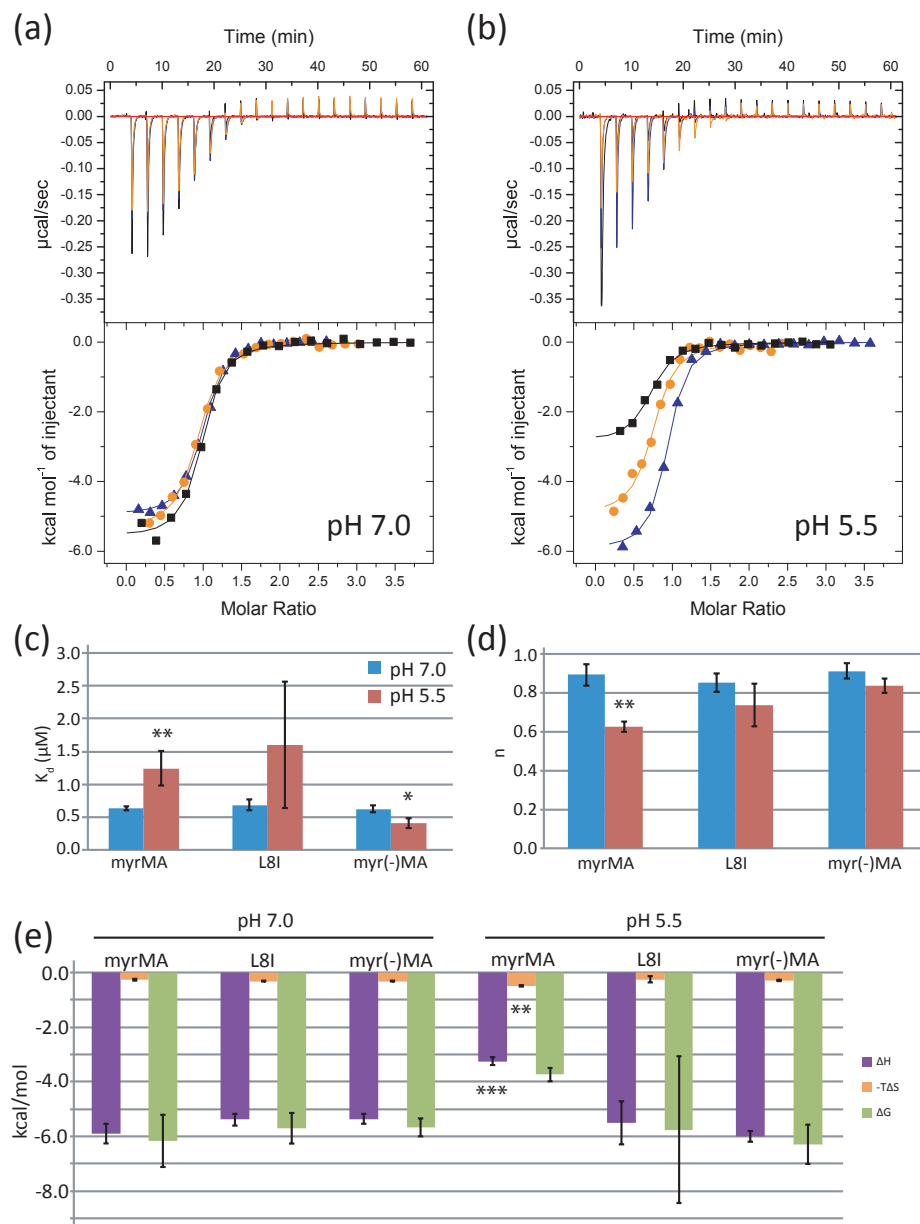


**Figure 3.7: Myristoyl group exposure weakens tRNA-MA interactions.** (a) WT myr(MA) (black), the exposure-deficient mutant L8I (orange), and myr(-)MA (blue) have similar binding profiles for tRNA<sup>Lys3</sup> at pH 7.0. (b) ITC titration curves at pH 5.5, when equilibrium of the myristoyl group shifts to the exposed conformation. (c)  $K_d$  values for the myrMA myristoylation mutants at pH 7.0 (blue) and pH 5.5 (red). (d) Stoichiometries for the myristoylation mutants at pH 7.0 (blue) and pH 5.5 (red). (e) Thermodynamic profiles for myrMA myristoylation mutants at pH 7.0 and pH 5.5. \* $p < 0.05$ , \*\* $p < 0.01$ , \*\*\* $p < 0.001$

**Table 3.1: Thermodynamic characterization of myrMA mutants with tRNA<sup>Lys3</sup>**

	$K_d$ ( $\mu$ M)	$n$	$\Delta H$ (kcal/mol)	$\Delta S$ (cal/mol/deg)
myrMA	$0.63 \pm 0.03$	$0.89 \pm 0.06$	$-5.9 \pm 0.4$	$8.9 \pm 1.3$
K30A	$2.51 \pm 0.19^{***}$	$1.09 \pm 0.16$	$-6.1 \pm 0.8$	$5.6 \pm 2.8$
K30T	$19 \pm 4^{**}$	$0.96 \pm 0.06$	$-4.2 \pm 0.6^*$	$7.8 \pm 2.4$
K18/30T	$17.3 \pm 0.9^{***}$	$0.96 \pm 0.02$	$-4.3 \pm 0.2^{**}$	$7.6 \pm 0.7$
K18T	$0.84 \pm 0.09^*$	$0.90 \pm 0.04$	$-7.3 \pm 0.6^*$	$3.7 \pm 2.1^*$
K32A	N/D	N/D	N/D	N/D
K32T	N/D	N/D	N/D	N/D
K26T	$3.2 \pm 0.6^{**}$	$0.87 \pm 0.03$	$-5.2 \pm 0.3^*$	$8.1 \pm 1.0$
K27T	$9.4 \pm 1.0^{***}$	$0.91 \pm 0.05$	$-5.15 \pm 0.01^*$	$6.0 \pm 0.2^*$
K26/27T	N/D	N/D	N/D	N/D

\*p&lt;0.05

\*\*p&lt;0.01

\*\*\*p&lt;0.001

**Table 3.2: Characterization of myristoyl group interactions with tRNA<sup>Lys3</sup>**

	$K_d$ ( $\mu$ M)	$n$	$\Delta H$ (kcal/mol)	$\Delta S$ (cal/mol/deg)
myrMA pH 7.0	$0.63 \pm 0.03$	$0.89 \pm 0.06$	$-5.9 \pm 0.4$	$8.9 \pm 1.3$
L8I pH 7.0	$0.68 \pm 0.08$	$0.85 \pm 0.05$	$-5.4 \pm 0.2$	$10.4 \pm 0.9$
myr(-)MA pH 7.0	$0.62 \pm 0.05$	$0.91 \pm 0.04$	$-5.4 \pm 0.2$	$10.7 \pm 0.5$
myrMA pH 5.5	$1.2 \pm 0.3^{**}$	$0.62 \pm 0.03^{**}$	$-3.25 \pm 0.14^{***}$	$16.3 \pm 0.8^{**}$
L8I pH 5.5	$1.6 \pm 1.0$	$0.74 \pm 0.11$	$-5.5 \pm 0.8$	$8.7 \pm 3.9$
myr(-)MA pH 5.5	$0.41 \pm 0.08^*$	$0.83 \pm 0.04$	$-6.0 \pm 0.2$	$9.4 \pm 1.0$

\*p&lt;0.05

\*\*p&lt;0.01

\*\*\*p&lt;0.001

## Chapter 4: tRNA's Role in Regulating Matrix-Membrane Interactions

### *Abstract*

Assembly of the HIV-1 virion begins when the myristoylated matrix domain (myrMA) of the Gag polyprotein targets the Gag-genome complex to the plasma membrane through interactions between myrMA's highly basic region and the membrane lipid phosphatidylinositol 4,5-bisphosphate [PI(4,5)P<sub>2</sub>]. In addition to interacting with PI(4,5)P<sub>2</sub>, myrMA will bind to specific tRNAs in the cytoplasm, and studies have found that treating myrMA with RNase will decrease myrMA's ability to discriminate between membranes containing and lacking PI(4,5)P<sub>2</sub>. Although a suggested role for tRNA-myrMA interactions is that they regulate myrMA's membrane-binding action and prevent myrMA from binding nonspecifically to membranes lacking PI(4,5)P<sub>2</sub>, <sup>1</sup>H-1D NMR liposome competition assays determined that the presence of tRNA alone is not enough to allow myrMA to discriminate between membranes. tRNA<sup>Lys3</sup> prevented binding to all membranes, including those containing high levels of PI(4,5)P<sub>2</sub> and those with raft-like compositions. Inducing myristoyl exposure by lowering the pH of the samples did not allow PI(4,5)P<sub>2</sub> to outcompete tRNA for myrMA binding, suggesting some other mechanism is required in addition to tRNA interactions to regulate assembly on the plasma membrane.

## *Introduction*

The HIV-1 matrix protein targets the Gag polyprotein to the plasma membrane for virion assembly through interactions between the highly basic region on MA and the membrane lipid phosphatidylinositol 4,5 bisphosphate [PI(4,5)P<sub>2</sub>] [40, 52, 53, 56]. PI(4,5)P<sub>2</sub> is primarily found in the plasma membrane at low concentrations, between 1% and 5% of the membrane lipids [132], and serves as a lipid target for many plasma membrane proteins [44, 133-136]. PI(4,5)P<sub>2</sub> serves as a precursor for phosphatidylinositol 3,4,5-trisphosphate and phosphatidylinositol 1,4,5-trisphosphate, which are also important signaling lipids for the plasma membrane [44]. Plasma membrane PI(4,5)P<sub>2</sub> levels are maintained through regulation of phosphatidylinositol-monophosphate kinases that synthesize PI(4,5)P<sub>2</sub> and phosphatidylinositol phosphatases that cleave the phosphates [137]. Depletion of PI(4,5)P<sub>2</sub> from the plasma membrane through overexpression of polyphosphoinositide 5-phosphatase IV (5ptaseIV) results in retargeting of Gag to late endosomes [40]. Alternatively, overexpressing PI(4,5)P<sub>2</sub> in the cell through a constitutively active Arf6 protein will retarget Gag to PI(4,5)P<sub>2</sub>-enriched vesicles, where budding can occur, leading to the conclusion that PI(4,5)P<sub>2</sub> is the signaling molecule MA targets in the plasma membrane [40].

Determination of the region of matrix responsible for membrane binding was determined through mutant studies. Highly basic region mutants, especially double mutants of lysine residues 30 and 32, can retarget Gag to multivesicular bodies [52, 53]. Adding charge to the basic patch region in the I18K/L20K mutant results in increased binding to the plasma membrane [53]. Increased membrane binding can

also be accomplished by through the K26T/K27T double mutation as well as the I18E/L20E mutation [53, 56]. Another basic patch mutant, K18T, will also decrease matrix's ability to bind to membranes [56].

While the highly basic region plays a vital role in membrane targeting, recent work has suggested that MA's ability to bind to RNA may also play a role in membrane specificity [56, 69]. Matrix binding to eight specific tRNAs in the cell, and HBR lysine residue mutants have decreased ability to bind to tRNAs [69]. Membrane flotation assays have indicated that MA loses its specificity for PI(4,5)P<sub>2</sub>-containing membranes upon the addition of RNases to degrade the RNAs left over from the *in vitro* translation reaction, similar to the phenotype observed for the K26T/K27T mutant [56, 69].

Work in this chapter further investigates the role tRNA may play in regulating membrane targeting through liposome competition assays. These assays used <sup>1</sup>H-1D NMR spectrometry in order to measure myrMA's ability to bind to liposomes in the presence and absence of tRNA, and the conditions that affected this equilibrium.

### *Materials and Methods*

#### *Protein Expression and Purification*

Detailed protocols can be found in Chapter 2. Briefly, HIV-1 NL4-3 strain myrMA was expressed using a pETDuet vector containing genes for both HIV-1 MA and human N-myristoyltransferase. Transformed BL21-DE3-RIL *E. coli* cells were grown in 2-4L LB broth at 37°C until OD<sub>600</sub> ~0.6-0.7. Cells were induced using isopropyl β-thiogalactoside (1 mM) and continued to grow for 3.5-4 hours. Following lysing by microfluidization, the supernatant was purified by polyethylenimine

precipitation (0.15% w/v) and the protein salted out with ammonium sulfate (at 50% saturation). The resuspended precipitate was purified using ion exchange chromatography (Q and SP columns; GE Healthcare), hydrophobicity chromatography (Butyl column; GE Healthcare), and size exclusion chromatography (Superdex 200 G75 column; GE Healthcare). Molecular weights and myristoylation efficiency were determined by electrospray ionization mass spectrometry.

#### *tRNA Synthesis and Purification*

Detailed protocols can be found in Chapter 2. Briefly, DNA oligonucleotides (IDT Tech) were annealed and ligated to form DNA templates containing a T7 promoter site and the tRNA sequences. tRNAs were synthesized *in vitro* by T7 polymerase, and purified using sequencing gels, followed by electroelution, NaCl washes to remove residual acrylamide, and water washes to remove excess ions. After addition of MgCl<sub>2</sub> to a concentration of 5 mM, tRNA samples were boiled for 3 minutes and snap-cooled on ice immediately before dialysis overnight in buffers used for experiments.

#### *Liposome Preparation*

Liposomes were prepared from stock solutions of 1-palmitoyl-2-oleoyl-*sn*-glycero-3-phosphocholine (POPC), L- $\alpha$ -phosphatidylserine (PS), L- $\alpha$ -phosphatidylinositol-4,5-bisphosphate [PI(4,5)P<sub>2</sub>], and 1-stearoyl-2-arachidonoyl-*sn*-glycero-3-phospho-(1'-myo-inositol-3',5'-bisphosphate) [PI(3,5)P<sub>2</sub>], L- $\alpha$ -phosphatidylethanolamine (PE), and cholesterol dissolved in chloroform. All lipids were purchased from Avanti Polar Lipids. Appropriate amounts of lipids were measured into tubes and dried for at least

2 hours (normally overnight) using a centrifugal vacuum. See Table 1 for lipid compositions approximating raft and non-raft membranes, and Table 2 for MT4 plasma membrane, and HIV-1 lipid envelope approximations. Values for non-raft and raft with and without PI(4,5)P<sub>2</sub> taken from Mercredi *et al.* [36]. Values for MT4 plasma membrane and HIV-1 lipid envelope calculated from work by Brügger *et al.* [51]. Sphingomyelin was eliminated from the calculation, as it is primarily a component of the outer leaflet of the plasma membrane [51, 133, 138]. Plasmalogen-phosphatidylethanolamine (pl-PE) was combined with PE in the calculation. Cholesterol ratio was kept constant with phospholipid concentration. Lipids were reconstituted in buffer, vortexed to dissolve the lipids, and allowed to rehydrate at 37°C for at least one hour. Lipid solutions were submitted to three freeze-thaw cycles (3 minutes on dry ice, followed by 3 minutes in RT water), and liposomes formed through extrusion of the solution through a 100 nm polycarbonate membrane 28 times. All liposomes were used on the day of preparation, and reconstituted to a concentration of 7.6 mM lipids.

#### *1D NMR Liposome Assay*

1D NMR data were obtained on a 600 MHz Bruker Avance III spectrometer equipped with a cryogenic probe. All data were collected at 35°C. myrMA samples were incubated at room temperature for at least 20 minutes and at 35°C for at least 5 minutes before collecting data in 3 mm NMR tubes. <sup>1</sup>H-1D spectra were acquired with 512 transients, 1 sec relaxation delay, 32768 time domain points, and a spectral window of 16233 Hz.

## *Results*

### *Modification of the $^1\text{H}$ -1D NMR Experiment*

ITC was initially favored over  $^1\text{H}$ -1D NMR experiments [36, 139] due to overlap between the tRNA signals and protein signals in the amide region. However, large heats of dilution associated with titrating liposomes into the sample resulted in an effort to modify the NMR binding experiment. The amide region, between 8.0 and 9.5 ppm, was integrated in previous works to determine the amount of signal loss associated with myrMA binding to liposomes, excluding the areas associated with unstructured regions as they should not decrease upon binding [36]. However, as tRNAs also have amide groups, they have signals in the 8.0 to 9.5 ppm region that make it difficult to determine which signals are associated with RNA and which are with protein when the protein is in complex (Figure 4.1a). Due to this, two upfield peaks (Figure 4.1b) were selected for monitoring. These peaks correspond to side chain protons in residues I34 (-0.2 ppm) and L21 (-0.3 ppm) [30]. I34 is near the N-terminal myristoyl group, and does not appear to shift upon binding to tRNA, indicating that tRNA binding does not promote myristoyl exposure. L21 is located in the basic patch of matrix. Upon binding to myrMA, the peak associated with the L21 side chains shifts, indicating that the chemical environment of the protons has changed and suggesting that tRNA may be binding nearby or may induce a conformational change. Thus L21 serves as an indicator of tRNA binding that can be used to monitor saturation of myrMA with RNA.

While use of these peaks solves the problem of overlapping residues, it does present an additional challenge upon the addition of liposomes. Addition of the

liposomes may lead to some peak broadening in the amide region, but the large area associated with the region prevents the broadening from interfering greatly with the calculation of binding. Integrating area in the amide region indicates that less than 15% of myrMA binds to the neutral phosphatidylcholine (POPC) liposomes. However, addition of POPC liposomes leads to significant broadening of I34 and L21 peaks, with area loss calculations giving the misleading calculation of binding at approximately 40%. (Table 3, Figure 4.1c). Since binding to POPC liposomes was slight and peak broadening appeared to occur equally for all liposome compositions, myrMA's ability to bind to negatively charged liposomes, including those bound to PI(4,5)P<sub>2</sub>, were compared to myrMA incubated with POPC liposomes instead of protein alone.

#### *Comparison of <sup>1</sup>H-1D NMR Binding Assay Using His-tagged and Untagged Protein*

Previous work in our lab looked at the ability of myrMA alone to bind to liposomes [36]. This protein had a C-terminal 6XHis tag (myrMA-His) in order to more efficiently purify the protein. Histidine tags commonly interfere with RNA-protein interactions, as RNA can bind to the positively charged residues [140]. Early work with the myrMA-His protein resulted in precipitation of the sample upon addition of tRNA. Removal of the 6XHis tag necessitated adding hydrophobicity and size exclusion chromatography steps in order to remove impurities.

I compared the spectra of the two proteins to ensure the untagged protein behaves similarly to the 6XHis-tagged protein (Figure 4.2a). The myrMA-His protein has additional area near 7.0 ppm, a region associated with amine side chains. There are also differences near 7.8 ppm, an area that can encompass histidine backbone

amides [141]. With exceptions in those regions, the spectra overlay well, indicating no major change in protein folding.

In addition to having a similar fold, the two proteins respond similarly to the addition of liposomes (Figure 4.2b,c). Addition of 3.8 mM POPC liposomes results in a slight reduction in signal for both proteins, with 5% PI(4,5)P<sub>2</sub> liposomes resulting in much larger decreases. When observing the upfield I34 and L21 peaks, both proteins show significant peak broadening upon addition of POPC liposomes, with a further and similar decrease in signal upon addition of PI(4,5)P<sub>2</sub>-containing liposomes. Taken together, this indicates that the two proteins behave similarly for the <sup>1</sup>H-1D NMR binding assay.

#### *Effect of Liposome Freeze-Thaw Cycles*

Freeze-thaw cycles are necessary in order to stabilize large unilamellar vesicles (LUVs), the type of liposome used in these studies [142-144]. Previous work extruded liposomes immediately after reconstituting the lipids in buffer and vortexing to dissolve the lipid films [36]. In order to determine if the implementation of freeze-thaw cycles affected the <sup>1</sup>H-1D NMR binding assay, I compared the binding of myrMA-His to POPC liposomes (Figure 4.3). myrMA-His had slight, but similar binding to the POPC liposomes that were frozen and thawed and those that were not.

The results of the NMR binding assays indicate that the lack of a freeze-thaw process will not detrimentally change the outcome of the liposome binding assay. Because the assay only requires a large vesicle for myrMA to bind to, and does not require the vesicles to be of uniform size or shape, it is possible that instable liposomes forming larger vesicles will not affect myrMA's ability to bind to those

vesicles. It is also possible the conditions and compositions used in these assays do not require freeze-thaw cycles in order to maintain stability for one day.

#### *Effect of Buffer Choice Liposome Binding*

While previous experiments [36] were completed using a sodium phosphate buffer, the use of magnesium in the buffer necessitated a change in buffer composition. T7-transcribed tRNA<sup>Lys3</sup> requires magnesium in order to fold into its correct shape, as it does not have the modified bases that stabilize the RNA in cells [73]. Addition of 5 mM MgCl<sub>2</sub> to the 50 mM NaPO<sub>4</sub> buffer resulted in precipitate forming in the dialysis buffer overnight. This was most likely due to the magnesium and phosphate ions forming insoluble salts.

Tris and HEPES buffers were compared to sodium phosphate in order to determine an alternative buffer to use. All three solutions were 50 mM buffer, pH 7.4, with 100 mM NaCl, 5 mM MgCl<sub>2</sub>, and 5 mM BME. Although the magnesium was added shortly before dialysis to the sodium phosphate buffer, some precipitate formed, thus the buffer strength may not be 50 mM and there may be slightly less magnesium in solution. Overall, the three samples had similar chemical shifts in the amide region (Figure 4.4a). Slight disagreements occurred in the 8.0 to 8.4 ppm and 6.4 ppm ranges. When looking at the upfield I34 and L21 signals, there is a large difference between the sodium phosphate buffer and the other two buffers (Figure 4b). The sodium phosphate buffer has approximately 1.5-fold more signal than either the Tris or HEPES buffers. The sodium phosphate buffer still has the most signal upon addition of tRNA<sup>Lys3</sup>, but there is less of a decrease in the HEPES signal in comparison (Figure 4c). The tRNA-myrMA complex sample in Tris buffer had more

noise in the sample, making it difficult to compare to the others, but it seems to have the large signal reduction seen in the myrMA sample alone.

myrMA bound strongly to 5% PI(4,5)P<sub>2</sub> liposomes in the absence of tRNA<sup>Lys3</sup> for each of the three buffers, with no distinguishable signal detected (Figure 4d), a result consistent with the results of Mercredi *et al.* [36]. While it is difficult to determine the amount of binding that occurred in the presence of tRNA due to the broadening of peaks associated with the addition of liposomes, some signal remained for all three buffers, indicating that tRNA<sup>Lys3</sup> can block at least some binding to liposomes (Figure 4e).

Although there is little apparent difference in the spectra for the HEPES and Tris buffers, the Tris buffer did not buffer the samples as well as the HEPES buffer. Upon the addition of acidic liposomes containing high concentrations of PI(4,5)P<sub>2</sub>, the pH of the samples in Tris buffer dropped more than the samples in HEPES buffer. HEPES buffer was used in all the following experiments as a result.

#### *RNA Alone is Not Sufficient to Regulate Membrane Binding*

If the hypothesis that tRNA is the sole regulatory mechanism allowing myrMA to discriminate between the plasma membrane and other cell membranes is correct, the presence of tRNA should prevent binding to negative liposomes lacking PI(4,5)P<sub>2</sub>. However, liposomes containing PI(4,5)P<sub>2</sub> should outcompete tRNA and bind to myrMA. Using the upfield signals of the methyl groups for I34 and L21, <sup>1</sup>H-1D NMR liposome assays were used to determine if tRNA could allow myrMA to discriminate between negative liposomes containing and lacking PI(4,5)P<sub>2</sub>. Since myrMA only slightly binds to neutral liposomes containing POPC, and the POPC

liposomes can induce broadening in the I34 and L21 peaks similar to negatively charged liposomes, all samples were compared to myrMA or the tRNA-myrMA complex incubated with POPC liposomes. In the absence of tRNA, myrMA bound indiscriminately to negatively charged membranes, with increased membrane binding correlating with negative charge of the liposome. As the concentration of phosphatidylserine (PS) in the liposomes increased, a higher percentage of myrMA bound, with most of the protein bound at a PS composition of 35% (Figure 4.5a). tRNA<sup>Lys3</sup> prevented binding to PS-containing liposomes, including those with high concentrations of PS similar to physiological concentrations of the inner leaflet [51, 133, 145], consistent with the hypothesis that tRNA regulates myrMA's ability to discriminate between membranes. A similar phenomenon occurred with liposomes containing phosphatidylinositol 3,5-bisphosphate (Figure 4.5b), a lipid with a similar charge as phosphatidylinositol 4,5-bisphosphate that is found in intercellular membranes at low concentrations during times of osmotic stress [146].

If tRNA allows myrMA to discriminate between membranes because PI(4,5)P<sub>2</sub> outcompetes tRNA for the basic patch, myrMA should bind to PI(4,5)P<sub>2</sub>-containing liposomes in both the presence and the absence of tRNA. Titrating PI(4,5)P<sub>2</sub>-containing liposomes into myrMA in the absence of tRNA resulted in a titration curve similar to the one seen for PI(3,5)P<sub>2</sub>-containing liposomes (Figure 4.5c). However, when saturated with tRNA<sup>Lys3</sup>, myrMA does not readily bind to PI(4,5)P<sub>2</sub>-containing liposomes. tRNA<sup>Lys3</sup> outcompeted the liposomes not just at physiologically relevant concentrations, but at concentrations far higher than would occur in a cell [147, 148] and those found enriched in HIV-1 virions [148].

Interestingly, this result was not specific to tRNA<sup>Lys3</sup> alone, and was also seen when incubating myrMA with tRNA<sup>IleGAU</sup> (Figure 4.6). In all cases, in the absence of tRNA, myrMA increasingly bound as the liposomes became more negative, with tRNA preventing binding (Figure 4.7).

#### *tRNA Prevents Binding to Raft-Like Liposomes*

Although tRNA prevented binding to liposomes containing high concentrations of PI(4,5)P<sub>2</sub>, it is possible that myrMA required the interactions between multiple phospholipids in order to successfully bind to model membranes in the presence of RNA. Evidence suggests that Gag assembles at raft-like microdomains enriched in cholesterol [45-49] and that the HIV-1 lipid envelope has a raft-like composition [50, 51]. Previous studies in our lab used model membranes with plasma membrane compositions mimicking the raft and non-raft domains of the plasma membrane. These studies found that myrMA required PI(4,5)P<sub>2</sub> to bind to non-raft liposomes, but would bind to raft domains in both the presence and absence of PI(4,5)P<sub>2</sub> [36]. We saw similar results in the absence of tRNA (Figure 4.8a). However, the presence of tRNA<sup>Lys3</sup> prevented binding to both rafts and non-rafts, even with the addition of PI(4,5)P<sub>2</sub> (Figure 4.8b).

The previous work took into consideration the composition of rafts and non-rafts as reported in Brügger *et al* [51]. and Chan *et al.* [148], but treated cholesterol as a phospholipid when calculating percentages. As cholesterol inserts into the fatty acid chains, treating it as a percentage of the phospholipids may skew the composition of the membranes when accounting for differences in the inner and outer leaflets. In order to confirm the result, liposomes with compositions similar to the plasma

membrane of MT4 cells and the lipid envelope of the HIV-1 virus as reported [51] were used as well. Differences in the composition of the inner and outer leaflet due to membrane asymmetry [133, 138, 145] were taken into account, keeping the ratio of cholesterol to phospholipid constant and only adjusting the percentages of the relevant phospholipids. These membranes had a stronger negative charge than those used previously due to increased concentrations of phosphatidylethanolamine, and had similar cholesterol concentrations. myrMA bound strongly to both the MT4 plasma membrane model and the HIV-1 envelope model, despite the absence of PI(4,5)P<sub>2</sub> (Figure 4.8c). No appreciable increase in binding occurred upon the addition of PI(4,5)P<sub>2</sub>. However, despite the high negative charge, tRNA<sup>Lys3</sup> still successfully prevented binding to all liposomes, including those with PI(4,5)P<sub>2</sub> (Figure 4.8d).

#### *The Effect of pH on Liposome Binding*

Chapter 3 discusses the role of the myristoyl group in myrMA-tRNA interactions. Myristoyl exposure weakens the interaction between myrMA and tRNA, and may play a role in membrane targeting, as myristoyl group exposure occurs as myrMA attaches to the plasma membrane. Unmyristoylated matrix mutants do not bind as well to the plasma membrane as the lack of myristoyl group prevents anchoring to the membrane [36, 37]. If myristoyl exposure weakens myrMA-tRNA interactions, perhaps myristoyl exposure would allow PI(4,5)P<sub>2</sub>-containing membranes to outcompete tRNA<sup>Lys3</sup>. Myristoyl exposure increases *in vitro* upon a decrease in pH or increase in concentration [31]. However, pH gradients exist in the

cell [130], making it likely that myrMA would encounter a lower pH while traveling through the cell.

To test this, liposomes were prepared in 50 mM HEPES buffer, 100 mM NaCl, 5 mM MgCl<sub>2</sub>, and 5 mM BME at pH 6.5, 7.0, and 7.4 (Figure 4.9). At pH 7.4, the myristoyl group is nearly fully sequestered [31]. myrMA bound almost completely to liposomes containing 5% PI(4,5)P<sub>2</sub> and 50% PS, but did not bind as well to liposomes containing 5% PI(3,5)P<sub>2</sub>, which is slightly less acidic than PI(4,5)P<sub>2</sub> due to the phosphate positions allowing stronger hydrogen bonding interactions to occur to stabilize the protonated form of the headgroup [149]. At pH 7.4, tRNA<sup>Lys3</sup> was able to prevent binding to PI(3,5)P<sub>2</sub> and PS liposomes. There was a slight decrease in signal for PI(4,5)P<sub>2</sub>-containing liposomes, but replicates from earlier samples (Figure 4.5) indicate this was probably not significant. At pH 7.0, myrMA should remain mostly sequestered. Results were similar to those at pH 7.4, with the PI(4,5)P<sub>2</sub> liposomes binding to myrMA in the absence of tRNA and tRNA<sup>Lys3</sup> preventing binding to 5% PI(4,5)P<sub>2</sub> liposomes. At pH 6.5, the myristoyl group should be predominately sequestered, with a significant population of the molecules in the exposed conformation [31]. Despite this, at pH 6.5 tRNA<sup>Lys3</sup> could successfully outcompete 5% PI(4,5)P<sub>2</sub> liposomes for myrMA.

#### *Work with Multimerized Matrix*

Many groups have shown that Gag has an RNA-dependent specific affinity for PI(4,5)P<sub>2</sub>-containing liposomes through membrane flotation assays [56, 69, 129]. Additionally, other labs have used fluorescence-based experiments to determine that PI(4,5)P<sub>2</sub> liposomes will outcompete DNA for bead-bound myrMA [62]. This leads

to the question of why their samples bind specifically to PI(4,5)P<sub>2</sub>-containing liposomes in the presence of RNA and in the previous experiments tRNA could fully block liposome binding.

The first clue may lie in the constructs used for the experiments. Most of the membrane binding assays found in the literature use full-length Gag in their studies [56, 69, 129], while work in this dissertation only uses the matrix domain. Gag has a much higher affinity for membranes than matrix alone, which is thought to be due to increased myristoyl exposure [38, 39]. While lowering the pH and promoting myristoyl exposure did not change the results of the liposome competition assays, there may be a role the myristoyl group plays when part of the full-length Gag polyprotein. Membrane targeting studies using the myrMA domain fused to a FK506-binding protein, which can be induced to form a dimer upon addition of a chemical agent, found that induction of the myrMA dimer led to increased plasma membrane binding [32], suggesting that Gag's increased membrane affinity may be due to Gag multimerization through the capsid domain. Further work using liposome flotation assays confirmed that multimerization of the matrix domain promoted matrix membrane binding [32]. While other studies have used the matrix domain alone, the matrix was bound to beads [62], which may have inadvertently mimicked the multimerization of Gag by tethering the protein in a highly concentrated state.

In order to test this hypothesis that Gag multimerization is essential for membrane selectivity, I constructed three matrix constructs with leucine zipper domains, capable of producing stable matrix dimers, trimers, and hexamers. The goal was to determine if multimerization weakened tRNA-myrMA interactions, and if so,

determine if multimerization allowed PI(4,5)P<sub>2</sub> to outcompete tRNA for matrix. These constructs were used instead of matrix-capsid constructs because the capsid-capsid interactions are difficult to control [150], and the equilibrium between monomer and multimer may affect ITC results. Unfortunately the multimerized matrix constructs were very difficult to purify, as they tended to aggregate in solution before completion of purification. This could be due to the myristoyl exposure causing aggregation and precipitation, as myristoyl exposure induced by concentration of myrMA can have a similar effect. Enough trimeric myrMA was purified in order to run an EMSA analysis (Figure 4.10), which had a band shift similar to the one observed for wild-type myrMA. However, there was not enough protein to complete ITC analysis or membrane competition assays, so it is impossible to determine if multimerization did indeed weaken the interaction to the point PI(4,5)P<sub>2</sub> could outcompete tRNA for myrMA binding.

The next set of experiments used a myristoylated matrix-capsid construct (myrMACA) in liposome binding assays to determine if multimerization could affect liposome binding. Although ITC experiments with a myristoylated matrix construct with the N-terminal domain of capsid (myrMACA<sup>NTD</sup>) only showed a slight decrease in affinity for tRNA<sup>Lys3</sup> compared to myrMA, one would not expect a large difference between the two constructs, as the main multimerization domain for the protein is in the C-terminal domain of capsid and myrMACA<sup>NTD</sup> should exist primarily as a monomer in solution [150, 151]. The addition of the C-terminal domain should reveal if the formation of dimers plays a role. The main reason for using the leucine zipper domains attached to matrix instead of myrMACA itself is that myrMACA does not

form very stable dimers, and this equilibrium between monomer and dimer could make it difficult to determine the protein's affinity for tRNA<sup>Lys3</sup> using the ITC. However, this equilibrium should not disrupt membrane binding assays in the NMR, as long as the protein still has resolved upfield peaks that do not overlap with RNA peaks. After successful purification of the myrMACA protein, liposome binding assays revealed that the protein loses its affinity for PI(4,5)P<sub>2</sub>-containing liposomes in the absence of tRNA (Figure 4.11), adding another layer to the question of how other domains of Gag affect membrane binding. Some have suggested that in the myrMACA construct, the capsid domain binds to the matrix domain [152], and it's possible that the liposome assay result is simply an artifact from a construct that does not exist in cells infected with the HIV virus. HSQC experiments determining if matrix peaks shift upon addition of the capsid protein could quickly determine if these MA-CA interactions are occurring, or if some other mechanism is responsible.

### *Discussion*

In order to determine if tRNA plays a regulatory role in myrMA-membrane interactions, a competition assay must measure myrMA's affinity for membranes in the presence of RNA and compare it to interactions in the absence of RNA. Initial trials with ITC were not successful, as titrating the liposomes into the cell resulted in large heats of dilution. <sup>1</sup>H-1D NMR liposome binding assays have been utilized in the past to measure myrMA's ability to bind liposomes [36]. The addition of RNA presented some challenges, as the amide region of the spectra used to determine binding also had signals from the RNA, making it difficult to discern signal loss due to binding. Well-resolved peaks upfield associated with I34 and L21 allow

measurement of signal loss upon RNA binding, as they are isolated from RNA signals. This assay does present a different challenge, as addition of liposomes causes these peaks to broaden. The effect of the broadening can be controlled by comparing normalizing binding to a neutral liposome, POPC, which binds less than 15% to myrMA but still broadens the I34 and L21 upfield peaks. While researching liposomes for this assay, many articles suggested freeze-thaw cycles in order to promote the stability of the liposomes [142-144]. Comparing  $^1\text{H}$ -1D NMR spectra with liposomes that underwent freeze-thaw cycles with those that did not, it was concluded that the freeze-thaw process did not negatively affect the assay and a freeze-thaw step was added to all future liposome preparations. Work with the 6XHis-tagged protein also indicated that the loss of the tag did not negatively affect the assay, allowing liposome binding assays through the use of NMR to determine if tRNA could play a role in myrMA's membrane binding.

If tRNA allows myrMA to discriminate between PI(4,5)P<sub>2</sub>-containing membranes and those that have other phospholipids, the addition of tRNA should prevent binding to liposomes lacking PI(4,5)P<sub>2</sub>, but should not fully abrogate binding to liposomes containing the lipid. While tRNA<sup>Lys3</sup> was able to prevent binding to negative liposomes that lacked PI(4,5)P<sub>2</sub>, it was also able to prevent binding to liposomes containing PI(4,5)P<sub>2</sub>. tRNA<sup>Lys3</sup> was not the only RNA able to prevent binding, as tRNA<sup>IleGAU</sup>, which is not predicted to bind specifically to myrMA [69], also prevented binding to PI(4,5)P<sub>2</sub>-containing liposomes. The tRNAs abrogated binding not just to liposomes containing low levels of PI(4,5)P<sub>2</sub>, but liposomes with high, non-physiologically relevant concentrations [147, 148]. These results were

consistent with the dissociation constants observed for tRNA<sup>Lys3</sup>-myrMA interactions reported in this work and myrMA-PI(4,5)P<sub>2</sub> interactions reported previously [36]. Mercredi *et al.* reported a K<sub>d</sub> apparent of  $10.2 \pm 2.1 \mu\text{M}$ , a 20-fold weaker interaction than the  $0.63 \pm 0.03 \mu\text{M}$  K<sub>d</sub> detected by ITC in this work.

It is possible that PI(4,5)P<sub>2</sub> alone is not enough to allow membranes to outcompete tRNA, as membranes are a mixture of different phospholipids. myrMA is reported to bind or to move to lipid rafts in the cell [49, 51, 148, 153, 154]. Liposome binding assays have reported that myrMA requires PI(4,5)P<sub>2</sub> to bind to non-raft membranes, but does not require PI(4,5)P<sub>2</sub> to bind to raft-like membranes [36]. I was able to replicate those results in the absence of tRNA<sup>Lys3</sup>, but found that the addition of cholesterol and other negative phospholipids associated with rafts did not allow the liposomes to outcompete tRNA<sup>Lys3</sup> even in the presence of PI(4,5)P<sub>2</sub>.

Others have completed liposome flotation assays in which PI(4,5)P<sub>2</sub> was able to outcompete tRNA for Gag binding [53, 56, 69]. The work in this chapter indicates that some other mechanism is required to regulate membrane binding and targeting other than the presence of tRNA. The other studies use Gag with both capsid and nucleocapsid domains instead of the matrix domain alone, which may account for the discrepancies seen between this work and others. Previous studies that had PI(4,5)P<sub>2</sub> outcompete RNA using matrix alone used matrix bound to beads [62, 63], which may result in a concentration shift that promotes myristoyl exposure. As shown in Chapter 3, myristoyl exposure weakens the interaction between tRNA and myrMA.

In order to test the theory that myristoyl group exposure weakened tRNA-myrMA interactions in order for PI(4,5)P<sub>2</sub> to outcompete tRNA, I performed a set of

liposome competition experiments at different pH values. As the pH decreases, the myristoyl group should become more exposed, leading to an increase in membrane binding. Despite lowering the pH to 6.5, no significant binding was observed with liposomes containing 5% PI(4,5)P<sub>2</sub>. At pH 6.5, there is more myristoyl exposure than at pH 7.0 [31], but the myrMA protein is still in the predominately sequestered conformation. There may be another mechanism needed in order to fully push the protein into a predominately exposed, membrane-binding conformation.

One possible conclusion is that multimerization of the Gag polypeptide through the capsid domain may be essential for forming higher order conformers, which then promote myristoyl exposure and weaken tRNA-myrMA interactions. This would account for the differences seen between our experiments and liposome flotation assays using the full Gag polypeptide. This multimerization may play the key role in allowing myrMA to discriminate between membranes. Work with constructs able to maintain a stable multimer were not successful, primarily due to the difficulty of purifying the constructs. If myristoyl exposure is promoted upon multimerization as reported [32], this could account for the difficulties in purifying the multimerized constructs. However, trimerization does not completely abolish tRNA binding, as the slight protein purified in the trimeric state also formed band shifts during EMSA analysis. Work with the myrMACA constructs was also inconclusive, as the construct lost its ability to bind to membranes in the absence of RNA. This could be due to MA-CA interactions, as the capsid domain has been reported to fold over and bind to the matrix domain [152]. However, the Gag protein

also has other domains, such as NC, and the MA-CA interactions may be an artifact of a construct that does not exist in a cell.

Future work should use Gag or other MA constructs with the ability to multimerize. One such possible construct is a MACA<sup>NTD</sup> construct with the A14C/E45E mutation, which can induce formation of a hexamer upon removal of reducing agent [151]. While the mutation has only been studied in capsid constructs, if myrMA links to MA through a flexible linker as reported [27] it is possible that this construct will work for these experiments. However, work with large constructs may make the <sup>1</sup>H-1D NMR binding assay difficult, as the complex may become too large to visualize on the NMR. Other liposome binding assays, such as liposome flotation assays, need to be considered in order to determine if multimerization plays a role in membrane specificity.

**Table 4.1: Percent compositions of non-raft and raft liposomes.**

	Non-Raft	Non-Raft + PI(4,5)P <sub>2</sub>	Raft	Raft + PI(4,5)P <sub>2</sub>
Cholesterol	17	17	44	44
PC	71	70	32	29
PE	6	6	8	8
PS	6	6	16	16
PI(4,5P) <sub>2</sub>	-	1	-	3

**Table 4.2: Percent compositions of model MT4 plasma membrane and HIV-1 lipid envelope liposomes.**

	MT4 PM	MT4 PM + PI(4,5)P <sub>2</sub>	HIV Lipid Envelope	HIV-1 Lipid Envelope + PI(4,5)P <sub>2</sub>
Cholesterol	32.4	32.4	32.4	32.4
PC	19.6	19.6	10.5	10.5
PE	27.7	27.7	35.2	35.2
PS	20.3	18.3	21.6	16.6
PI(4,5P) <sub>2</sub>	-	2	-	5

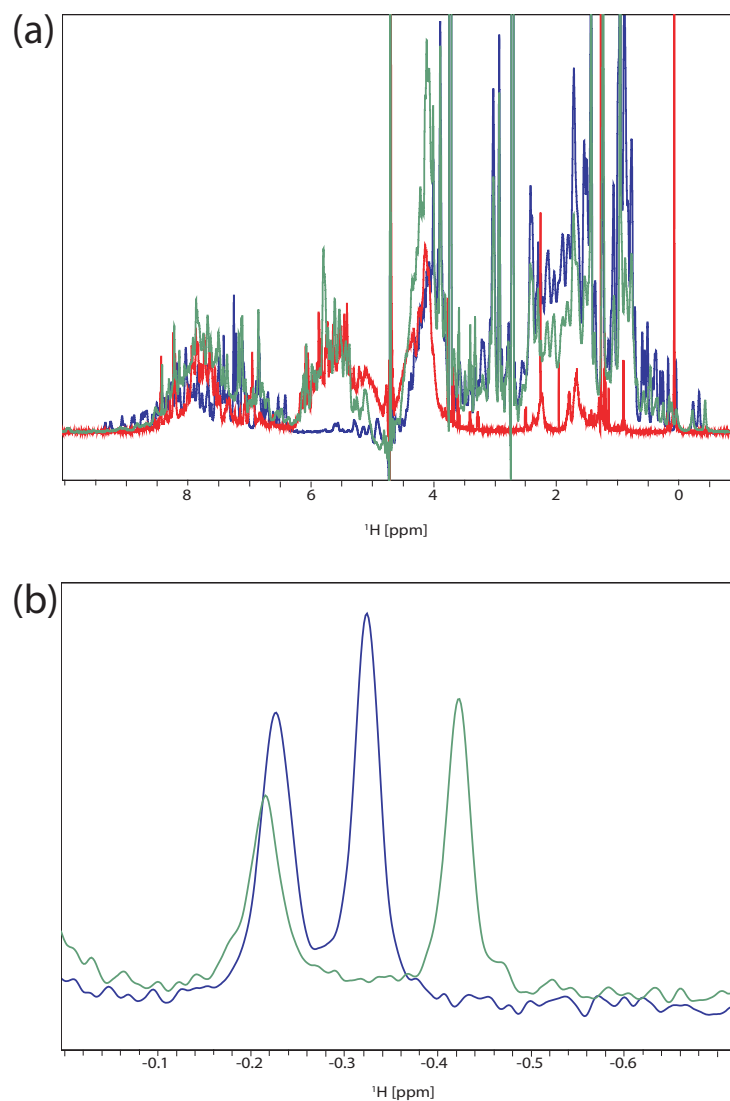


**Figure 4.1: <sup>1</sup>H-1D NMR spectra of myrMA and the myrMA-tRNA<sup>Lys3</sup> complex.** (a) Previous NMR liposome binding assays used the amide region signal loss (8.0 to 9.5 ppm) to determine binding to liposomes. The myrMA protein (blue) has signal overlap with tRNA signals (red) in the myrMA-tRNA<sup>Lys3</sup> complex (green) that make it difficult to use this region to determine myrMA's ability to bind liposomes in the presence of RNA. (b) Liposome binding experiments using RNA looked at signal loss for two upfield shifted side chain methyl groups, I34 (-0.2 ppm) and L21 (-0.3 ppm). L21 shifts upon addition of tRNA to the sample (-0.45 ppm).

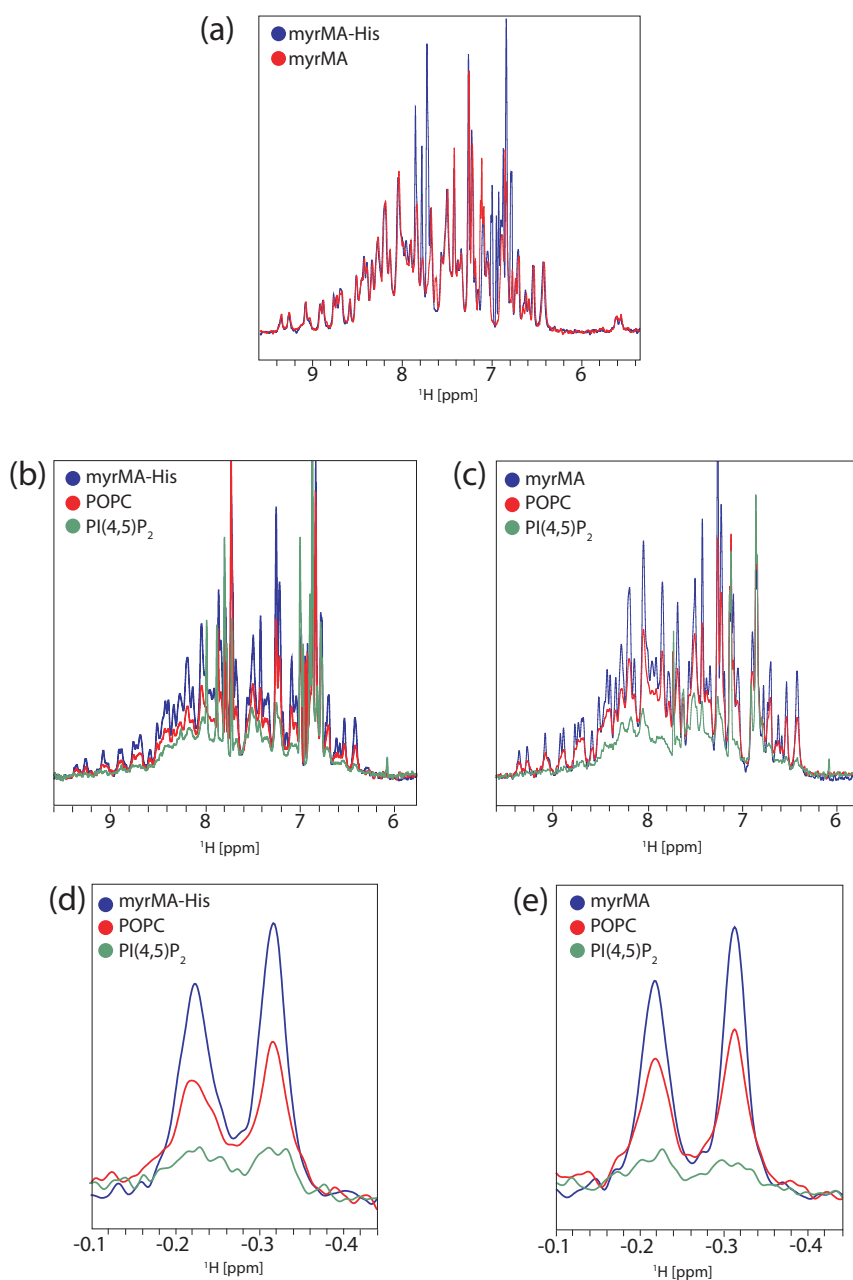


**Figure 4.2: Comparison of the 6XHis-tagged and untagged myrMA proteins.** (a) Untagged myrMA has a similar fold as 6XHis-tagged myrMA, as they have similar  $^1\text{H}$ -1D spectra. Both the myrMA-His protein (b) and untagged protein (c) bind similarly to neutral and negative liposomes. (d) The peak broadening of the upfield methyl side chain signals upon addition of liposomes is similar for the His-tagged protein (d) and untagged protein (e). All samples in 50 mM  $\text{NaPO}_4$ , pH 7.4, 100 mM  $\text{NaCl}$ , 5 mM  $\text{MgCl}_2$ , and 5 mM BME.

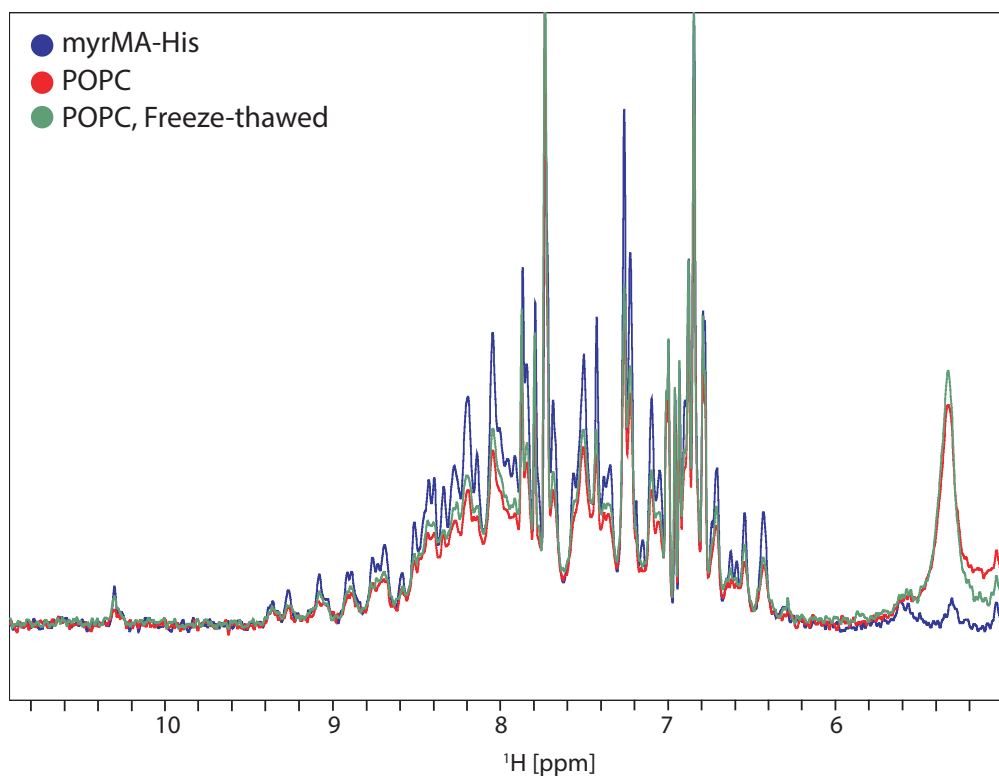


**Figure 4.3: Effect of freeze-thaw cycles on myrMA-liposome interactions.** Little binding occurs upon addition of POPC liposomes (<15%). Liposomes that underwent freeze-thaw cycles (red) bound similarly to myrMA as those that did not (green).

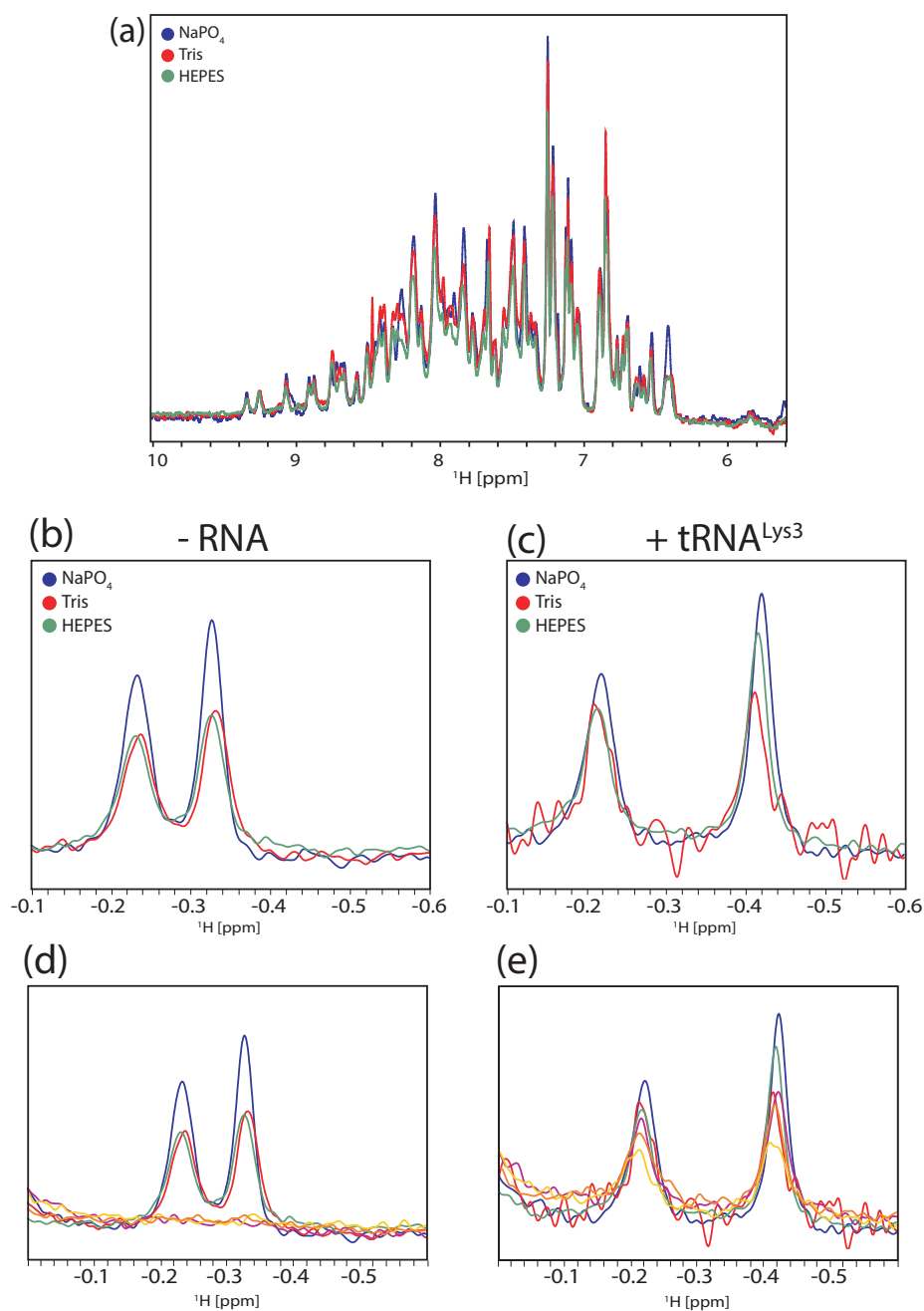


**Figure 4.4: Buffer effect on liposome binding assay.** (a) Signals in the amide region were similar for all three buffers tested. Signal sensitivity decreased in the upfield methyl region for the Tris and HEPES buffer in the absence (b) and presence (c) of  $\text{tRNA}^{\text{Lys3}}$ . myrMA bound completely to 5% PI(4,5) $\text{P}_2$  liposomes in the absence of tRNA (d), but not in the presence (e) of tRNA.

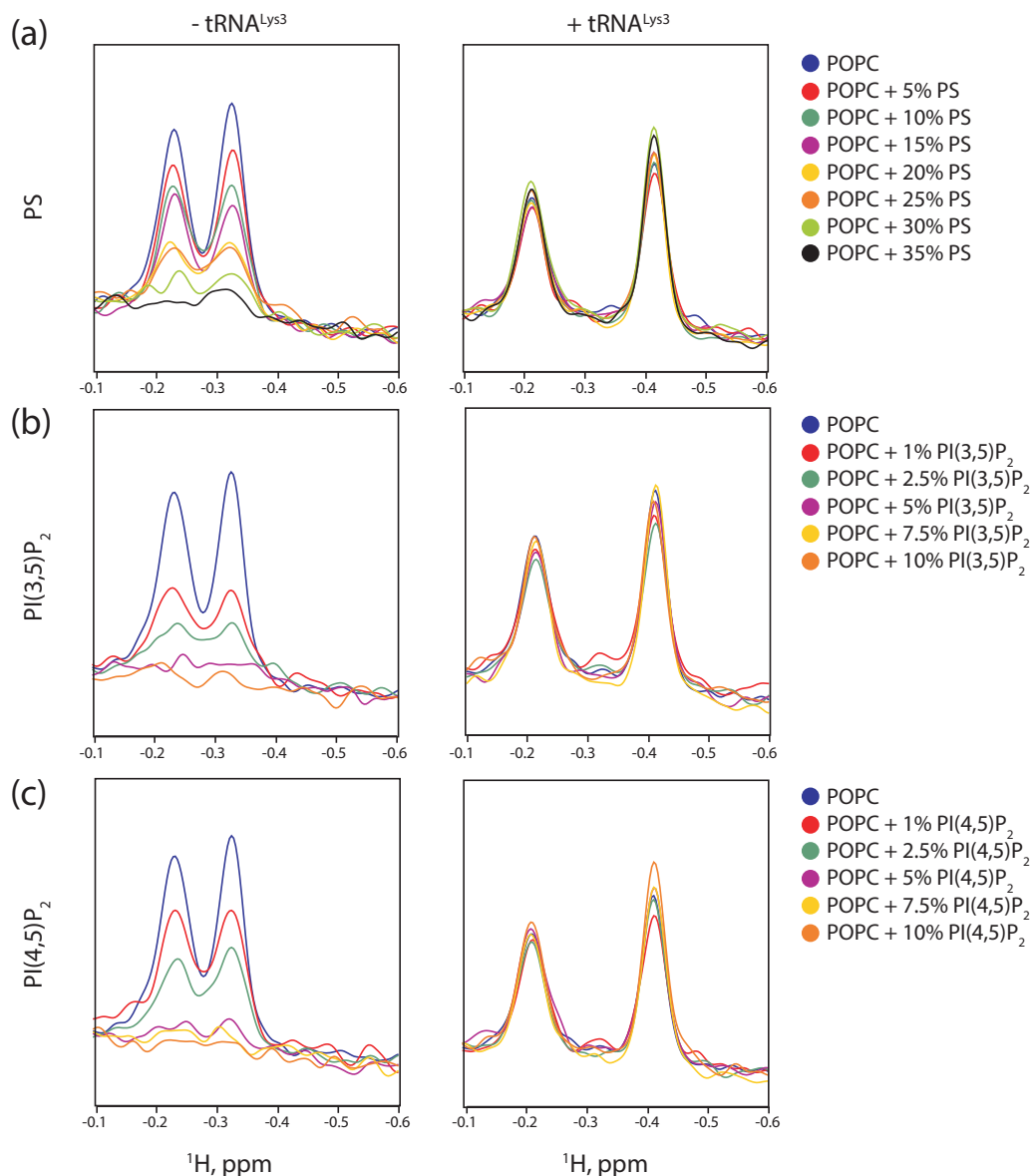


**Figure 4.5: Negative phospholipids, including PI(4,5)P<sub>2</sub> cannot outcompete tRNA<sup>Lys3</sup>.** (a) <sup>1</sup>H-1D NMR spectra of myrMA titrated with liposomes containing increasing amount of PS in the absence (left) and presence (right) of tRNA<sup>Lys3</sup>. (b) <sup>1</sup>H-1D NMR spectra of myrMA titrated with liposomes containing increasing amount of PI(3,5)P<sub>2</sub> in the absence (left) and presence (right) of tRNA<sup>Lys3</sup>. (c) <sup>1</sup>H-1D NMR spectra of myrMA titrated with liposomes containing increasing amount of PI(4,5)P<sub>2</sub> in the absence (left) and presence (right) of tRNA<sup>Lys3</sup>.

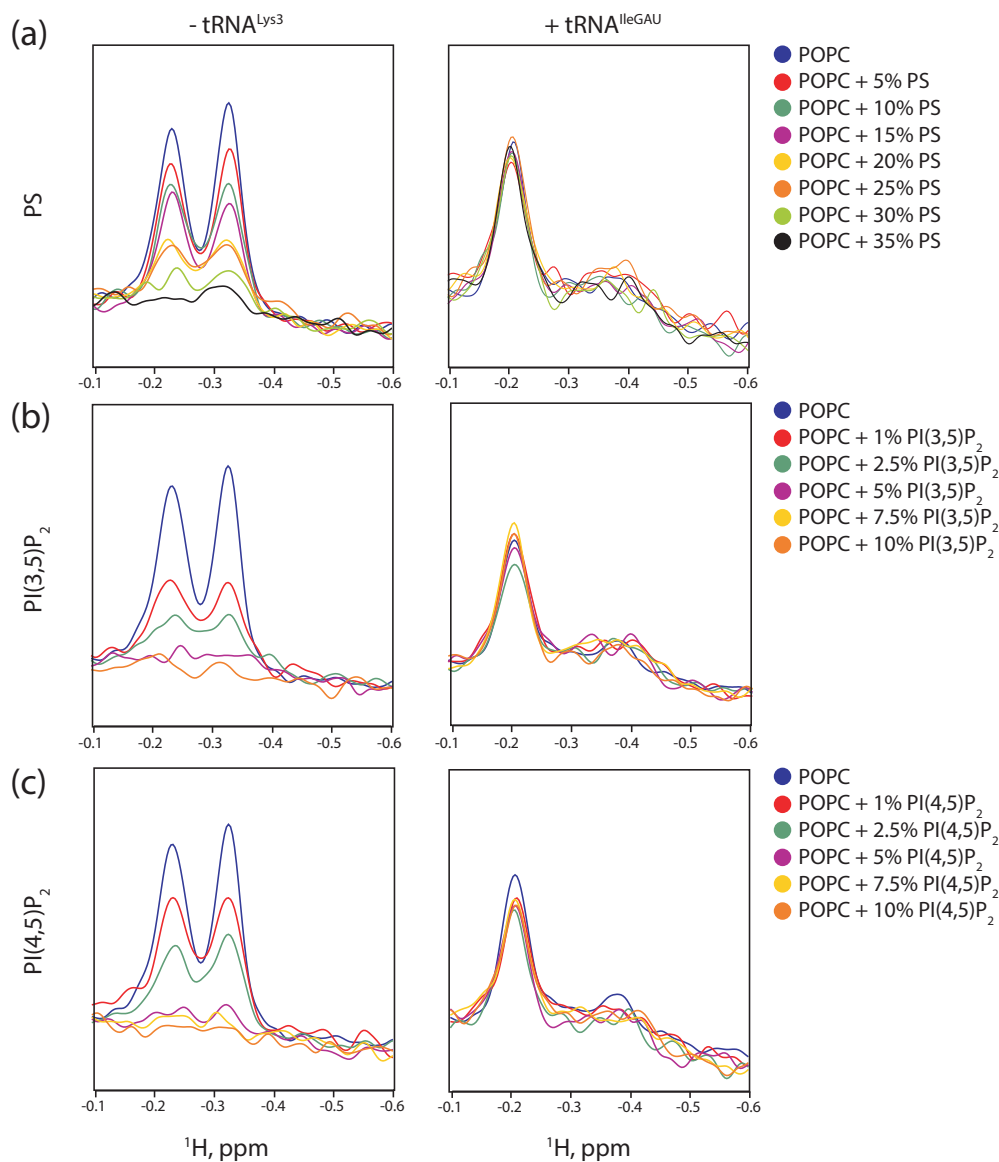


**Figure 4.6: tRNA<sup>IleGAU</sup> prevents binding to negatively charged liposomes.** (a)  $^1\text{H}$ -1D NMR spectra of myrMA titrated with liposomes containing increasing amount of PS in the absence of RNA (left) and presence of tRNA<sup>IleGAU</sup> (right). (b)  $^1\text{H}$ -1D NMR spectra of myrMA titrated with liposomes containing increasing amount of PI(3,5) $\text{P}_2$  in the absence of RNA (left) and presence of tRNA<sup>IleGAU</sup> (right). (c)  $^1\text{H}$ -1D NMR spectra of myrMA titrated with liposomes containing increasing amount of PI(3,5) $\text{P}_2$  in the absence of RNA (left) and presence of tRNA<sup>IleGAU</sup> (right).

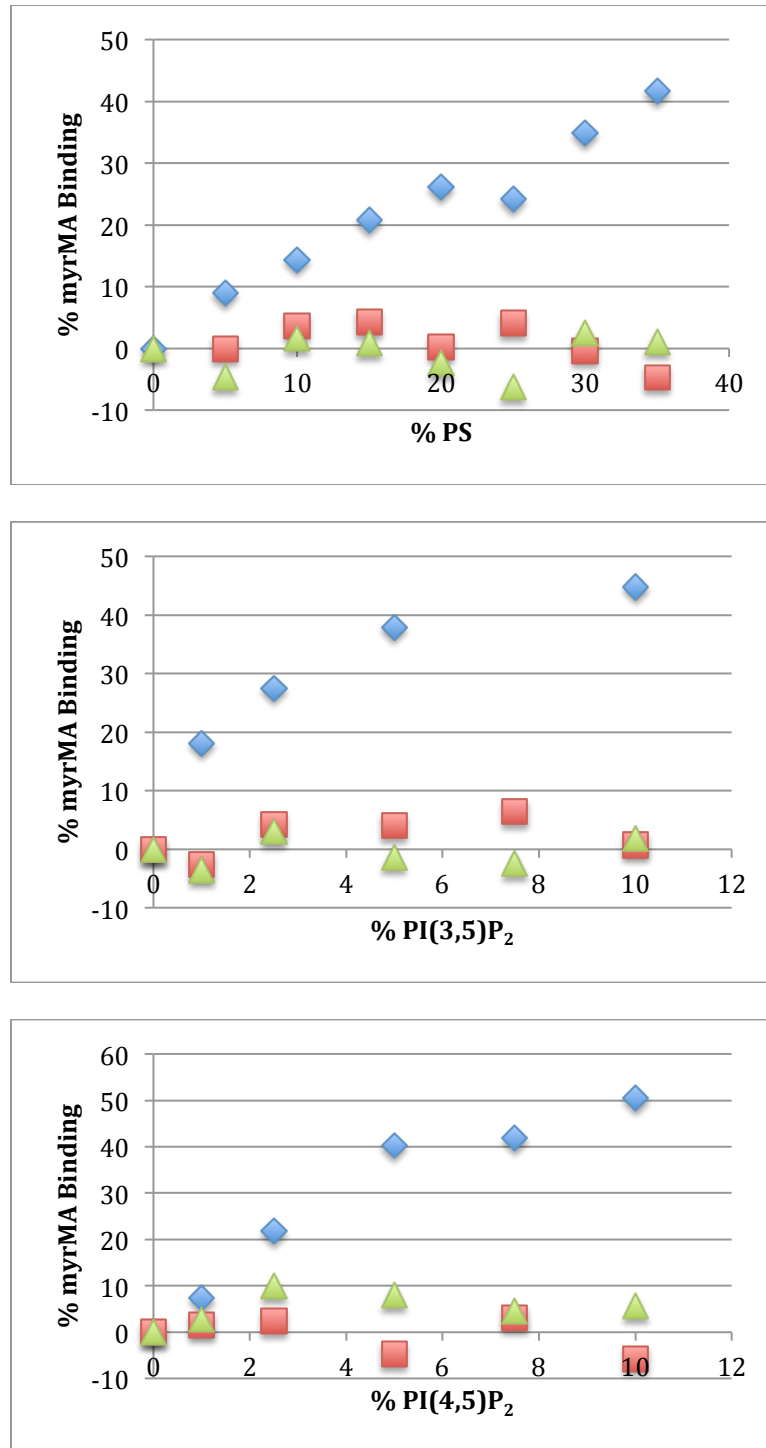


**Figure 4.7: Liposome binding in the presence and absence of tRNA.** In the absence of tRNA (blue circles), myrMA has increased binding as the percentage of negative lipid increases in the liposome. The presence of tRNA<sup>Lys3</sup> (red squares) and tRNA<sup>IleGAU</sup> (green triangles) prevent liposome binding. Area used to calculate % myrMA binding were normalized to myrMA's signal loss upon binding to POPC liposomes.

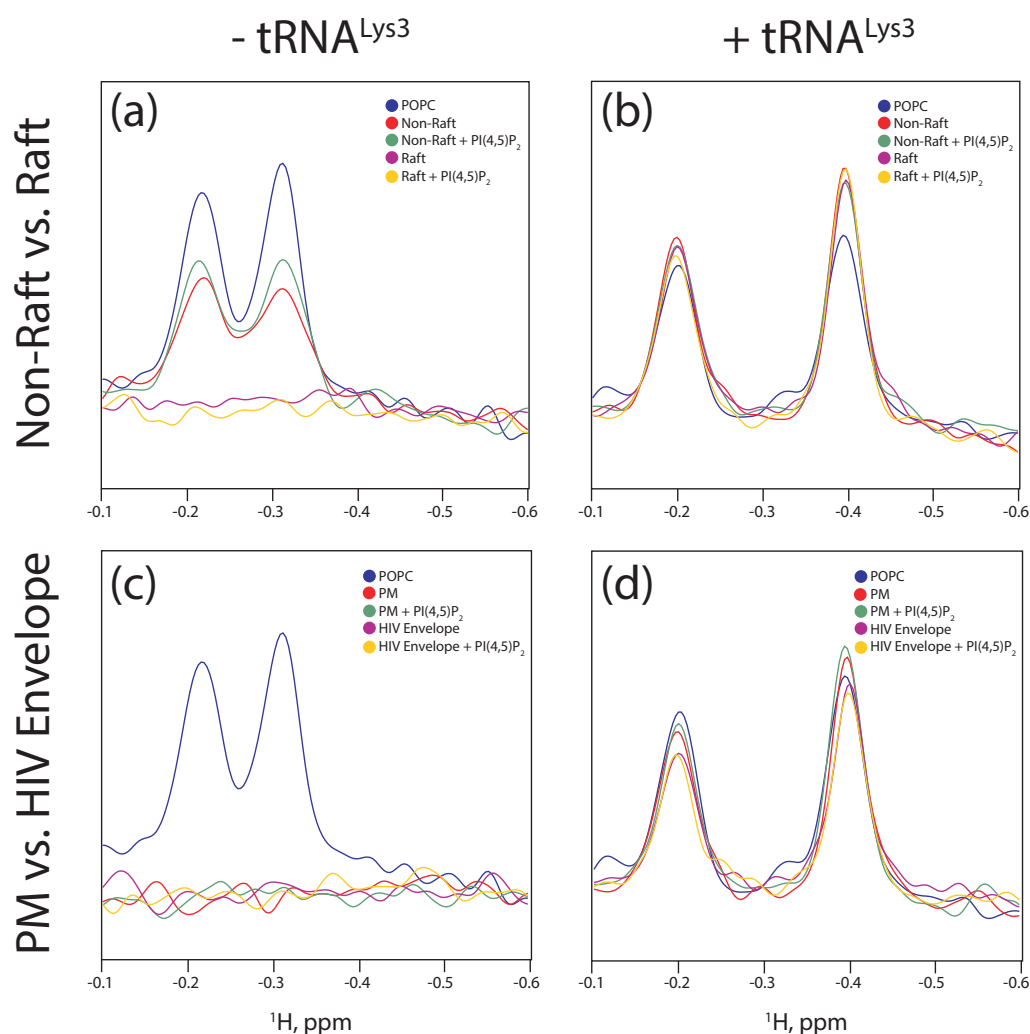


**Figure 4.8:  $\text{tRNA}^{\text{Lys3}}$  prevents myrMA interactions with raft-like liposomes.** (a) Interactions between myrMA and liposomes with raft and non-raft compositions in the absence of  $\text{tRNA}^{\text{Lys3}}$ . (b) Interactions between myrMA and liposomes with raft and non-raft compositions in the presence of  $\text{tRNA}^{\text{Lys3}}$ . (c) Titration of myrMA with liposomes approximating the inner leaflet of MT4 cells and the HIV-1 lipid envelope in the absence of RNA. (d) Titration of myrMA with liposomes approximating the inner leaflet of MT4 cells and the HIV-1 lipid envelope in the presence of tRNA.

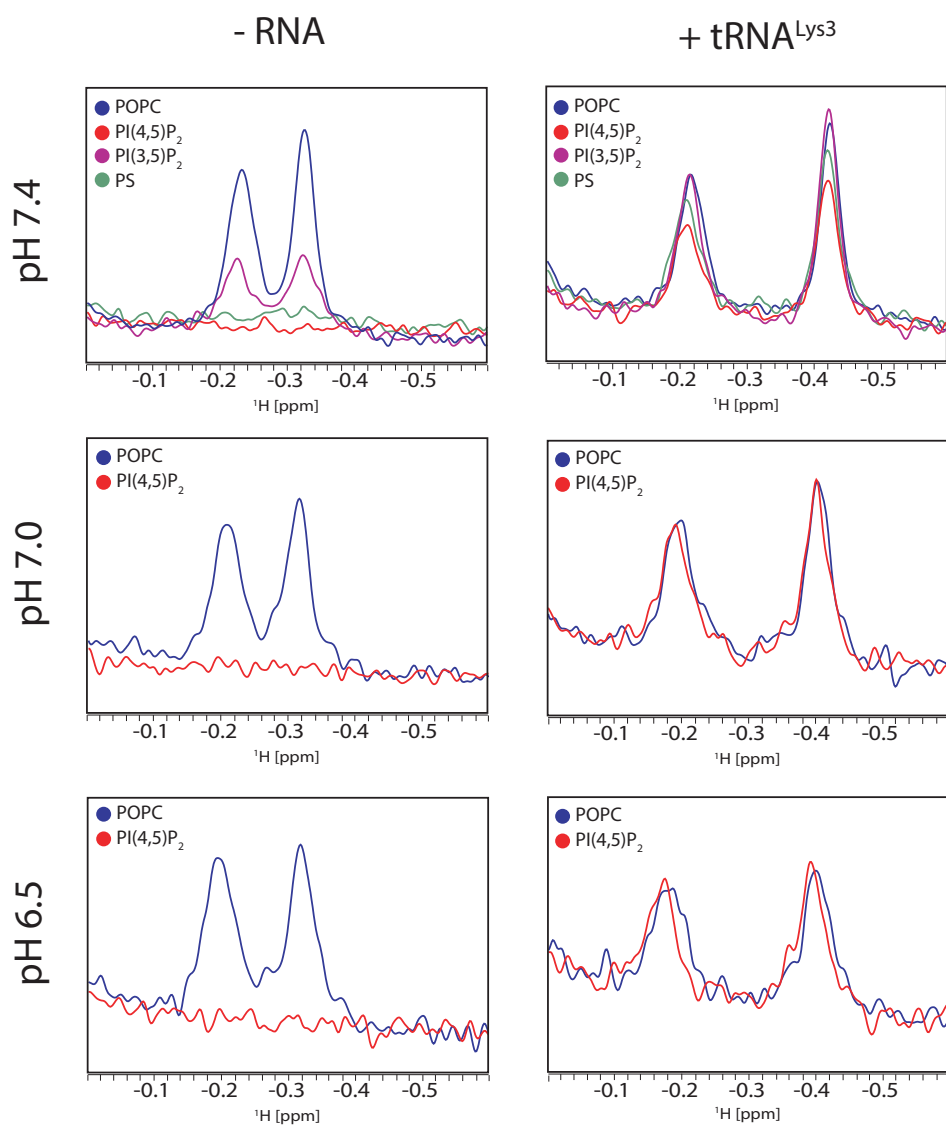


**Figure 4.9: Reducing the pH does not allow PI(4,5)P<sub>2</sub>-containing liposomes to outcompete tRNA<sup>Lys3</sup>.** At pH 7.4, myrMA will bind to negative liposomes in the absence of tRNA<sup>Lys3</sup>, but binding is blocked upon addition of tRNA. A similar result is obtained at pH 7.0 and pH 6.5.

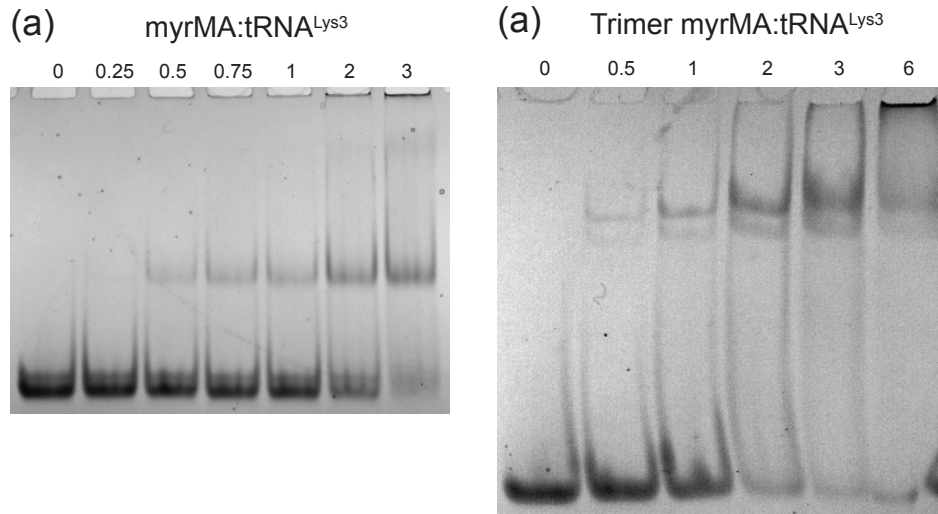


**Figure 4.10: Role of multimerization on tRNA binding.** Monomeric myrMA bound similarly to tRNA<sup>Lys3</sup> (a) as the trimeric myrMA protein (b). Each molar ratio is in units of monomer to tRNA.

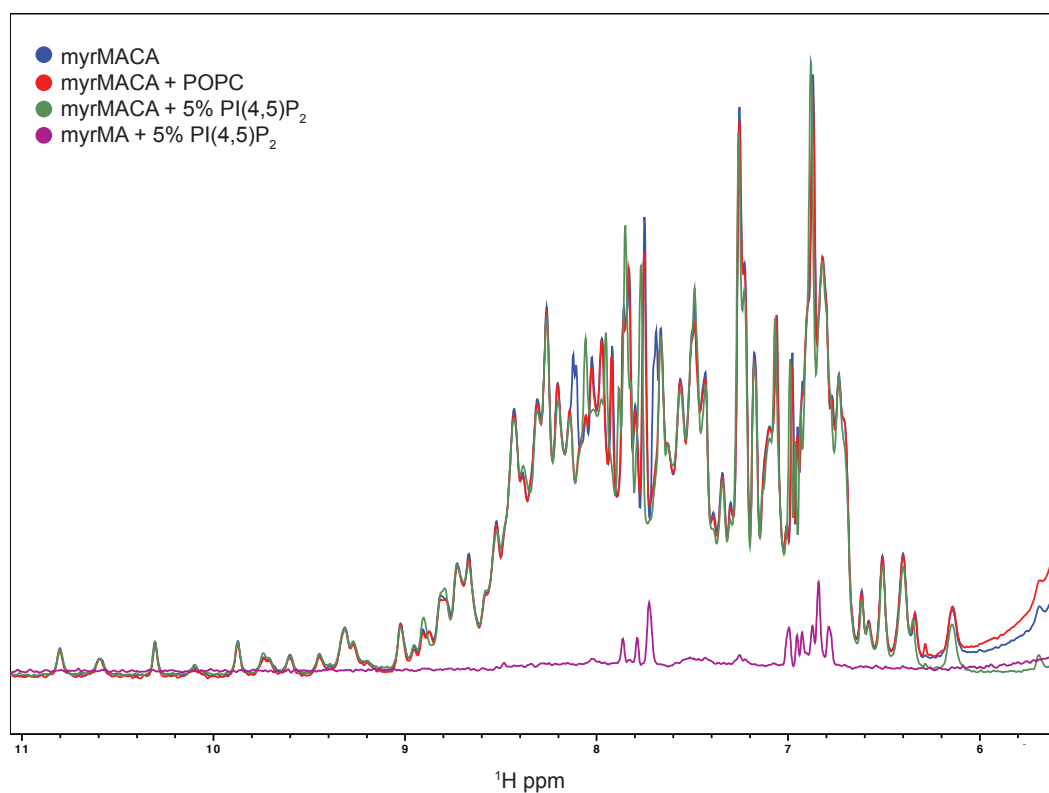


**Figure 4.11: myrMACA does not bind to PI(4,5)P<sub>2</sub>-containing liposomes.** myrMACA (blue) does not bind to POPC liposomes (red) or liposomes containing 5% PI(4,5)P<sub>2</sub> (green), although myrMA has almost complete binding at that percentage of PI(4,5)P<sub>2</sub> (purple).

## Chapter 5: Significance and Future Perspectives

### *Summary and Significance of Dissertation Studies*

The matrix domain has a known role in targeting the Gag polyprotein to the plasma membrane for virion assembly [1, 31, 36, 40, 41, 46, 49, 52-57, 68, 155-157]. Matrix does so through interactions between the highly basic region (HBR) on the protein and the plasma membrane lipid phosphatidylinositol 4,5-bisphosphate [PI(4,5)P<sub>2</sub>] [1, 36, 40, 41, 53-56]. Upon binding to the plasma membrane, the N-terminal myristoyl group on matrix will adopt an exposed conformation, anchoring the Gag polyprotein to the plasma membrane [38, 39, 123, 124]. Work in the field has proposed a nucleic acid-binding ability as well, first proposed as a role matrix plays in the preintegration complex that transports newly reverse transcribed viral DNA to the host nucleus for integration into the host genome [65, 66]. Later work with liposome flotation assays determined that RNA can play a role in membrane selectivity, as the addition of RNases to Gag samples translated from rabbit reticulocyte serum lost their ability to target only PI(4,5)P<sub>2</sub>-containing liposomes, and began binding to liposomes containing other negative phospholipids [32, 56]. Debate existed as to whether or not this was physiologically relevant or an artifact of the in vitro system until CLIP studies determined that matrix will bind to eight specific tRNAs in the cytoplasm of infected cells [69]. However, myrMA does not bind to tRNAs in virions, and treatment of cellular lysates with RNases led to an increase in endogenous membrane binding during membrane flotation assays, leading to the conclusion that matrix-tRNA interactions play a role in regulating membrane binding [69].

My work sought to further investigate this hypothesis in order to determine how matrix-tRNA interactions regulate membrane binding. Experiments primarily used one of the eight specific tRNAs that bound to matrix, tRNA<sup>Lys3</sup>, as it is the primer for reverse transcription and is packaged into virions [11, 12, 82]. The first step in the characterization process used HSQC experiments to determine the matrix residues affected by binding to tRNA<sup>Lys3</sup>. The NMR spectra indicated that the residues affected by binding included R22, K26, K30, L31 and K32, which are located in the HBR of the matrix protein. Other residues affected by RNA binding were located near the HBR, in the N-termini of helices II and V and the C-terminus of helix I. This binding region was consistent with the binding region for a 15mer RNA oligonucleotide determined by the Barklis laboratory [63]. More importantly, the results indicated that the tRNA binding region on matrix is also the region that confers specificity to PI(4,5)P<sub>2</sub>-containing membranes, giving further evidence that these two processes may be linked.

Many studies have looked at the role of specific lysine residues in membrane binding through the use of HBR mutants [36, 53, 55, 56]. The K18T, K18T/K30T, and K30T/K32T mutants decrease Gag's ability to bind to PI(4,5)P<sub>2</sub>-containing liposomes in liposome flotation assays [56]. Additionally, the K32E mutation was shown to play the major role in membrane disruption for K30E/K32E mutants, as the single K32T mutant could disrupt liposome binding in NMR assays using myrMA [36]. Since these mutations are known to affect membrane binding, work in this dissertation investigated whether they also play a role in tRNA binding. Isothermal titration calorimetry experiments with K18, K30, and K32 mutants determined that

K18 did not play a major role in tRNA-matrix interactions, but K30 and K32 did, with K32 playing the largest role and completely abolishing matrix's ability to bind tRNA. Interestingly, the K30A mutant did not disrupt matrix-tRNA interactions as much as the K30T mutant, suggesting that the tRNA-matrix interaction is not due to electrostatics alone.

Another basic patch mutant, K26T/K27T, has a different phenotype than the other HBR mutants. The K26T/K27T Gag mutant binds to PI(4,5)P<sub>2</sub>-containing membranes similarly to the wild-type protein, but will also bind non-specifically to other negative liposomes [56]. This is the same result obtained by adding RNases to the Gag samples used in liposome flotation assays, suggesting that these residues may play a role in RNA binding in addition to membrane binding [56]. The CLIP studies also looked at this mutant, and found that K26T/K27T Gag did not bind to as many tRNAs as the wild-type Gag, further linking the lysine residues to RNA-binding [69]. When observing the K26T, K27T, and K26/K27T mutants' ability to bind tRNA<sup>Lys3</sup> using ITC, I found that the K26T slightly weakened the myrMA-tRNA<sup>Lys3</sup> interaction, with K27T playing a larger role, and the mutations working synergistically to abolish tRNA binding in the double mutant. This leads to the question of whether or not these two residues play a role in membrane binding, or if they mainly regulate tRNA interactions, resulting in Gag mistargeting once myrMA loses the ability to bind RNA. It is of note that both the K32T and K26T/K27T mutants abolish tRNA<sup>Lys3</sup> binding, but have very different phenotypes when it comes to membrane binding. I hypothesize that the K32 residue is needed for electrostatic interactions with PI(4,5)P<sub>2</sub> and tRNA<sup>Lys3</sup>, and when mutated the protein loses the

ability to bind to both. However, K26 and K27 are only needed to stabilize the tRNA interaction, and are not essential for the PI(4,5)P<sub>2</sub> interaction to take place. Further structural work is needed in order to determine the mechanism of the myrMA-tRNA<sup>Lys3</sup> interaction, so that it can be compared to myrMA's PI(4,5)P<sub>2</sub>-binding mechanism and confirm or deny the proposed role for the three residues.

After determining that the HBR lysine residues play a large role in tRNA-myrMA interactions, the next step was to determine if the myristoyl group may also regulate myrMA's ability to bind to RNA. The myristoyl group is primarily sequestered in matrix's hydrophobic pocket, but becomes exposed upon binding to PI(4,5)P<sub>2</sub> [41]. ITC studies using wild-type protein, a myristoyl-deficient L8I mutant, and an unmyristoylated mutant, determined that as the myristoyl group becomes more exposed, the tRNA<sup>Lys3</sup>-matrix interaction weakens. This led to a proposed mechanism, where tRNA binds to the HBR of matrix, preventing binding nonspecific binding to membranes other than the plasma membrane. Upon encountering PI(4,5)P<sub>2</sub> in the plasma membrane, the lipid would outcompete the tRNA for the HBR, displacing the RNA and allowing binding. This binding would promote myristoyl exposure, anchoring Gag to the plasma membrane and further preventing tRNA binding after matrix arrives at the membrane.

In order to test this hypothesis, NMR-based liposome assays observed matrix's ability to bind to various liposomes in the presence and absence of tRNAs. If the hypothesis is correct, myrMA should bind to negative liposomes lacking PI(4,5)P<sub>2</sub> in the absence of tRNA, with the addition of tRNA preventing binding. However, myrMA should bind to PI(4,5)P<sub>2</sub>-containing liposomes in both the presence and

absence of tRNA. This is consistent with what was proposed and seen by others using membrane flotation assays [56, 69]. When observing myrMA's binding to liposomes containing increasing amounts of phosphatidylserine (PS) and phosphatidylinositol 3,5-bisphosphate [PI(3,5)P<sub>2</sub>], I saw that in the absence of tRNA myrMA had increased binding to the liposomes as the liposomes became more negative. However, consistent with the hypothesis and the results of others, tRNA was able to block membrane binding to the negative liposomes lacking PI(4,5)P<sub>2</sub>. myrMA bound to PI(4,5)P<sub>2</sub>-containing liposomes in the absence of tRNA, but did not bind to those liposomes in the presence of tRNA, suggesting that the model for PI(4,5)P<sub>2</sub>-specificity is not complete. These results were consistent with previous NMR liposome binding assays and the ITC results, as myrMA binds to liposomes with an apparent  $K_d$  of  $10.2 \pm 2.1 \mu\text{M}$  [36], while myrMA binds to tRNA<sup>Lys3</sup> with a  $K_d$  of  $0.63 \pm 0.03 \mu\text{M}$  in a 15-fold stronger interaction.

Although the results of the competition assays were in agreement with some *in vitro* studies, Gag must bind to the plasma membrane in order for viral replication to occur. Some papers have suggested that Gag targets not just PI(4,5)P<sub>2</sub>, but also lipid rafts on the plasma membrane [46, 48, 49, 51, 123, 153]. These regions have increased concentrations of cholesterol and other negative phospholipids that may enhance binding in a cell. Liposome competition assays were completed using membranes mimicking both rafts and non-rafts, both with and without PI(4,5)P<sub>2</sub>, and found that myrMA bound well to the raft-like liposomes in the absence of tRNA but that tRNA<sup>Lys3</sup> could successfully prevent binding to raft-like liposomes, including those that contained PI(4,5)P<sub>2</sub>.

The previous liposome competition assays were performed at pH 7.4 in order to keep them consistent with past experiments, but this is most likely not the pH near the plasma membrane of the cell [130, 131, 158]. It was possible that the myristoyl group played the key role in membrane specificity, as myristoyl exposure weakens myrMA-tRNA interactions. Full length Gag has a higher affinity for membranes than the matrix domain, which may be due to an increase in myristoyl exposure upon multimerization [32, 38, 39]. Additionally, at pH 7.4 myrMA's myristoyl group should be nearly fully sequestered [31]. Liposome competition assays at lower pH were used in order to determine if the myristoyl group plays this key role in regulating tRNA interactions and thus membrane interactions. However, even at pH 6.5, PI(4,5)P<sub>2</sub>-containing liposomes could not outcompete tRNA<sup>Lys3</sup> for binding, suggesting that there is some other mechanism involved in how tRNA regulates myrMA-membrane interactions.

### *Future Perspectives*

The next step is to determine what other mechanisms beyond myrMA interactions with tRNAs regulate myrMA's ability to discriminate between membranes. While the  $K_d$  values obtained for myrMA-tRNA interactions and myrMA-PI(4,5)P<sub>2</sub> interactions are consistent with the results of the <sup>1</sup>H-1D competition assays, many other groups have been able to show Gag will specifically bind to PI(4,5)P<sub>2</sub>-containing membranes in the presence of RNA [32, 56, 62, 69, 75].

One major difference between the NMR-based competition experiments and the flotation experiments are the constructs used. Due to size limitations, the NMR-based experiments used the matrix domain alone, which has a lower affinity for

membranes than the full-length Gag [38, 39]. This increased affinity conferred by the presence of the other domains of the Gag polyprotein may be necessary to allow myrMA to bind membranes in the presence of tRNAs. Consistent with this idea, membrane flotation assays that use the full-length Gag see Gag bind to PI(4,5)P<sub>2</sub>-containing membranes, but not to other negative liposomes in the presence of tRNA [56, 129].

If other domains of the Gag polyprotein are required to confer membrane specificity, the next step should investigate which parts of Gag are required and how they affect membrane binding. One likely candidate is the capsid domain, which allows multimerization of the Gag polyprotein. Multimerization of the matrix protein has been shown to enhance membrane binding, as chimeric myrMA fused to a FK506-binding protein (FKBP) have increased plasma membrane binding upon addition of a chemical agent that induces dimerization of the FKBP domain [32]. Further work using liposome flotation assays confirmed that multimerization of matrix increased binding to liposomes, with protein forming a hexamer through a Ccmk4 domain having the most binding [32]. While another study has used the matrix domain alone and successfully had PI(4,5)P<sub>2</sub>-containing liposomes outcompete nucleic acids, the matrix was tethered to a bead [62], which may mimic the multimerization process. This study also used a DNA oligonucleotide, which may not bind as tightly as tRNA, making it easier PI(4,5)P<sub>2</sub> to outcompete the nucleic acid for binding. If multimerization plays a role in membrane binding, this may be a crucial step that allows PI(4,5)P<sub>2</sub> to outcompete tRNA. It is possible that the act of multimerization weakens the tRNA-myrMA interaction, whether through increased

local concentration that promotes myristoyl exposure, through steric hindrance preventing myrMA-tRNA interactions, or through some other mechanism. It is also possible that the concentration of positive charge induced through multimerization allows myrMA to target PI(4,5)P<sub>2</sub> with higher affinity. The mechanism could be some or all of these processes (Figure 5.1).

The nucleocapsid (NC) domain of the Gag polyprotein may also play a role in membrane specificity. The NC domain binds to the viral RNA genome, allowing Gag to traffic the genome to plasma membrane for incorporation into virions [8]. In the absence of tRNA, Gag will target the membrane in vesicle flotation assays equally in the presence of five RNAs, which are available to bind to the NC domain [75]. However, in the presence of tRNA, Gag bound to RNAs containing the 5' UTR of the HIV-1 genome bound to membranes more than Gag molecules bound to other RNAs [75]. Some have suggested that Gag multimerizes upon NC binding to the genome [159], which would further link multimerization to membrane selection.

Future studies should investigate the role these domains may play in membrane selectivity. Due to the size of multimerized Gag, non-NMR based assays, such as liposome flotation assays, may be necessary to determine the role the multimerization plays membrane selectivity. Formation of stable dimers, trimers, and hexamers of myrMA are difficult to purify, potentially because of the enhanced myristoyl exposure. There are protocols for purifying a Gag in *E. coli* [160], so constructs using part or all of Gag may be the most useful for these experiments.

To complement studies investigating the role of other domains of the Gag polyprotein, a structure of matrix in complex with tRNA can give useful information

about the mechanism of the interaction, such as confirmation that the highly basic region is the domain that binds to tRNA<sup>Lys3</sup>. The structure could also determine how myristoyl exposure affects binding, and whether exposure of the myristoyl group creates a barrier to prevent myrMA-tRNA interactions or some other mechanism weakens the tRNA-myrMA interaction.

In addition to studies with HIV-1 Gag, work with other retroviral Gag proteins could determine if RNAs play a similar role in membrane specificity. Work with RSV Gag proteins found that tRNAs do not greatly perturb its ability to bind to membranes, suggesting that the RSV matrix domain may not interact with RNAs [32]. Determining if RNAs, particularly tRNAs, play a role in HIV-2 and other similarly related retroviruses, such as SIV, could further the understanding of how the mechanism works. Additionally, comparing these Gag molecules to other retroviruses, such as RSV Gag, could lead to insights into the evolutionary process for retroviruses and how they adapted for their hosts.

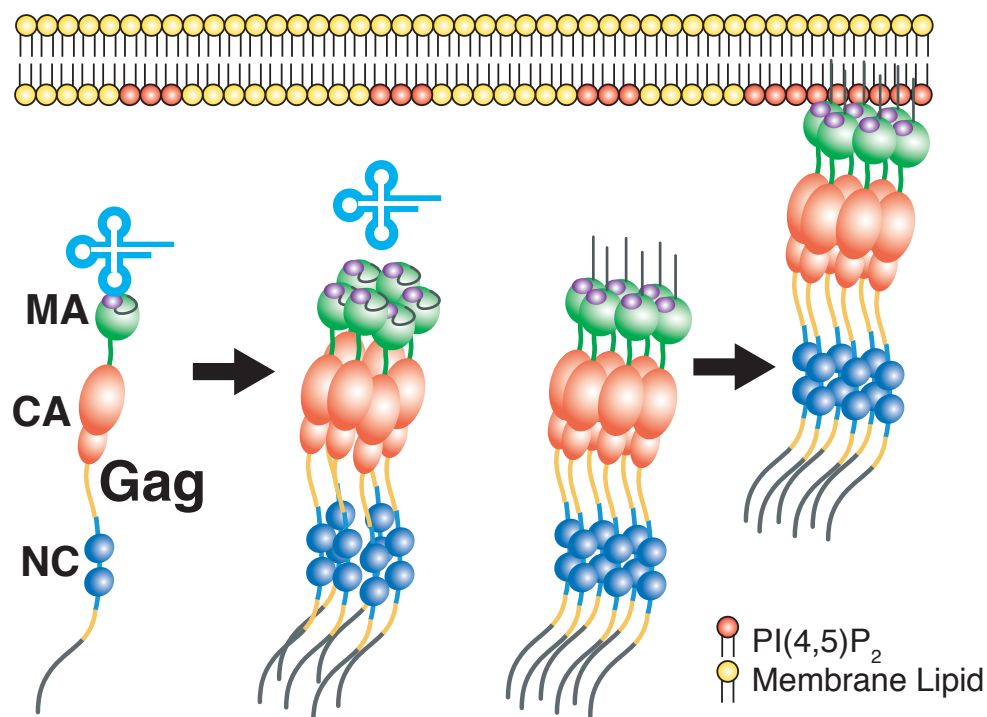


**Figure 5.1: Proposed mechanism for Gag targeting to the plasma membrane.** tRNA binds to the basic patch of the matrix domain of Gag, preventing premature binding to membranes lacking PI(4,5)P<sub>2</sub>. In this proposed mechanism, the multimerization of the Gag polypeptide through the capsid domain either increases the affinity of the protein for PI(4,5)P<sub>2</sub> clusters in the membrane, allowing PI(4,5)P<sub>2</sub> to outcompete tRNA for the basic patch, or the multimerization of Gag promotes myristoyl exposure, weakening the MA-tRNA interaction. One or a combination of both of these processes allows the membrane to outcompete tRNA for the basic patch, allowing Gag to bind to the plasma membrane and viral assembly to begin.

## Appendices

### *Protein DNA Sequences*

#### HIV-1 NL4-3 MA

ATGGGTGCGAGAGCGTCGGTATTAAGCGGGGGAGAATTAGATAAATGGG  
AAAAAATTCGGTTAAGGCCAGGGGGAAAGAAACAATATAAACTAAAACA  
TATAGTATGGGCAAGCAGGGAGCTAGAACGATTCGCAGTTAATCCTGGCC  
TTTLAGAGACATCAGAAGGCTGTAGACAAATACTGGGACAGCTACAACCA  
TCCCTTCAGACAGGATCAGAAGAAGCTTAGATCATTATATAATACAATAGC  
AGTCCTCTATTGTGTGCATCAAAGGATAGATGTAAAAGACACCAAGGAAG  
CCTTAGATAAGATAGAGGAAGAGCAAAACAAAAGTAAGAAAAAGGCACA  
GCAAGCAGCAGCTGACACAGGAAACAACAGCCAGGTCAGCCAAAATTAC  
TAA

#### HIV-1 NL4-3 MACA<sup>NTD</sup>

ATGGGTGCGAGAGCGTCGGTATTAAGCGGGGGAGAATTAGATAAATGGG  
AAAAAATTCGGTTAAGGCCAGGGGGAAAGAAACAATATAAACTAAAACA  
TATAGTATGGGCAAGCAGGGAGCTAGAACGATTCGCAGTTAATCCTGGCC  
TTTLAGAGACATCAGAAGGCTGTAGACAAATACTGGGACAGCTACAACCA  
TCCCTTCAGACAGGATCAGAAGAAGCTTAGATCATTATATAATACAATAGC  
AGTCCTCTATTGTGTGCATCAAAGGATAGATGTAAAAGACACCAAGGAAG  
CCTTAGATAAGATAGAGGAAGAGCAAAACAAAAGTAAGAAAAAGGCACA  
GCAAGCAGCAGCTGACACAGGAAACAACAGCCAGGTCAGCCAAAATTAC  
CCTATAGTGCAGAACCTCCAGGGGGCAAATGGTACATCAGGCCATATCACC  
TAGAACTTTAAATGCATGGGTAAAAGTAGTAGAAGAGAAGGCTTTCAGCC  
CAGAAGTAATAACCATGTTTTTCAGCATTATCAGAAGGAGCCACCCACAA  
GATTTAAATACCATGCTAAACACAGTGGGGGGACATCAAGCAGCCATGCA  
AATGTTAAAAGAGACCATCAATGAGGAAGCTGCAGAATGGGATAGATTG  
CATCCAGTGCATGCAGGGCCTATTGCACCAGGCCAGATGAGAGAACCAA  
GGGGAAGTGACATAGCAGGAACTACTAGTACCCTTCAGGAACAAATAGG  
ATGGATGACACATAATCCACCTATCCCAGTAGGAGAAATCTATAAAAGAT  
GGATAATCCTGGGATTAAATAAAATAGTAAGAATGTATAGCCCTACCAGC  
ATTCTGTAA

#### HIV-1 NL4-3 MACA

ATGGGTGCGAGAGCGTCGGTATTAAGCGGGGGAGAATTAGATAAATGGG  
AAAAAATTCGGTTAAGGCCAGGGGGAAAGAAACAATATAAACTAAAACA  
TATAGTATGGGCAAGCAGGGAGCTAGAACGATTCGCAGTTAATCCTGGCC  
TTTLAGAGACATCAGAAGGCTGTAGACAAATACTGGGACAGCTACAACCA

TCCCTTCAGACAGGATCAGAAGAAGCTTAGATCATTATATAATACAATAGC  
 AGTCCTCTATTGTGTGCATCAAAGGATAGATGTAAAAGACACCAAGGAAG  
 CCTTAGATAAGATAGAGGAAGAGCAAAACAAAAGTAAGAAAAAGGCACA  
 GCAAGCAGCAGCTGACACAGGAAACAACAGCCAGGTCAGCCAAAATTAC  
 CCTATAGTGCAGAACCTCCAGGGGCAAATGGTACATCAGGCCATATCACC  
 TAGAACTTTAAATGCATGGGTAAAAGTAGTAGAAGAGAAGGCTTTCAGCC  
 CAGAAGTAATACCCATGTTTTTCAGCATTATCAGAAGGAGCCACCCACAA  
 GATTTAAATACCATGCTAAACACAGTGGGGGGACATCAAGCAGCCATGCA  
 AATGTTAAAAGAGACCATCAATGAGGAAGCTGCAGAATGGGATAGATTG  
 CATCCAGTGCATGCAGGGCCTATTGCACCAGGCCAGATGAGAGAACCAA  
 GGGGAAGTGACATAGCAGGAACTACTAGTACCCTTCAGGAACAAATAGG  
 ATGGATGACACATAATCCACCTATCCCAGTAGGAGAAATCTATAAAAGAT  
 GGATAATCCTGGGATTAAATAAAATAGTAAGAATGTATAGCCCTACCAGC  
 ATTCTGGACATAAGACAAGGACCAAAGGAACCCTTTAGAGACTATGTAGA  
 CCGATTCTATAAACTCTAAGAGCCGAGCAAGCTTCACAAGAGGTAAAAA  
 ATTGGATGACAGAAACCTTGTTGGTCCAAAATGCGAACCCAGATTGTAAG  
 ACTATTTTAAAAGCATTGGGACCAGGAGCGACACTAGAAGAAATGATGA  
 CAGCATGTCAGGGAGTGGGGGGACCCGGCCATAAAGCAAGAGTTTTGTA  
 A

#### Human N-myristoyltransferase

ATGGCCGACGAGAGTGAAACCGCAGTTAAGCCGCCTGCCCCGCCTCTGCCGCAAAT  
 GATGGAAGGCAACGGTAATGGCCACGAGCACTGCAGTGACTGCGAGAACGAAGAG  
 GACAACAGTTACAACCGTGGTGGTCTGAGCCCTGCAAACGACACCGGCGCCAAAAA  
 AAAGAAAAAAAACAGAAGAAAAAAAAGGAGAAAGGTAGCGAAACCGATAGCGC  
 CCAGGACCAGCCTGTGAAAATGAACAGCCTGCCGGCAGAGCGCATCCAGGAGATCC  
 AGAAGGCCATTGAGCTGTTCAGCGTGGGTGAGGGCCCTGCCAAGACAATGGAAGAG  
 GCCAGCAAGCGCAGCTACCAGTTCTGGGACACACAACCGGTGCCGAAGTTAGGCGA  
 GGTGGTTAACACACACGGTCCGGTTGAACCGGATAAGGACAACATCCGTCAGGAGC  
 CGTACACATTACCGCAAGGCTTCACATGGGATGCCTTAGACCTGGGTGATCGCGGCG  
 TGCTGAAGGAGTTATACACACTGCTGAACGAGAACTATGTGGAGGACGACGACAAT  
 ATGTTCCGCTTTGACTATAGCCCGGAATTCCTGCTGTGGGCATTACGTCCGCCTGGTT  
 GGCTGCCGCAATGGCATTGTGGTGTTCGCGTGGTGAGCAGTCGTAAGCTGGTGGGTT  
 TCATCAGTGCCATCCCTGCCAACATCCACATCTACGACACCGAGAAGAAGATGGTTG  
 AGATCAACTTTCTGTGCGTTCACAAAAAGCTGCGCAGTAAGCGCGTTGCCCTGTGC  
 TGATTCGTGAGATCACCCGCCGCGTGCATCTGGAAGGCATCTTCCAAGCCGTGTATA  
 CCGCAGGCGTGGTTCTGCCGAAGCCTGTGGGCACATGCCGTTACTGGCACCGTAGTC  
 TGAACCCTCGCAAACCTGATCGAGGTGAAGTTCAGCCATCTGAGCCGTAACATGACC  
 ATGCAGCGTACCATGAAGCTGTACCGCCTGCCGGAAACACCTAAGACAGCCGGCTT  
 ACGTCCGATGGAGACCAAGGACATTCCGGTGGTTCACCAGCTGCTGACACGCTACCT  
 GAAACAGTTCCACCTGACCCCTGTTATGAGCCAAGAAGAGGTTGAGCACTGGTTTTA  
 TCCGCAGGAGAATATCATTGACACCTTCGTGGTGGAAAACGCCAACGGCGAGGTGA  
 CCGACTTCCTGAGCTTTTACACCCTGCCGAGCACCATTAAGAACCATCCGACCCATA  
 AGAGTCTGAAGGCCGCTACAGTTTCTACAACGTGCACACCCAGACCCCGCTGTTAG  
 ATCTGATGAGCGACGCCCTGGTGCTGGCAAAGATGAAAGGCTTTGATGTGTTCAATG

CACTGGATTTAATGGAGAACAAGACCTTCCTGGAGAAGCTGAAGTTCGGCATCGGT  
GACGGCAATCTGCAATACTACCTGTACAATTGGAAGTGCCCGAGTATGGGCGCCGA  
AAAAGTGGGTCTGGTTTTACAATAA

*tRNA Sequences*

tRNA<sup>Lys3</sup> (Sequence from Bénas, *et al.* [76])

5' GCCCGGAUAG CUCAGUCGGU AGAGCAUCAG ACUUUUAUUC  
UGAGGGUCCA GGGUUCAAGU CCCUGUUCGG GCGCCA 3'

tRNA<sup>GlyGCC</sup> (NCBI GenBank ID: K00208.1)

5' GCATTGGTGG TTCAGTGGTA GAATTCTCGC CTGCCACGCG  
GGAGGCCCGG GTTCGATTCC CGGCCAATGC ACCA 3'

tRNA<sup>IleGAU</sup> (NCBI GenBank ID: HG983860.1)

5' GGCCGGTTAG CTCAGTTGGT AAGAGCGTGG TGCTGATAAC  
ACCAAGGTCG CGGGCTCGAC TCCCGCACCG GCCA 3'

## Bibliography

- [1] Freed EO. HIV-1 assembly, release and maturation. *Nature Reviews Microbiology*. 2015;13:484-96.
- [2] Nyamweya S, Hegedus A, Jaye A, Rowland-Jones S, Flanagan KL, Macallan DC. Comparing HIV-1 and HIV-2 infection: Lessons for viral immunopathogenesis. *Rev Med Virol*. 2013;23:221-40.
- [3] UNAIDS. Global AIDS Update 2016. World Health Organization; 2016.
- [4] CDC. Statistics Overview | Statistics Center | HIV/AIDS | CDC. 2017.
- [5] CDC. HIV Surveillance Report 2015. Diagnoses of HIV Infection in the United States and Dependent Areas, 2015. 2015 ed: Division of HIV/AIDS Prevention; National Center for HIV/AIDS, Viral Hepatitis, STD, and TB Prevention; Centers for Disease Control and Prevention (CDC); U.S. Department of Health and Human Services; 2016.
- [6] Cihlar T, Fordyce M. Current status and prospects of HIV treatment. *Current Opinion in Virology*. 2016;18:50-6.
- [7] Svarovskaia ES, Cheslock SR, Zhang WH, Hu WS, Pathak VK. Retroviral mutation rates and reverse transcriptase fidelity. *Front Biosci*. 2003;8:d117-34.
- [8] Turner B, Summers M. Structural biology of HIV. *Journal of Molecular Biology*. 1999;285:1–32.
- [9] Deng HK, Unutmaz D, KewalRamani VN, Littman DR. Expression cloning of new receptors used by simian and human immunodeficiency viruses. *Nature*. 1997;388:296-300.
- [10] Sarafianos SG, Marchand B, Das K, Himmel DM, Parniak MA, Hughes SH, et al. Structure and function of HIV-1 reverse transcriptase: molecular mechanisms of polymerization and inhibition. *J Mol Biol*. 2009;385:693-713.
- [11] Kleiman L. tRNA<sup>Lys3</sup>: The Primer tRNA for Reverse Transcription in HIV-1. *IUBMB Life*. 2002;53:107-14.
- [12] Kleiman L, Jones C, Musier-Forsyth K. Formation of the tRNA<sup>Lys</sup> Packaging Complex in HIV-1. *FEBS Lett*. 2010;584:359.
- [13] Miller MD, Farnet CM, Bushman FD. Human immunodeficiency virus type 1 preintegration complexes: studies of organization and composition. *J Virol*. 1997;71:5382-90.
- [14] Fouchier RAM, Meyer BE, Simon JHM, Fischer U, Albright AV, González-Scarano F, et al. Interaction of the Human Immunodeficiency Virus Type 1 Vpr Protein with the Nuclear Pore Complex. *J Virol*. 1998;72:6004-3016.
- [15] Dahabieh M, Battivelli E, Verdin E. Understanding HIV Latency: The Road to an HIV Cure. *Annu Rev Med*. 2015;66:407-21.
- [16] Wu Y. HIV-1 gene expression: lessons from provirus and non-integrated DNA. *Retrovirology*. 2004;1:13.
- [17] Karn J, Stoltzfus CM. Transcriptional and Posttranscriptional Regulation of HIV-1 Gene Expression. *Cold Spring Harb Perspect Med*. 2012;2:a006916.
- [18] Suhasini M, Reddy TR. Cellular proteins and HIV-1 Rev function. *Curr HIV Res*. 2009;7:91-100.

- [19] Keane SC, Summers MF. NMR Studies of the Structure and Function of the HIV-1 5'-Leader. *Viruses*. 2016;8.
- [20] Kharytonchyk S, Monti S, Smaldino PJ, Van V, Bolden NC, Brown JD, et al. Transcriptional start site heterogeneity modulates the structure and function of the HIV-1 genome. *Proc Natl Acad Sci U S A*. 2016;113:13378-83.
- [21] Carlson LA, Briggs JA, Glass B, Riches JD, Simon MN, Johnson MC, et al. Three-dimensional analysis of budding sites and released virus suggests a revised model for HIV-1 morphogenesis. *Cell Host Microbe*. 2008;4:592-9.
- [22] Adamson CS, Salzwedel K, Freed EO. Virus Maturation as a Novel HIV-1 Therapeutic Target. *Expert Opin Ther Targets*. 2009;13:895-908.
- [23] Fiorentini S, Marini E, Caracciolo S, Caruso A. Functions of the HIV-1 matrix protein p17. *New Microbiol*. 2006;29:1-10.
- [24] Nermut MV, Hockley DJ, Jowett JB, Jones IM, Garreau M, Thomas D. Fullerene-like organization of HIV gag-protein shell in virus-like particles produced by recombinant baculovirus. *Virology*. 1994;198:288-96.
- [25] Fassati A, Goff SP. Characterization of intracellular reverse transcription complexes of human immunodeficiency virus type 1. *J Virol*. 2001;75:3626-35.
- [26] Checkley MA, Luttge BG, Freed EO. HIV-1 envelope glycoprotein biosynthesis, trafficking, and incorporation. *J Mol Biol*. 2011;410:582-608.
- [27] Massiah MA, Starich MR, Paschall C, Summers MF, Christensen AM, Sundquist WI. Three-dimensional structure of the human immunodeficiency virus type 1 matrix protein. *J Mol Biol*. 1994;244:198-223.
- [28] Hill CP, Worthylake D, Bancroft DP, Christensen AM, Sundquist WI. Crystal structures of the trimeric human immunodeficiency virus type 1 matrix protein: implications for membrane association and assembly. *Proc Natl Acad Sci U S A*. 1996;93:3099-104.
- [29] Alfadhli A, Huseby D, Kapit E, Colman D, Barklis E. Human Immunodeficiency Virus Type 1 Matrix Protein Assembles on Membranes as a Hexamer<sup>▽</sup>. *J Virol*. 2007;81:1472-8.
- [30] Tang C, Loeliger E, Luncsford P, Kinde I, Beckett D, Summers MF. Entropic switch regulates myristate exposure in the HIV-1 matrix protein. *Proc Natl Acad Sci U S A* 2004. p. 517-22.
- [31] Fledderman EL, Fujii K, Ghanam RH, Waki K, Prevelige PE, Freed EO, et al. Myristate Exposure in the HIV-1 Matrix Protein is Modulated by pH. *Biochemistry*. 2010;49:9551-62.
- [32] Dick RA, Kamynina E, Vogt VM. Effect of Multimerization on Membrane Association of Rous Sarcoma Virus and HIV-1 Matrix Domain Proteins. *Journal of Virology*. 2013;87:13598-608.
- [33] Tedbury PR, Novikova M, Ablan SD, Freed EO. Biochemical evidence of a role for matrix trimerization in HIV-1 envelope glycoprotein incorporation. *Proc Natl Acad Sci U S A*. 2016;113:E182-90.
- [34] Bryant M, Ratner L. Myristoylation-dependent replication and assembly of human immunodeficiency virus 1. *Proc Natl Acad Sci U S A*. 1990;87:523-7.
- [35] Spearman P, Wang JJ, Vander Heyden N, Ratner L. Identification of human immunodeficiency virus type 1 Gag protein domains essential to membrane binding and particle assembly. *J Virol*. 1994;68:3232-42.

- [36] Mercredi PY, Bucca N, Loeliger B, Gaines CR, Mehta M, Bhargava P, et al. Structural and Molecular Determinants of Membrane Binding by the HIV-1 Matrix Protein. *Journal of Molecular Biology*. 2016;428:1637–55.
- [37] Bouamr F, Scarlata S, Carter C. Role of myristylation in HIV-1 Gag assembly. *Biochemistry*. 2003;42:6408-17.
- [38] Zhou W, Resh MD. Differential membrane binding of the human immunodeficiency virus type 1 matrix protein. *J Virol*. 1996;70:8540-8.
- [39] Spearman P, Horton R, Ratner L, Kuli-Zade I. Membrane binding of human immunodeficiency virus type 1 matrix protein in vivo supports a conformational myristyl switch mechanism. *J Virol*. 1997;71:6582-92.
- [40] Ono A, Ablan SD, Lockett SJ, Nagashima K, Freed EO. Phosphatidylinositol (4,5) biphosphate regulates HIV-1 Gag targeting to the plasma membrane. *Proc Natl Acad Sci U S A*. 2004;101:14889-94.
- [41] Saad JS, Miller J, Tai J, Kim A, Ghanam RH, Summers MF. Structural basis for targeting HIV-1 Gag proteins to the plasma membrane for virus assembly. *Proc Natl Acad Sci U S A* 2006. p. 11364-9.
- [42] Shkriabai N, Datta SA, Zhao Z, Hess S, Rein A, Kvaratskhelia M. Interactions of HIV-1 Gag with assembly cofactors. *Biochemistry*. 2006;45:4077-83.
- [43] Campbell S, Fisher RJ, Towler EM, Fox S, Issaq HJ, Wolfe T, et al. Modulation of HIV-like particle assembly in vitro by inositol phosphates. *Proc Natl Acad Sci U S A*. 2001;98:10875-9.
- [44] Heo WD, Inoue T, Park WS, Kim ML, Park BO, Wandless TJ, et al. PI(3,4,5)P3 and PI(4,5)P2 Lipids Target Proteins with Polybasic Clusters to the Plasma Membrane. *Science*. 2006;314:1458-61.
- [45] Nguyen DH, Hildreth JE. Evidence for budding of human immunodeficiency virus type 1 selectively from glycolipid-enriched membrane lipid rafts. *J Virol*. 2000;74:3264-72.
- [46] Ono A, Waheed AA, Freed EO. Depletion of cellular cholesterol inhibits membrane binding and higher-order multimerization of human immunodeficiency virus type 1 Gag. *Virology*. 2007;360:27-35.
- [47] Waheed AA, Freed EO. Lipids and membrane microdomains in HIV-1 replication. *Virus Res*. 2009;143:162-76.
- [48] Graham DR, Chertova E, Hilburn JM, Arthur LO, Hildreth JE. Cholesterol depletion of human immunodeficiency virus type 1 and simian immunodeficiency virus with beta-cyclodextrin inactivates and permeabilizes the virions: evidence for virion-associated lipid rafts. *J Virol*. 2003;77:8237-48.
- [49] Ono A, Freed EO. Plasma membrane rafts play a critical role in HIV-1 assembly and release. *PNAS*. 2001;98:13925-30.
- [50] Aloia RC, Tian H, Jensen FC. Lipid composition and fluidity of the human immunodeficiency virus envelope and host cell plasma membranes. *Proc Natl Acad Sci U S A*. 1993;90:5181-5.
- [51] Brügger B, Glass B, Haberkant P, Leibrecht I, Wieland FT, Kräusslich H-G. The HIV lipidome: A raft with an unusual composition. *PNAS*. 2006;103:2641-6.
- [52] Ono A, Freed EO. Cell-Type-Dependent Targeting of Human Immunodeficiency Virus Type 1 Assembly to the Plasma Membrane and the Multivesicular Body. *J Virol*. 2004;78:1552-63.

- [53] Ono A, Orenstein JM, Freed EO. Role of the Gag Matrix Domain in Targeting Human Immunodeficiency Virus Type 1 Assembly. *Journal of Virology*. 2000;74:2855-66.
- [54] Freed EO, Englund G, Martin MA. Role of the basic domain of human immunodeficiency virus type 1 matrix in macrophage infection. *J Virol*. 1995;69:3949-54.
- [55] Freed EO, Orenstein JM, Buckler-White AJ, Martin MA. Single amino acid changes in the human immunodeficiency virus type 1 matrix protein block virus particle production. *J Virol*. 1994;68:5311-20.
- [56] Chukkapalli V, Oh SJ, Ono A. Opposing mechanisms involving RNA and lipids regulate HIV-1 Gag membrane binding through the highly basic region of the matrix domain. *Proceedings of the National Academy of Sciences*. 2010;107:1600-5.
- [57] Chukkapalli V, Hogue IB, Boyko V, Hu W-S, Ono A. Interaction between the Human Immunodeficiency Virus Type 1 Gag Matrix Domain and Phosphatidylinositol-(4,5)-Bisphosphate Is Essential for Efficient Gag Membrane Binding. *J Virol*. 2008;82:2405-17.
- [58] Todd GC, Duchon AA, Inlora J, Olson ED, Musier-Forsyth K, Ono A. Inhibition of HIV-1 Gag-membrane interactions by specific RNAs. *RNA*. 2016.
- [59] Ott DE, Coren LV, Gagliardi TD. Redundant roles for nucleocapsid and matrix RNA-binding sequences in human immunodeficiency virus type 1 assembly. *J Virol*. 2005;79:13839-47.
- [60] Purohit P, Dupont S, Stevenson M, Green MR. Sequence-specific interaction between HIV-1 matrix protein and viral genomic RNA revealed by in vitro genetic selection. *RNA*. 2001;7:576-84.
- [61] Lochrie MA, Waugh S, Pratt DG, Clever J, Parslow TG, Polisky B. In vitro selection of RNAs that bind to the human immunodeficiency virus type-1 gag polyprotein. *Nucleic Acids Res*. 1997;25:2902-10.
- [62] Alfadhli A, Still A, Barklis E. Analysis of human immunodeficiency virus type 1 matrix binding to membranes and nucleic acids. *Journal Of Virology*. 2009;83:12196-203.
- [63] Alfadhli A, McNett H, Tsagli S, Bächinger HP, Peyton DH, Barklis E. HIV-1 Matrix Protein Binding to RNA. *J Mol Biol*. 2011;410:653-66.
- [64] Cimorelli A, Luban J. Translation Elongation Factor 1-Alpha Interacts Specifically with the Human Immunodeficiency Virus Type 1 Gag Polyprotein. *J Virol*. 1999;73:5388-401.
- [65] Cai M, Huang Y, Craigie R, Clore GM. Structural Basis of the Association of HIV-1 Matrix Protein with DNA. *PLoS One*. 2010;5.
- [66] Hearps AC, Wagstaff KM, Piller SC, Jans DA. The N-Terminal Basic Domain of the HIV-1 Matrix Protein Does Not Contain a Conventional Nuclear Localization Sequence But Is Required for DNA Binding and Protein Self-Association. *Biochemistry*. 2008;47:2199-210.
- [67] Datta SA, Heinrich F, Raghunandan S, Krueger S, Curtis JE, Rein A, et al. HIV-1 Gag Extension: Conformational Changes Require Simultaneous Interaction with Membrane and Nucleic Acid. *J Mol Biol*. 2011;406:205-14.
- [68] Chukkapalli V, Inlora J, Todd GC, Ono A. Evidence in Support of RNA-Mediated Inhibition of Phosphatidylserine-Dependent HIV-1 Gag Membrane Binding in Cells. *Journal of Virology*. 2013;87:7155-9.

- [69] Kutluay SB, Zang T, Blanco-Melo D, Powell C, Jannain D, Errando M, et al. Global Changes in the RNA Binding Specificity of HIV-1 Gag Regulate Virion Genesis. *Cell*. 2014;159:1096-109.
- [70] Jiang M, Mak J, Ladha A, Cohen E, Klein M, Rovinski B, et al. Identification of tRNAs incorporated into wild-type and mutant human immunodeficiency virus type 1. *J Virol*. 1993;67:3246-53.
- [71] Mak J, Jiang M, Wainberg MA, Hammariskjold ML, Rekosh D, Kleiman L. Role of Pr160gag-pol in mediating the selective incorporation of tRNA(Lys) into human immunodeficiency virus type 1 particles. *J Virol*. 1994;68:2065-72.
- [72] Huang Y, Mak J, Cao Q, Li Z, Wainberg MA, Kleiman L. Incorporation of excess wild-type and mutant tRNA(3Lys) into human immunodeficiency virus type 1. *J Virol*. 1994;68:7676-83.
- [73] Puglisi EV, Puglisi JD. Probing the conformation of human tRNA<sup>3Lys</sup> in solution by NMR. *FEBS Letters*. 2007;581:5307-14.
- [74] Puglisi EV, Puglisi JD. Secondary structure of the HIV reverse transcription initiation complex by NMR. *J Mol Biol*. 2011;410:863-74.
- [75] Carlson L-A, Bai Y, Keane SC, Doudna JA, Hurley JH. Reconstitution of selective HIV-1 RNA packaging in vitro by membrane-bound Gag assemblies. *eLife*. 2016;5:e14663.
- [76] Bénas P, Bec G, Keith G, Marquet R, Ehresmann C, Ehresmann B, et al. The crystal structure of HIV reverse-transcription primer tRNA(Lys,3) shows a canonical anticodon loop. *RNA*. 2000;6:1347-55.
- [77] Walker SC, Engelke DR. Ribonuclease P: the evolution of an ancient RNA enzyme. *Crit Rev Biochem Mol Biol*. 2006;41:77-102.
- [78] Phizicky EM, Hopper AK. tRNA biology charges to the front. *Genes Dev*. 2010;24:1832-60.
- [79] Vogel A, Schilling O, Spath B, Marchfelder A. The tRNase Z family of proteins: physiological functions, substrate specificity and structural properties. *Biol Chem*. 2005;386:1253-64.
- [80] Pang YLJ, Poruri K, Martinis SA. tRNA synthetase: tRNA Aminoacylation and beyond. *Wiley Interdiscip Rev RNA*. 2014;5:461-80.
- [81] Stapulionis R, Deutscher MP. A channeled tRNA cycle during mammalian protein synthesis. *Proc Nat Acad*. 1995;92:718-7161.
- [82] Kleiman L, Cen S. The tRNA<sup>Lys</sup> packaging complex in HIV-1. *The International Journal of Biochemistry & Cell Biology*. 2004;36:1776-86.
- [83] Mak J, Kleiman L. Primer tRNAs for reverse transcription. *J Virol*. 1997;71:8087-95.
- [84] Raba M, Limburg K, Burghagen M, Katze JR, Simsek M, Heckman JE, et al. Nucleotide sequence of three isoaccepting lysine tRNAs from rabbit liver and SV40-transformed mouse fibroblasts. *Eur J Biochem*. 1979;97:305-18.
- [85] Huang Y, Khorchid A, Wang J, Parniak MA, Darlix JL, Wainberg MA, et al. Effect of mutations in the nucleocapsid protein (NCp7) upon Pr160(gag-pol) and tRNA(Lys) incorporation into human immunodeficiency virus type 1. *J Virol*. 1997;71:4378-84.
- [86] Khorchid A, Javanbakht H, Wise S, Halwani R, Parniak MA, Wainber MA, et al. Sequences within Pr160gag-pol affecting the selective packaging of primer tRNA<sup>Lys3</sup> into HIV-11. *J Mol Biol*. 2000;299:17-26.

- [87] Kaminska M, Shalak V, Francin M, Mirande M. Viral hijacking of mitochondrial lysyl-tRNA synthetase. *J Virol.* 2007;81:68-73.
- [88] Kaminska M, Francin M, Shalak V, Mirande M. Role of HIV-1 Vpr-induced apoptosis on the release of mitochondrial lysyl-tRNA synthetase. *FEBS Lett.* 2007;581:3105-10.
- [89] Javanbakht H, Halwani R, Cen S, Saadatmand J, Musier-Forsyth K, Gottlinger H, et al. The interaction between HIV-1 Gag and human lysyl-tRNA synthetase during viral assembly. *J Biol Chem.* 2003;278:27644-51.
- [90] Javanbakht H, Cen S, Musier-Forsyth K, Kleiman L. Correlation between tRNA<sup>Lys3</sup> aminoacylation and its incorporation into HIV-1. *J Biol Chem.* 2002;277:17389-96.
- [91] Isel C, Ehresmann C, Marquet R. Initiation of HIV Reverse Transcription. *Viruses.* 2010;2:213-43.
- [92] Cen S, Khorchid A, Javanbakht H, Gabor J, Stello T, Shiba K, et al. Incorporation of lysyl-tRNA synthetase into human immunodeficiency virus type 1. *J Virol.* 2001;75:5043-8.
- [93] Cen S, Javanbakht H, Niu M, Kleiman L. Ability of wild-type and mutant lysyl-tRNA synthetase to facilitate tRNA(Lys) incorporation into human immunodeficiency virus type 1. *J Virol.* 2004;78:1595-601.
- [94] Gabor J, Cen S, Javanbakht H, Niu M, Kleiman L. Effect of altering the tRNA(Lys)(3) concentration in human immunodeficiency virus type 1 upon its annealing to viral RNA, GagPol incorporation, and viral infectivity. *J Virol.* 2002;76:9096-102.
- [95] Cen S, Javanbakht H, Kim S, Shiba K, Craven R, Rein A, et al. Retrovirus-specific packaging of aminoacyl-tRNA synthetases with cognate primer tRNAs. *J Virol.* 2002;76:13111-5.
- [96] Guo F, Cen S, Niu M, Javanbakht H, Kleiman L. Specific inhibition of the synthesis of human lysyl-tRNA synthetase results in decreases in tRNA(Lys) incorporation, tRNA(3)(Lys) annealing to viral RNA, and viral infectivity in human immunodeficiency virus type 1. *J Virol.* 2003;77:9817-22.
- [97] Saadatmand J, Guo F, Cen S, Niu M, Kleiman L. Interactions of reverse transcriptase sequences in Pol with Gag and LysRS in the HIV-1 tRNA<sup>Lys3</sup> packaging/annealing complex. *Virology.* 2008;380:109-17.
- [98] Isel C, Marquet R, Keith G, Ehresmann C, Ehresmann B. Modified nucleotides of tRNA(3Lys) modulate primer/template loop-loop interaction in the initiation complex of HIV-1 reverse transcription. *J Biol Chem.* 1993;268:25269-72.
- [99] Isel C, Ehresmann C, Keith G, Ehresmann B, Marquet R. Initiation of reverse transcription of HIV-1: secondary structure of the HIV-1 RNA/tRNA(3Lys) (template/primer). *J Mol Biol.* 1995;247:236-50.
- [100] Hargittai MR, Gorelick RJ, Rouzina I, Musier-Forsyth K. Mechanistic insights into the kinetics of HIV-1 nucleocapsid protein-facilitated tRNA annealing to the primer binding site. *J Mol Biol.* 2004;337:951-68.
- [101] Feng YX, Campbell S, Harvin D, Ehresmann B, Ehresmann C, Rein A. The human immunodeficiency virus type 1 Gag polyprotein has nucleic acid chaperone activity: possible role in dimerization of genomic RNA and placement of tRNA on the primer binding site. *J Virol.* 1999;73:4251-6.

- [102] Roldan A, Warren OU, Russell RS, Liang C, Wainberg MA. A HIV-1 minimal gag protein is superior to nucleocapsid at in vitro annealing and exhibits multimerization-induced inhibition of reverse transcription. *J Biol Chem*. 2005;280:17488-96.
- [103] Huang Y, Wang J, Shalom A, Li Z, Khorchid A, Wainberg MA, et al. Primer tRNA<sup>3</sup>Lys on the viral genome exists in unextended and two-base extended forms within mature human immunodeficiency virus type 1. *J Virol*. 1997;71:726-8.
- [104] Guo F, Saadatmand J, Niu M, Kleiman L. Roles of Gag and NCp7 in facilitating tRNA(Lys)(3) Annealing to viral RNA in human immunodeficiency virus type 1. *J Virol*. 2009;83:8099-107.
- [105] Jones CP, Datta SAK, Rein A, Rouzina I, Musier-Forsyth K. Matrix Domain Modulates HIV-1 Gag's Nucleic Acid Chaperone Activity via Inositol Phosphate Binding. *Journal of Virology*. 2011;85:1594-603.
- [106] Cen S, Khorchid A, Gabor J, Rong L, Wainberg MA, Kleiman L. Roles of Pr55(gag) and NCp7 in tRNA(3)(Lys) genomic placement and the initiation step of reverse transcription in human immunodeficiency virus type 1. *J Virol*. 2000;74:10796-800.
- [107] Skripkin E, Isel C, Marquet R, Ehresmann B, Ehresmann C. Psoralen crosslinking between human immunodeficiency virus type 1 RNA and primer tRNA<sup>3</sup>(Lys). *Nucleic Acids Res*. 1996;24:509-14.
- [108] Isel C, Lanchy JM, Le Grice SF, Ehresmann C, Ehresmann B, Marquet R. Specific initiation and switch to elongation of human immunodeficiency virus type 1 reverse transcription require the post-transcriptional modifications of primer tRNA<sup>3</sup>Lys. *Embo j*. 1996;15:917-24.
- [109] Sundaram M, Durant PC, Davis DR. Hypermodified nucleosides in the anticodon of tRNA<sup>Lys</sup> stabilize a canonical U-turn structure. *Biochemistry*. 2000;39:12575-84.
- [110] Kapust RB, Tozser J, Fox JD, Anderson DE, Cherry S, Copeland TD, et al. Tobacco etch virus protease: mechanism of autolysis and rational design of stable mutants with wild-type catalytic proficiency. *Protein Eng*. 2001;14:993-1000.
- [111] Li Z, Shalom A, Huang Y, Mak J, E A, MA W, et al. Multiple Forms of tRNA<sup>Lys3</sup>in HIV-1. *Biochemical and Biophysical Research Communications*. 1996;227:530-40.
- [112] Lorenz C, Lünse C, Mörl M. tRNA Modifications: Impact on Structure and Thermal Adaptation. *Biomolecules*. 2017;7:35.
- [113] Roe BA. Studies on human tRNA. I. The rapid, large scale isolation and partial fractionation of placenta and liver tRNA. *Nucleic Acids Res*. 1975;2:21-42.
- [114] Watanabe K, Hayashi N, Oyama A, Nishikawa K, Ueda T, Miura K. Unusual anticodon loop structure found in E.coli lysine tRNA. *Nucleic Acids Res*. 1994;22:79-87.
- [115] Tan ZJ, Chen SJ. Salt Contribution to RNA Tertiary Structure Folding Stability. *Biophys J*. 2011;101:176-87.
- [116] Tran T, Liu Y, Marchant J, Monti S, Seu M, Zaki J, et al. Conserved determinants of lentiviral genome dimerization. *Retrovirology*. 2015;12:83.
- [117] Chan PP, Lowe TM. GtRNAdb: a database of transfer RNA genes detected in genomic sequence. *Nucleic Acids Res*. 2009;37:D93-7.
- [118] Kutluay SB, Bieniasz PD. Analysis of the initiating events in HIV-1 particle assembly and genome packaging. *PLoS Pathog*. 2010;6:e1001200.
- [119] Jouvenet N, Bieniasz PD, Simon SM. Imaging the biogenesis of individual HIV-1 virions in live cells. *Nature*. 2008;454:236-40.

- [120] Jouvenet N, Simon SM, Bieniasz PD. Imaging the interaction of HIV-1 genomes and Gag during assembly of individual viral particles. *Proc Natl Acad Sci U S A*. 2009;106:19114-9.
- [121] Jouvenet N, Simon SM, Bieniasz PD. Visualizing HIV-1 assembly. *J Mol Biol*. 2011;410:501-11.
- [122] Zhou W, Parent LJ, Wills JW, Resh MD. Identification of a membrane-binding domain within the amino-terminal region of human immunodeficiency virus type 1 Gag protein which interacts with acidic phospholipids. *J Virol*. 1994;68:2556-69.
- [123] Ding L, Derdowski A, Wang J-J, Spearman P. Independent Segregation of Human Immunodeficiency Virus Type 1 Gag Protein Complexes and Lipid Rafts. *J Virol*. 2003;77:1916-26.
- [124] Li H, Dou J, Ding L, Spearman P. Myristoylation Is Required for Human Immunodeficiency Virus Type 1 Gag-Gag Multimerization in Mammalian Cells. *J Virol*. 2007;81:12899-910.
- [125] Alfadhli A, Barklis E. The roles of lipids and nucleic acids in HIV-1 assembly. *Frontiers in Microbiology*. 2014;5:1-11.
- [126] Hermida-Matsumoto L, Resh MD. Human immunodeficiency virus type 1 protease triggers a myristoyl switch that modulates membrane binding of Pr55(gag) and p17MA. *J Virol*. 1999;73:1902-8.
- [127] Saad JS, Loeliger E, Luncsford P, Liriano M, Tai J, Kim A, et al. Point mutations in the HIV-1 matrix protein turn off the myristyl switch. *J Mol Biol*. 2007;366:574-85.
- [128] Paillart JC, Göttlinger HG. Opposing Effects of Human Immunodeficiency Virus Type 1 Matrix Mutations Support a Myristyl Switch Model of Gag Membrane Targeting. *J Virol*. 1999;73:2604-12.
- [129] Todd GC, Duchon A, Inlora J, Olson ED, Musier-Forsyth K, Ono A. Inhibition of HIV-1 Gag-membrane interactions by specific RNAs. *RNA*. 2017;23:395-405.
- [130] Casey JR, Grinstein S, Orlowski J. Sensors and regulators of intracellular pH. *Nature Reviews Molecular Cell Biology*. 2009;11:50-61.
- [131] Makutonina A, Voss TG, Plymale DR, Fermin CD, Norris CH, Vigh S, et al. Human immunodeficiency virus infection of T-lymphoblastoid cells reduces intracellular pH. *J Virol*. 1996;70:7049-55.
- [132] Martin TFJ. Role of PI(4,5)P2 in Vesicle Exocytosis and Membrane Fusion. *Subcell Biochem*. 2012;59:111-30.
- [133] van Meer G, Voelker DR, Feigenson GW. Membrane lipids: where they are and how they behave. *Nat Rev Mol Cell Biol*. 2008;9:112-24.
- [134] van Meer G, de Kroon AIPM. Lipid map of the mammalian cell. *Journal of Cell Science*. 2011;124:5-8.
- [135] Lemmon MA. Phosphoinositide Recognition Domains. *Traffic*. 2003;4:201-13.
- [136] Lemmon MA. Membrane recognition by phospholipid-binding domains. *Nature Reviews Molecular Cell Biology*. 2008;9:99-111.
- [137] Gericke A, Leslie NR, Lösche M, Ross AH. PI(4,5)P2-Mediated Cell Signaling: Emerging Principles and PTEN as a Paradigm for Regulatory Mechanism. *Adv Exp Med Biol*. 2013;991:85-104.
- [138] Devaux PF, Morris R. Transmembrane Asymmetry and Lateral Domains in Biological Membranes. *Traffic*. 2004;5:241-6.

- [139] Ceccon A, D'Onofrio M, Zanzoni S, Longo DL, Aime S, Molinari H, et al. NMR investigation of the equilibrium partitioning of a water-soluble bile salt protein carrier to phospholipid vesicles. *Proteins*. 2013;81:1776-91.
- [140] Milojevic T, Sonnleitner E, Romeo A, Djinovic-Carugo K, Blasi U. False positive RNA binding activities after Ni-affinity purification from *Escherichia coli*. *RNA Biol*. 2013;10:1066-9.
- [141] BMRB. Full Chemical Shift Statistics. 2017.
- [142] Sriwongsitanon S, Ueno M. Effect of Freeze-Thawing Process on the Size and Lamellarity of PEG-Lipid Liposomes. *Open Colloid Science Journal*. 2011;4:1-6.
- [143] Castile JD, Taylor KMG. Factors affecting the size distribution of liposomes produced by freeze-thaw extrusion - ScienceDirect. *International Journal of Pharmaceutics*. 1999;188:87-95.
- [144] Lipids AP. Liposome Preparation. 2017.
- [145] Marquardt D, Geier B, Pabst G. Asymmetric Lipid Membranes: Towards More Realistic Model Systems. *Membranes*. 2015;5:180-96.
- [146] McCartney AJ, Zhang Y, Weisman LS. Phosphatidylinositol 3,5-bisphosphate: low abundance, high significance. *Bioessays*. 2014;36:52-64.
- [147] McLaughlin S, Murray D. Plasma membrane phosphoinositide organization by protein electrostatics. *Nature*. 2005;438:605-11.
- [148] Chan R, Uchil PD, Jin J, Shui G, Ott DE, Mothes W, et al. Retroviruses Human Immunodeficiency Virus and Murine Leukemia Virus Are Enriched in Phosphoinositides. *Journal of Virology*. 2008;82:11228-38.
- [149] Kooijman EE, King KE, Gangoda M, Gericke A. Ionization Properties of Phosphatidylinositol Polyphosphates in Mixed Model Membranes. *Biochemistry*. 2009;48:9360-71.
- [150] Shin R, Tzou YM, Krishna NR. Structure of a monomeric mutant of the HIV-1 capsid protein†. *Biochemistry*. 2011;50:9457-67.
- [151] Pornillos O, Ganser-Pornillos BK, Banumathi S, Hua Y, Yeager M. Disulfide bond stabilization of the hexameric capsomer of human immunodeficiency virus. *J Mol Biol*. 2010;401:985-95.
- [152] Datta SA, Curtis JE, Ratcliff W, Clark PK, Crist RM, Lebowitz J, et al. Conformation of the HIV-1 Gag protein in solution. *J Mol Biol*. 2007;365:812-24.
- [153] Campbell SM, Crowe SM, Mak J. Lipid rafts and HIV-1: from viral entry to assembly of progeny virions. *J Clin Virol*. 2001;22:217-27.
- [154] Lorizate M, Sachsenheimer T, Glass B, Habermann A, Gerl MJ, Kräusslich HG, et al. Comparative lipidomics analysis of HIV-1 particles and their producer cell membrane in different cell lines. *Cellular Microbiology*. 2013;15:292-304.
- [155] Chukkapalli V, Ono A. Molecular Determinants that Regulate Plasma Membrane Association of HIV-1 Gag. *Journal of Molecular Biology*. 2011;410:512-24.
- [156] Inlora J, Collins DR, Trubin ME, Chung JY, Ono A. Membrane binding and subcellular localization of retroviral Gag proteins are differentially regulated by MA interactions with phosphatidylinositol-(4,5)-bisphosphate and RNA. *MBio*. 2014;5:e02202.
- [157] Olety B, Ono A. Roles played by acidic lipids in HIV-1 Gag membrane binding. *Virus Research*. 2014;193:108–15.

- [158] Rink TJ, Tsien RY, Pozzan T. Cytoplasmic pH and free Mg<sup>2+</sup> in lymphocytes. *The Journal of Cell Biology*. 1982;95:189-96.
- [159] Khorchid A, Halwani R, Wainberg MA, Kleiman L. Role of RNA in Facilitating Gag/Gag-Pol Interaction. *J Virol*. 2002;76:4131-7.
- [160] McKinstry WJ, Hijnen M, Tanwar HS, Sparrow LG, Nagarajan S, Pham ST, et al. Expression and purification of soluble recombinant full length HIV-1 Pr55(Gag) protein in *Escherichia coli*. *Protein Expr Purif*. 2014;100:10-8.

